Dominguez Channel Estuary Model Study
Model Data, Calibration and Verification Report

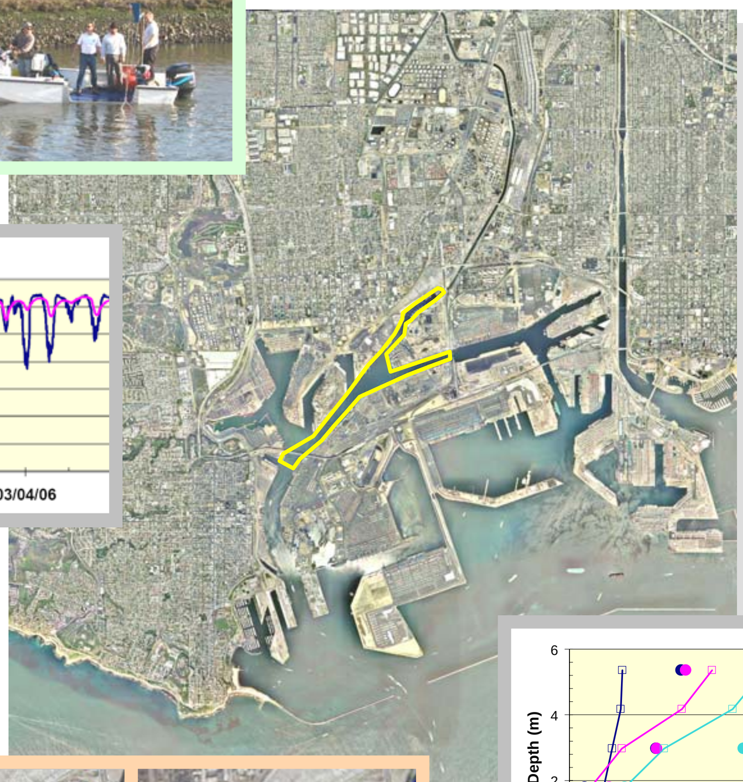

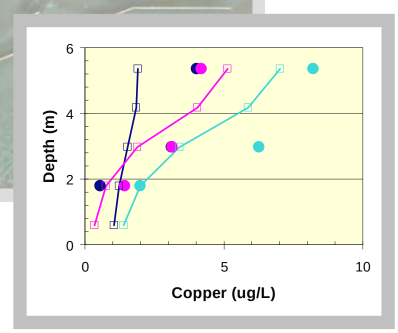

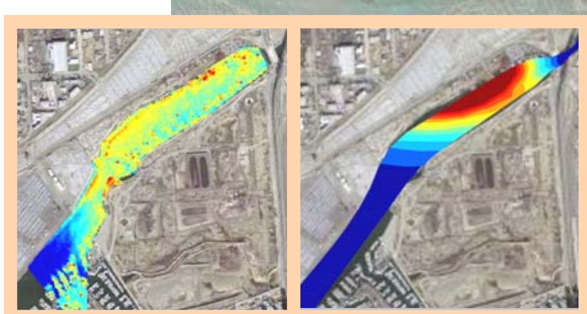

Prepared for:

Port of Los Angeles

Prepared by:

Everest International Consultants, Inc.

EVEREST

August, 2006

DOMINGUEZ CHANNEL ESTUARY MODEL STUDY

MODEL DATA, CALIBRATION AND VERIFICATION

REPORT

Prepared For:

Port of Los Angeles
Environmental Management Division
425 S. Palos Verdes Street
San Pedro, CA 90731

Contact: Andrew Jirik

Prepared By:

Everest International Consultants, Inc.
444 West Ocean Boulevard. Suite 1104
Long Beach, CA 90802

Contacts: David Cannon, Ying Poon

August 2006

Funding for this project has been provided in full or in part through an Agreement with the State Water Resources Control Board (SWRCB) pursuant to the Costa-Machado Water Act of 2000 (Proposition 13) and any amendments thereto for the implementation of California's Nonpoint Source Pollution Control Program. The contents of this document do not necessarily reflect the views and policies of the SWRCB, nor does mention of trade names or commercial products constitute endorsement or recommendation for use.

TABLE OF CONTENTS

LIST OF TABLES

LIST OF FIGURES

1. INTRODUCTION

1.1 BACKGROUND

In November 2003, the California State Water Resources Control Board awarded a Proposition 13 Grant to the Port of Los Angeles (Port) to conduct the Dominguez Channel Hydrodynamic and Water Quality Study now known as the Dominguez Channel Estuary Model Study (DCEMS). In December 2003, the Port issued a request for proposals and performed an extensive consultant selection process that was completed in July 2004. In August 2004, the Port retained a team of consultants lead by Everest International Consultants, Inc. (Everest) to conduct the DCEMS. The team is presented in Table 1.1, along with the primary responsibilities for each team member.

Table 1.1 Dominguez Channel Estuary Model Study Team

TEAM MEMBER	PRIMARY RESPONSIBILITIES
Everest International Consultants, Inc. (Everest)	Contract management, project management, numerical model evaluation, numerical model development, and project report preparation
Science Applications International Corporation (SAIC)	Field program management and coordination, field data collection and management, field data QA/QC, and field program report preparation
Applied Ocean Sciences (AOS)	Dye tracer study management and coordination, dye tracer study data collection and management, dye tracer study data QA/QC, and dye tracer study report preparation
Southern California Coastal Waters Research Project (SCCWRP)	Watershed loading integration
Flow Simulations, LLC	Numerical model development
Merkel & Associates, Inc. (M&A)	Field data collection support

The Everest Team began working on the DCEMS in September 2004 and work on the contract was completed in August 2006. The DCEMS involved coordination with the Port, Los Angeles Regional Water Quality Control Board (LARWQCB), U.S. Environmental Protection Agency (EPA), and a Scientific Review Board (SRB) composed of members from the academia and consulting professions, as well as federal and local governmental agencies. The purpose and objectives of the DCEMS are presented in Sections 1.2 and 1.3. The content of the rest of this report is discussed in Section 1.4.

1.2 PURPOSE

The purpose of the DCEMS is to develop a hydrodynamic and water quality model (Dominguez Channel Estuary Model or DCEM) that the LARWQCB can use to accurately predict water elevations, velocities, and pollutant transport in the estuarine and marine portions of the Dominguez Channel. The Port anticipates that the LARWQCB will utilize the DCEM for the development and implementation of Total Maximum Daily Loads (TMDLs) within the Dominguez Channel Watershed and Los Angeles/Long Beach Harbor Complex.

1.3 OBJECTIVES

The following objectives were developed to achieve the study purpose presented above.

1. Evaluate hydrodynamic and water quality models for the study area.
2. Select a hydrodynamic and water quality models for DCEM development.
3. Obtain and assemble existing data for calibration and validation of the DCEM.
4. Identify data gaps necessary to develop the DCEM.
5. Conduct a field data collection program to fill the identified data gaps.
6. Set up the DCEM system and associated input data files.
7. Perform model simulations necessary to calibrate and validate the DCEM.
8. Prepare a report summarizing the input data files and output data files
9. Prepare a report summarizing the calibration and validation process.

1.4 REPORT CONTENT

The first five objectives (Items 1 through 5) are summarized in other deliverables that were previously submitted as part of the DCEMS. This report focuses on the last four objectives above (Items 6 through 9). Although not identified in the DCEMS scope of work as a deliverable, it was determined that a summary of the calibration and validation process (i.e., Item 9 above) would be important for improving the overall usefulness of the DCEMS for use in the TMDL development and implementation process. Therefore, this report includes a summary of the calibration and validation process that was used to develop the DCEM.

2. MODEL DEVELOPMENT AND SETUP

2.1 OVERVIEW

The Dominguez Channel Estuary Model (DCEM) developed for this study is a three-dimensional (3-D) calibrated hydrodynamic and water quality model for the Dominguez Channel Estuary (Estuary). The DCEM focuses on the estuary portion, which extends from the tidally influence portion of the Dominguez Channel (at Vermont Avenue) down to the upstream portion of the Consolidated Slip (Figure 2.1). The goals of the DCEM are to:

- Simulate hydrodynamic conditions in the Estuary
- Simulate the mixing and transport of pollutants through the Estuary
- Allow integration with other models being developed for the area
- Enable access and use by other stakeholders

The DCEM was designed and developed to achieve these goals. It is anticipated that in the future, the DCEM will be used with other models being developed for the San Pedro Bay area, such as the Dominguez Channel Watershed Model, Los Angeles River Estuary and San Gabriel River Estuary Model, and Harbor Area Circulation Model, as part of the TMDL development and implementation process.

2.2 MODEL SELECTION

Model selection and approval involved an iterative process between the SRB, LARWQCB, and Port that occurred between October 2004 and May 2005. The model selection process involved an initial screening of potential models, comparison and evaluation of the potential hydrodynamic models, and comparison of potential water quality models. In each step of the selection process, recommendations were made to the SRB and LARWQCB and concerns were addressed to assist the decision-making process. This section provides a brief summary of the selection process. Details of the selection process can be found in the following technical memorandums that were prepared and submitted previously as part of the study.

Figure 2.1 Dominguez Channel Estuary Model (DCEM) Study Area

- October 12, 2004 – "Scientific Review Board Meeting 2 Briefing – Model Selection"
- November 4, 2004 – "*Hydrodynamic Model Summary Report Draft*"
- December 1, 2004 – "*Water Quality Model Summary Report Draft*"
- May 2, 2005 – "*Water Quality Model Summary Report – Addendum*"

2.2.1 Initial Screening

Models considered for the DCEM were non-proprietary, 3-D hydrodynamic and water quality models. The use of a non-proprietary model is consistent with the Proposition 13 grant requirement to provide all model codes (i.e., executable and source code) to the LARWQCB. This also allows easier integration with future models, as well as access for other stakeholders that will utilize the model. After the initial screening of potential models, the hydrodynamic models recommended for evaluation were CH3D-WES, EFDC, and RMA10. Since each of these hydrodynamic models also has a corresponding water quality model - CE-QUAL-ICM/TOXI, WASP/TOXI, and RMA11, these water quality models were also selected for further evaluation.

2.2.2 Model Evaluation and Selection

The three hydrodynamic models (CH3D, EFDC, and RMA10) were first evaluated on technical strengths and weaknesses based on: 1) mathematical formulation, 2) numerical methods, 3) watershed model interfacing, and 4) similar applications experience in the Harbor Area and TMDL developments. On the basis of mathematical formulation, there are more similarities than differences between these models. The major difference being that CH3D uses a k-epsilon model for turbulent closure, which is better suited for channel flows, while EFDC and RMA10 use a modified Mellor-Yamada turbulent closure model, which is best suited for ocean models. However, both closure models are similar for estuary applications. CH3D and EFDC have nearly identical numerical methods that vary substantially from RMA10, the latter has greater numerical stability problems with fast moving flows.

Based on the mathematical formulation and numerical method, CH3D and EFDC were determined to be better suited than RMA10. In terms of interfacing with a watershed model, EFDC is slightly more flexible than CH3D in handling flow, salinity, and temperature at different water layers. Based on model application experience, CH3D has a long history with applications in the Los Angeles and Long Beach Harbor Areas for tidal circulation and water quality studies and was used for the Cabrillo Beach TMDL development. However, EFDC has been used for TMDL development in the Los Angeles River and many other TMDL development studies throughout the nation.

In general, the three corresponding water quality models are capable or can be configured to simulate the necessary water quality constituents for the DCEMS. WASP6 and CE-QUAL-ICM/TOXI are similar water quality models with comparable eutrophication subroutines and the same subroutines for simulating toxic constituents. Both models are also exchangeable with the CH3D and EFDC hydrodynamic models. The use of RMA11 requires the RMA10 hydrodynamic model, which was previously determined to be less suitable than EFDC or CH3D for this study.

The initial evaluation of the EFDC model was based on the version of EFDC that has only the hydrodynamic components with a linkage to the WASP water quality model. Over the course of the model selection process, another version (full version) of EFDC that can simulate both hydrodynamics and water quality became available. An evaluation of this version of EFDC determined that the water quality component of this full version has similar water quality modeling capabilities to WASP plus some additional capabilities that WASP does not have. Meanwhile, EPA retained Tetra Tech, Inc. to use EFDC to develop a hydrodynamic and water quality model for the LA/LB Harbors including the Los Angeles River Estuary and San Gabriel River Estuary in support of TMDL development. Further discussions between the SRB, LARWQCB, and EPA were held regarding the coordination of this study and the Tetra Tech study. It was determined that it would be advantageous for future TMDL development for the region if both modeling efforts are using the same EFDC model. Otherwise, substantial effort will be required to merge two different models together before they can be used for future TMDL development.

In summary, the EFDC was selected as the model for the DCEMS for the following reasons.

- EFDC is a non-proprietary model (source code available) with similar or better capabilities compared to other hydrodynamic/water quality models that were evaluated.
- EFDC combines the hydrodynamic and water quality components in one single model, hence the hydrodynamics and water quality components are dynamically linked.
- EFDC has been selected by EPA for TMDL development for the greater Los Angeles and Long Beach Harbors. Using the same model for the development of DCEM will facilitate the merging of DCEM with the harbor-wide model in the future.

2.3 EFDC Description

EFDC is a 1-, 2-, or 3-D hydrodynamic and water quality model that has been used by EPA for TMDL developments in river, lake, estuary, wetland, and coastal regions in the US. The model was originally developed by Dr. John Hamrick at the Virginia Institute of Marine

Science and currently is maintained by Tetra Tech, Inc. for the EPA. The EFDC model has three primary components – hydrodynamics, sediment-toxic transport and fate, and water quality (eutrophication) integrated into a single model. The hydrodynamic component is dynamically coupled to salinity and temperature transport, as well as to sediment-toxic transport and water quality components.

The hydrodynamic component is similar to the Princeton Ocean Model (Blumberg and Mellor 1987). EFDC solves the 3-D Reynold-Averaged Navier-Stokes equations assuming incompressible flow and hydrostatic pressure distribution with dynamically coupled salinity and temperature transport, which accounts for density variations. Additional hydrodynamic features include a modified Mellor-Yamada level 2.5 turbulence closure formulation (Mellor and Yamada 1982 and Galperin et al 1988), wetting and drying, controlled flow structures, vegetation resistance, wave-current boundary layers and wave induced currents, embedded single port buoyant jet module based on the CORMIX model for couple near-field and far-field mixing analyses, and Lagrangian particle tracking scheme.

The hydrodynamic component provides the dynamics for the sediment transport and fate, which is in turn linked to the toxic or contaminant transport and fate. EFDC can simulate multiple classes of cohesive and noncohesive sediment as suspended load and bed load, as well as sediment deposition and resuspension (Tetra Tech 2002). The sediment transport component can be coupled with the hydrodynamics to represent changes in bed topography and can also be coupled with a spectral wave model for wave induced resuspension. EFDC is capable of simulating an arbitrary number of toxics (e.g., metals and hydrophobic organics) and interactions with any of the sediment-classes, dissolved organic carbon, and particulate organic carbon. The toxic transport is based on the same advection-diffusion scheme used for salinity and temperature.

The water quality component in EFDC is basically an eutrophication model that simulates eutrophication and sediment biogeochemical (diagenesis) processes. The water quality simulation capability is based on a 21-state variable water column eutrophication model coupled with a 27-state variable sediment biogeochemical process model.

2.4 DCEM SETUP

2.4.1 Grid Setup

The primary focus of the DCEM is the estuary portion, which extends from the tidally influence portion of the Dominguez Channel at Vermont Avenue down through the Consolidated Slip and into the Main Channel of the Port, as shown previously in Figure 2.1. However, the model domain extends beyond the Estuary to include the entire harbor area since the hydrodynamics of the Estuary are dynamically linked to the harbor area.

EFDC can use either a Cartesian or curvilinear, orthogonal horizontal grid. For the DCEM, a curvilinear, orthogonal grid was determined to be more suitable to capture flows within the Estuary. The model grid was designed with a higher resolution (i.e., smaller grid cells) in the estuary portion with progressively larger cells in the harbor area and ocean portions. In the design of the numerical model grid, a balance must be achieved between the grid resolution (e.g., grid cell size and total number of cells) and computation time. Smaller grid cells provide greater level of detail in model predictions, but tend to be less stable and require smaller computational time steps, which increases computation time.

EFDC uses a stretched or sigma vertical coordinate. In other words, each model grid cell is divided into the same number of vertical layers regardless of the water depth. The DCEM was specified with five, evenly-spaced vertical layers in the water column. For example, a cell with a water depth of 5 meters is represented with five 1-m layers and a cell with a water depth of 20 meters is represented with five 4-m layers.

Two grids with different grid cell resolutions in the harbor area and ocean, shown in Figure 2.2, were developed and tested for the required grid resolution to provide adequate model resolutions (e.g., water elevations and velocities) for the study area and at the same time can be run with reasonable computation time. Both grids shown in Figure 2.2 have the same setup for the Dominguez Channel, Consolidated Slip, and Cerritos Channel areas (areas of most interest for this study) that are defined with three cells across the channel. The fine grid contains a total of 25,530 horizontal cells, while the coarse grid has 2,031 cells. For the fine grid, the Main Channel is defined by seven cells across the channel. The Harbor Area is defined with approximately 100 x 50 m cells and the ocean by 100 x 200 m cells. For the coarse grid, the cells in the Harbor and ocean areas ranged from 100 x 200 m to 1,000 x 900 m cells. In addition, the model grid boundaries were specified with curvilinear edges and a semi-circular ocean boundary. Both grids have five layers to represent the water column.

A 16-day test simulation was conducted on both grids to compare the model predicted hydrodynamic conditions in the areas of interest (the four ADP monitoring locations shown in Figure 2.2) and the required computation time. A comparison of the predicted water surface elevations using the fine and coarse grids are shown in Figure 2.3. The results indicate that using either the fine or coarse grids will result in almost the same predicted water surface elevations. The predicted velocities at the four measurement locations in the Estuary are compared in Figure 2.4. The results show that using either the fine or coarse grid will result in essentially the same predicted velocities at the Dominguez Channel (S. Pacific Drive) and Berth 200G, while there are small differences in the predicted velocities at the other two locations (Berth 206 and Berth 173).

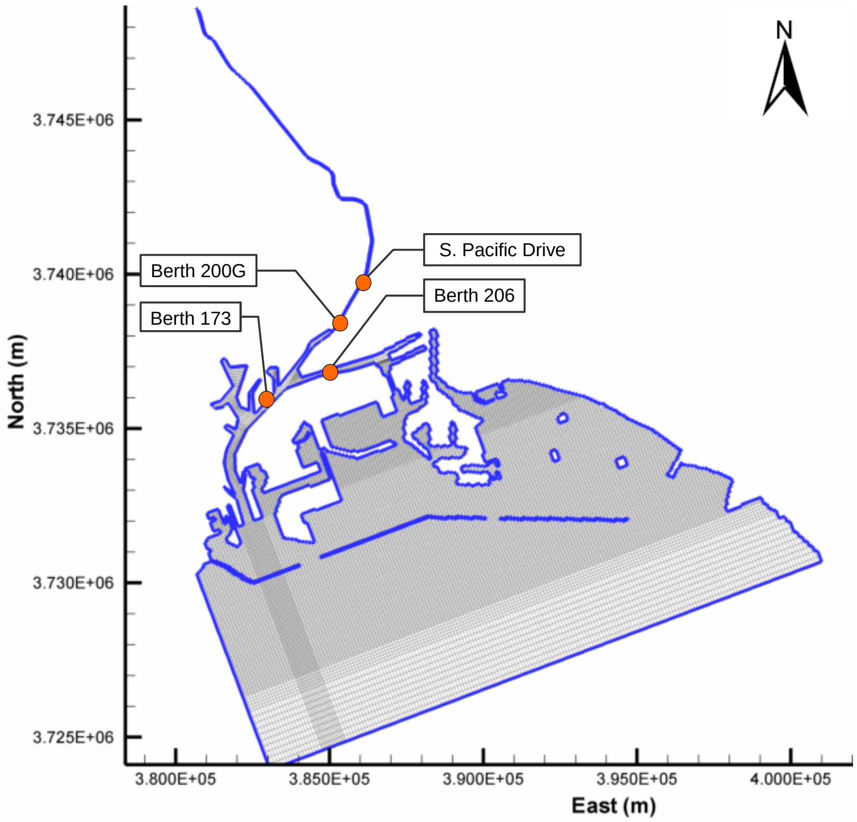

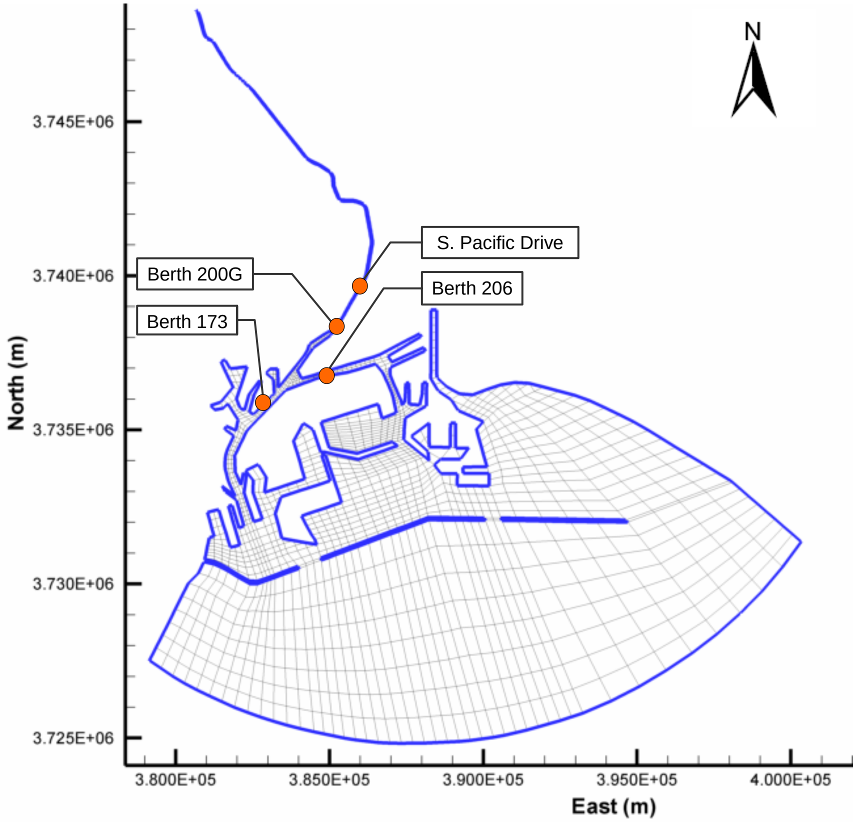

Figure 2.2 Fine and Coarse Grids

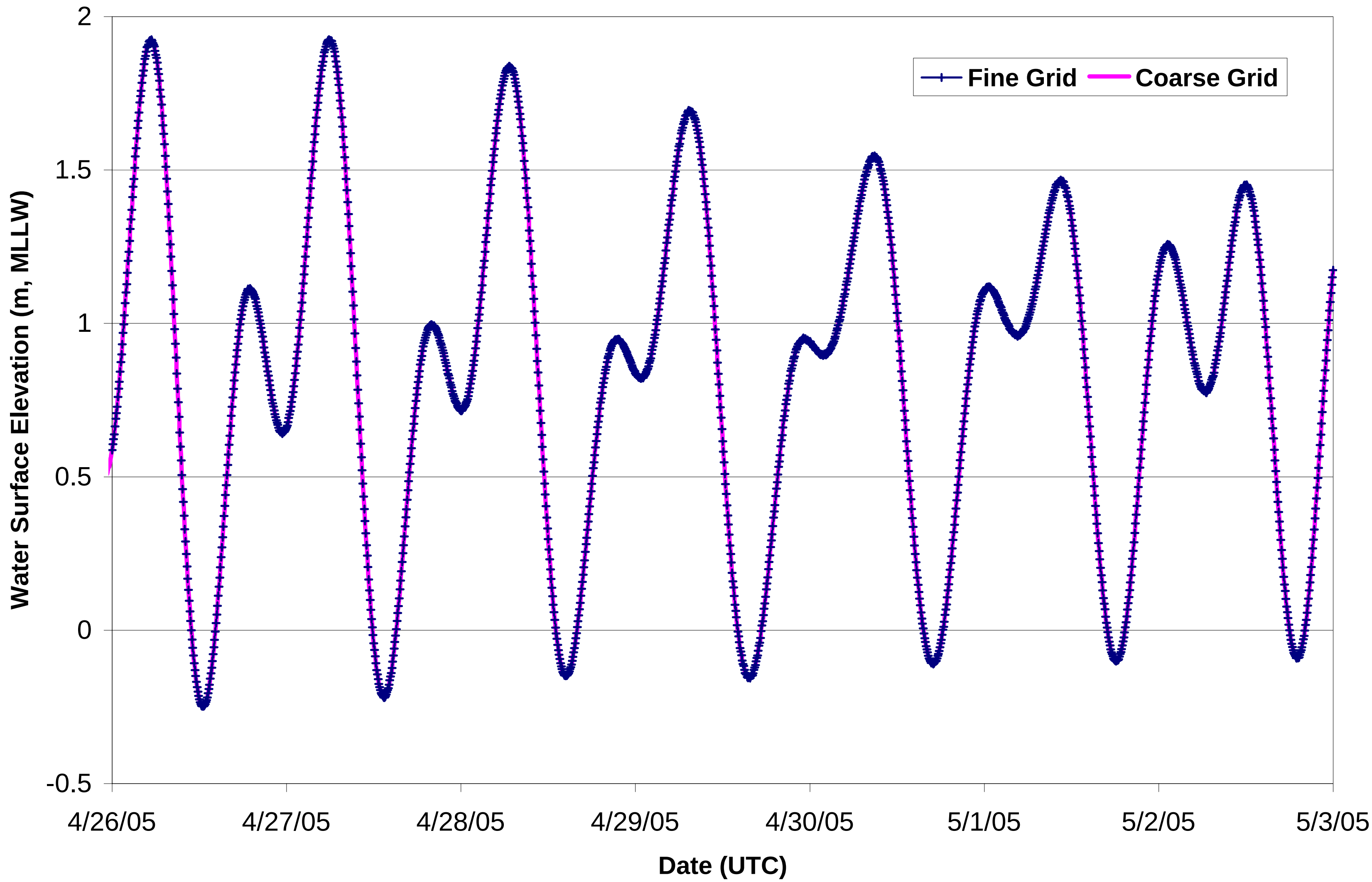

Figure 2.3 Comparison of Water Surface Elevations for Fine and Coarse Grids

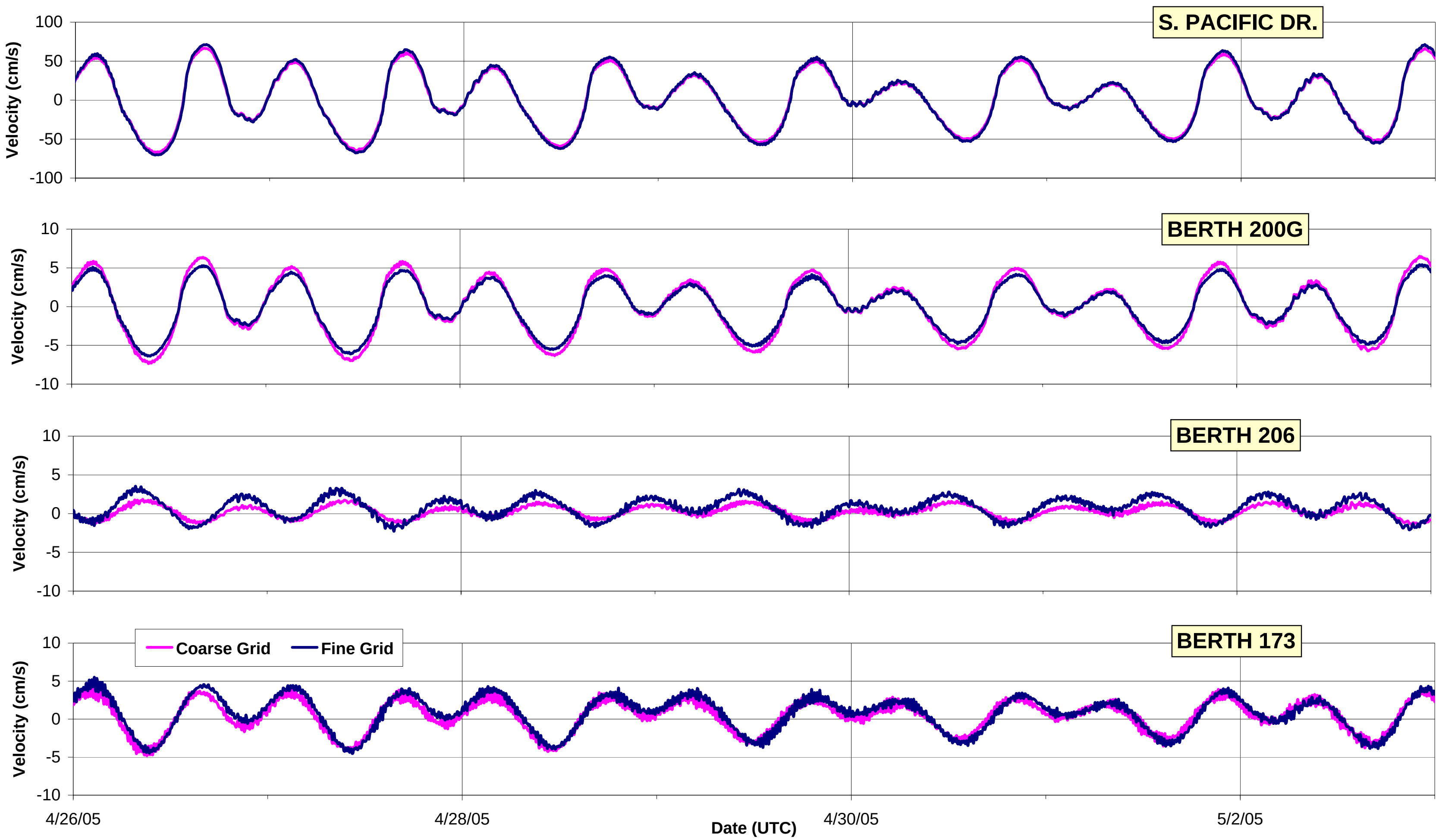

Figure 2.4 Comparison of Velocities for Fine and Coarse Grids

Most of the calibration simulations need to be run for 60 days (30 days for spin-up and 30 days calibration period), it would take about 19 hours and 30 minutes to run the model with the coarse grid, but about 12 days with the fine grid. Judging that the model predicted velocities using either the fine or coarse grid produces are similar in the study area, the coarse grid was selected for the DCEM.

2.4.2 Bathymetry

Bathymetry data for the DCEM were a composite of data from various sources. As shown in Figure 2.5, bathymetry data for the Dominguez Channel were from a Port March 2006 survey. The U.S. Army Corps of Engineers (USACE) survey data for the Los Angeles Channel Deepening Project in 2005 were used for the Main Channel and parts of the Los Angeles Harbor. The rest of the model domain was based on the 2004 NOAA Charts (Numbers 18749 and 18751), supplemented by other survey data conducted by USACE in 2001. The DCEM grid with the composite bathymetry data incorporated is shown in Figure 2.6.

2.4.3 Storm Drains

Storm drains discharge flows into the estuary from the watershed. As shown in Figure 2.7, the Dominguez Channel Watershed was divided into 19 drainage areas to capture all the storm drain sources. The names of the drainage areas shown in the figure are based on either the closest cross street to the discharge location in the Dominguez Channel or the discharge location in the Harbor Area. The DCEM storm drains and the corresponding drainage area characteristics are provided in Table 2.1. In some cases, multiple storm drains were grouped together and represented as one single storm drain source. These nineteen storm drain locations are represented by the red dots in Figure 2.7.

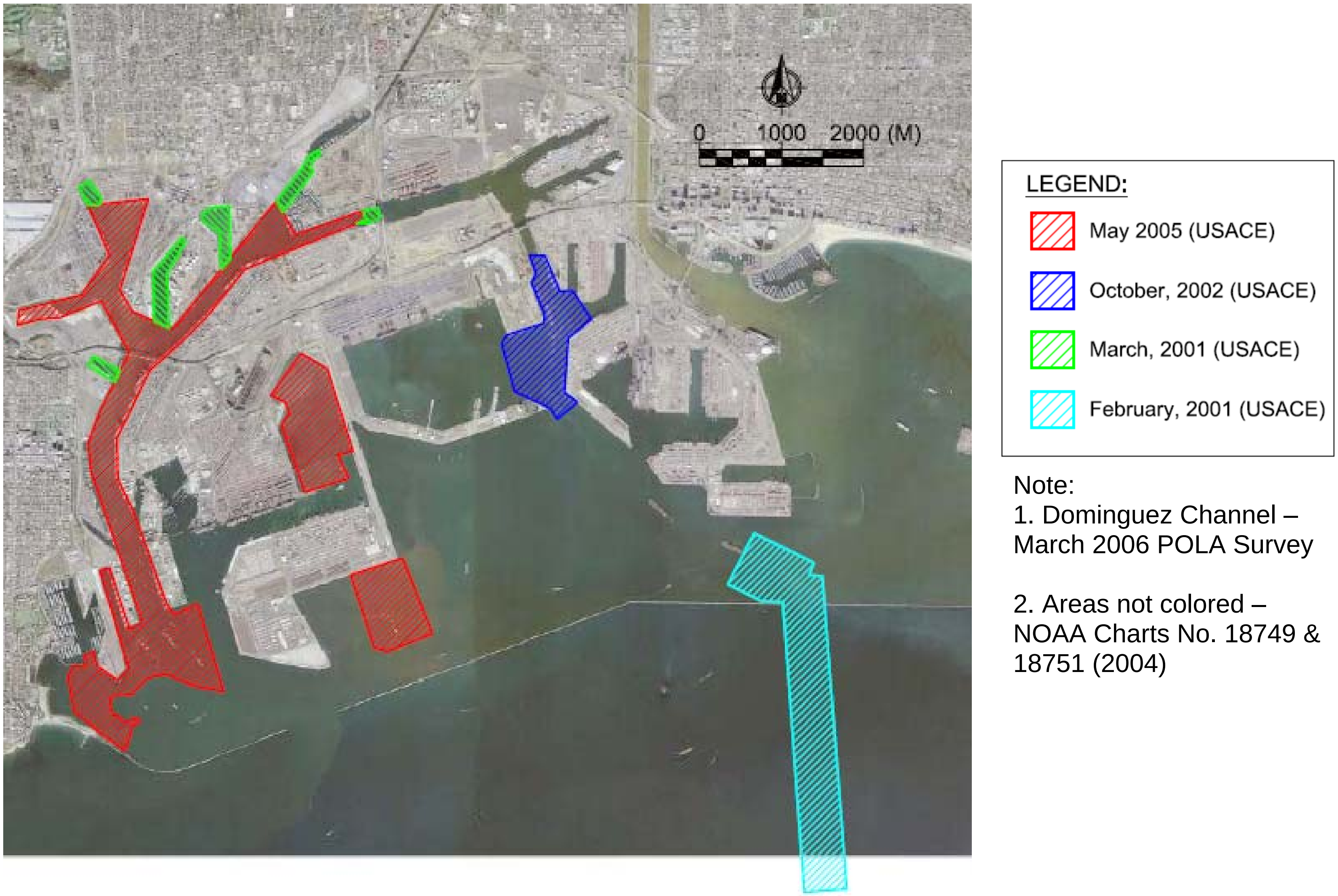

Note:
1. Dominguez Channel – March 2006 POLA Survey

2. Areas not colored – NOAA Charts No. 18749 & 18751 (2004)

Figure 2.5 Bathymetry Data Sources

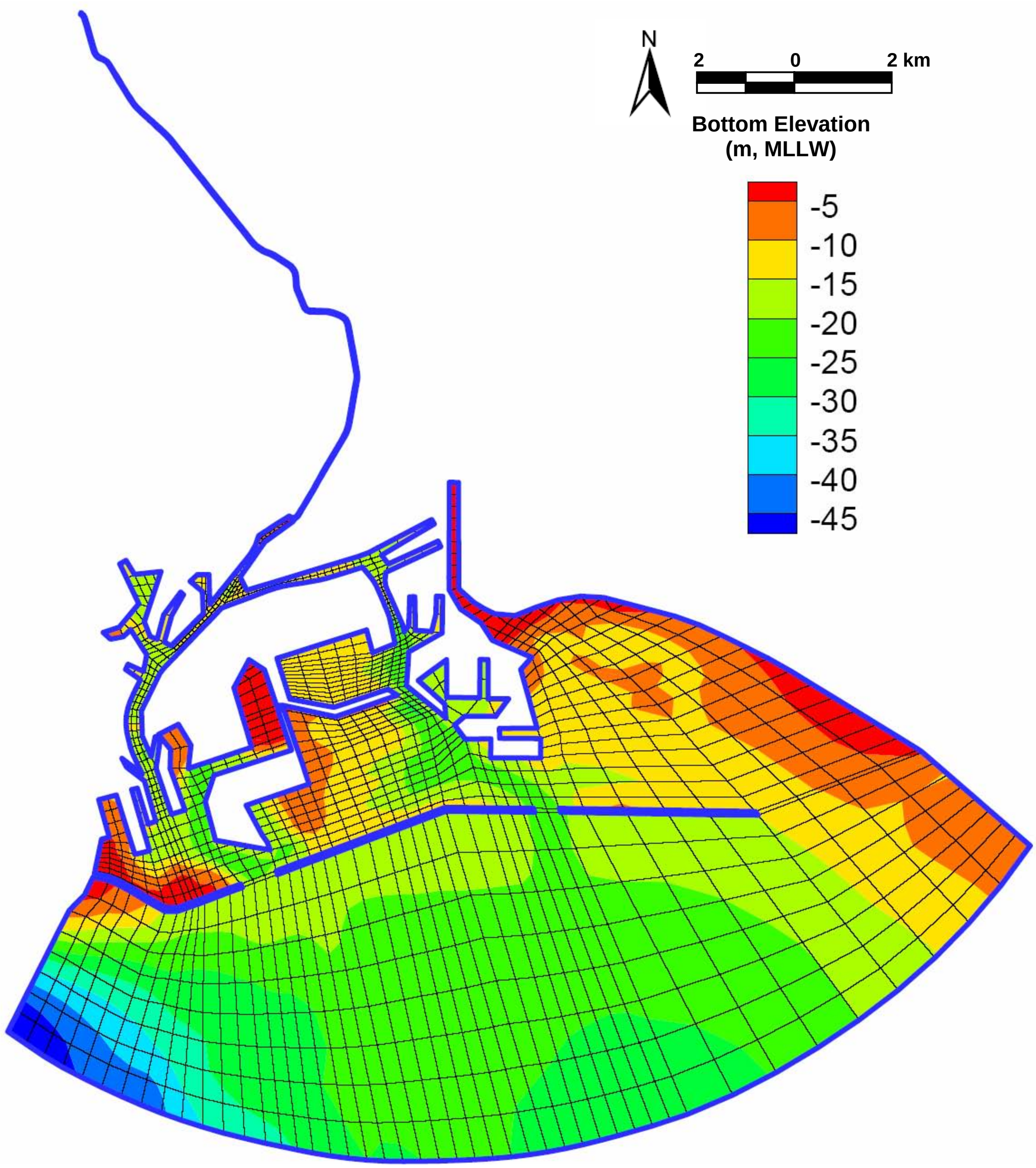

Figure 2.6 DCEM Model Grid and Bathymetry

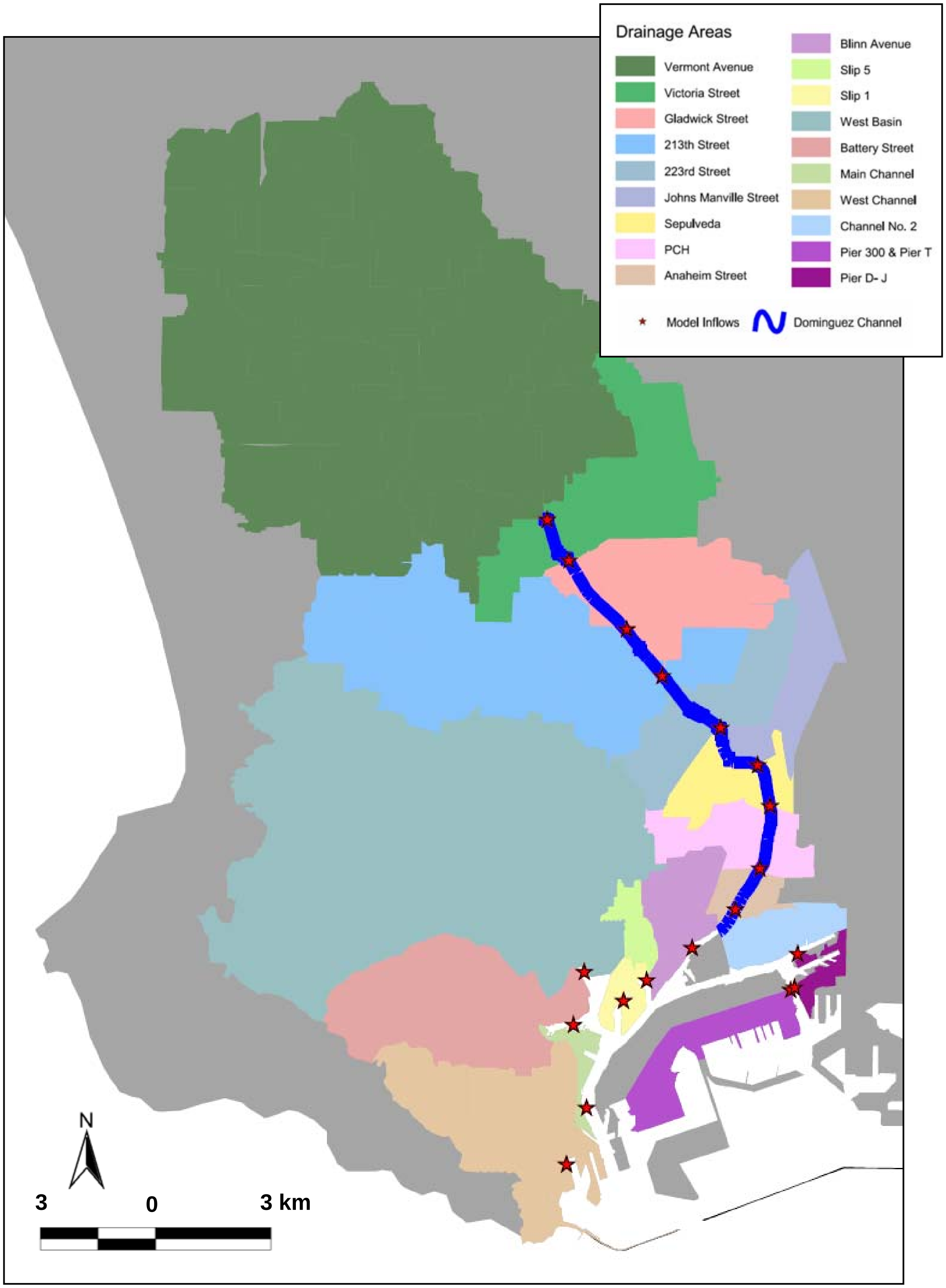

Figure 2.7 Storm Drain Drainage Areas and Model Inflow Locations

Table 2.1 Storm Drain Inflows for DCEM

STORM DRAIN	DRAINAGE AREA (km^2)	PERCENT OF WATERSHED (%)
Vermont Avenue	103.36	33.0
Victoria Street	15.19	4.8
Gladwick Street	11.77	3.8
213th Street	30.32	9.7
223rd Street	8.11	2.6
Johns Manville Street	5.90	1.9
Sepulveda	4.34	1.4
PCH	2.07	0.7
Anaheim Street	5.14	1.6
Blinn Avenue	4.60	1.5
Slip 5	1.60	0.5
Slip 1	1.46	0.5
West Basin	66.99	21.4
Battery Street	15.27	4.9
Main Channel	1.07	0.3
West Channel	14.29	4.6
Channel No. 2	3.34	1.1
Pier 300 & Pier T	0.71	0.2
Pier D - J	1.10	0.4

2.4.4 Power Station

The Harbor Generating Station is the only power station currently operating in the Harbor Area that requires cooling water for a steam turbine (Unit 5). The Harbor Generating Station withdraws cooling water from the northwest corner of Slip 5 and discharges in the northeast corner of the West Basin. This was simulated as a withdrawal-return flow using the design flow rate of 4.73 m^3/sec (108 MGD). Although, cooling water intake is not continuously operated at design conditions; between 2000 and 2004, Unit 5 was operated at 29% capacity on average. Test runs with the EFDC model indicate that even at design conditions, the cooling water intake and discharge would not affect the hydrodynamics in the study area; results show that predicted velocities at the four monitoring locations are the same with or without the power station operation. Nevertheless, the power station operation was incorporated into the DCEM for completeness.

3. FIELD DATA

3.1 OVERVIEW

A field data collection program (Field Program) was designed to collect suitable data for the development, calibration, and verification of the DCEM, as well as to augment existing hydrodynamic and water quality monitoring. The Field Program consisted of monitoring hydrodynamic and water quality conditions in or near the estuary over a one-year period from February 2005 through March 2006. Data collected under the Field Program included hydrodynamic (water surface elevations and velocities) and water quality data from fixed monitoring stations, vessel-based surveys, salinity distributions, estuary water quality samples, storm drain pollutographs, a dye study, and meteorological data. Details of the field program are provided in the Field Implementation and Validation Plan (Everest 2005) and the reports prepared by the Field Program (SAIC, 2006a, 2006b).

An overview of the Field Program is provided in Table 3.1 and the water quality parameters are listed in Table 3.2. Field data monitoring locations are shown in Figure 3.1 and coordinates of the fixed locations are provided in Table 3.3. The following sections provide a brief description of the field data collected, as well as the methodology for processing the field data for use in the DCEM calibration. In addition, field data collected by others in the study area that were used in the development of the DCEM are also discussed. These additional data used for model development include:

- NOAA LA Outer Harbor tide gage data
- NOAA PORTS® meteorological data
- Pollutographs collected by the Port at Artesia
- Sediment data collected by the Port in the Consolidated Slip and Dominguez Channel
- Sediment and water quality data collected as part of the Ports of Long Beach and Los Angeles Biological Baseline Study

Table 3.1 Field Program Summary

FIELD DATA	INSTRUMENT	MEASUREMENTS	FREQUENCY	DATE*
Fixed Monitoring	ADP	Pressure Water Temperature Velocity magnitude and direction	Continuous	2/26/05 to 3/15/06
Vessel-Based Surveys	ADCP	Velocity Profiles	Dry Weather	2/26/05
			Wet Weather	2/27 – 2/28/06
Salinity Distributions	CTD	Suite A Profiles	Dry Weather	5/17/05
		Salinity and continuous wet weather salinity Temperature Pressure Conductivity Suite A Profiles Beam Attenuation Profiles Colored Dissolved Organic Matter Chlorophyll Fluorescence	Wet Weather	2/27 – 2/28/06
Estuary Water Quality	CTD and discrete samples	Suite A Profiles TSS	Monthly	2/26/05 – 2/28/06
		Suite A Profiles	Wet Weather	2/27 – 2/28/06
		Suite B	Dry Weather	5/17/05 and 8/18/05
			Wet Weather	2/27 – 2/28/06
Pollutographs	Discrete samples	TSS and Suite B	Wet Weather	2/27 – 2/28/06
Dye Tracer Study	Fluorometer ISCO batch samples	Dye Concentration and Profiles Aerial Photo Dye Contours	Dry Weather	5/17/05
Meteorological Data	MET	Wind Speed, Direction, and Gust Air Temperature, Relative Humidity, Dew Point Temperature, Solar Radiation, Barometric Pressure	Continuous	2/26/05 – 3/22/06
PORTS® **	MET	Wind Speed, Direction, and Gust Air Temperature and Pressure	Continuous	2/26/05 – 3/22/06
Artesia Pollutograph**	Autosampler and stage	TSS and Suite B Flow	Dry Weather	5/17/05 and 8/18/05
			Wet Weather	2/27 – 2/28/06

* *Field data date and time in Coordinated Universal Time (UTC)*
** *Additional field data provided by the Port of Los Angeles*

Table 3.2 Suite A and Suite B Water Quality Parameters

<table>
<tr><th colspan="4">SUITE A</th></tr>
<tr><td>Density
Dissolved Oxygen (DO)</td><td>pH
Salinity</td><td colspan="2">Temperature
Transmissivity</td></tr>
<tr><th colspan="4">SUITE B</th></tr>
<tr><th>CONVENTIONAL</th><th>METALS</th><th>PESTICIDES / PCBS</th><th>PAHS</th></tr>
<tr><td>Dissolved Organic Carbon (DOC)
Total Organic Carbon (TOC)
Hardness
Alkalinity
Ammonia</td><td>Aluminum
Arsenic
Cadmium
Chromium
Copper
Iron
Lead
Mercury
Nickel
Selenium
Silver
Zinc</td><td>Aldrin
Alpha-BHC
Beta-BHC
Gamma-BHC
Delta-BHC
Chlordane
4,4-DDD
4,4-DDE
4,4-DDT
Dieldrin
Endosulfan I
Endosulfan II
Endosulfan Sulfate
Heptachlor
Heptachlor Expoxide
Endrin
Endrin aldehyde
Methoxychlor
Toxaphene
Aroclor 1016
Aroclor 1221
Aroclor 1232
Aroclor 1242
Aroclor 1248
Aroclor 1254
Aroclor 1260</td><td>Acenaphthene
Acenaphthylene
Anthracene
Benzo(a)anthracene
Benzo(b)fluoranthene
Benzo(k)fluoranthene
Benzo(a)pyrene
Benzo(e)pyrene
Benzo(ghi)perylene
Chrysene
Dibenzo(ah)anthracene
Fluorene
Fluoranthene
Indeno(1,2,3-cd)pyrene
Napthalene
Perylene
Phenanthrene</td></tr>
</table>

Table 3.3 Fixed Station Locations

STATION	LOCATION	TYPE	LATITUDE	LONGITUDE
Sepulveda	Channel	CTD	33.80579000	-118.2277900
S. Pacific Drive		ADP	33.78483340	-118.2353806
E. I Street		CTD	33.78295228	-118.2366820
Berth 200G	Harbor	ADP / CTD	33.77657267	-118.2437419
Berth 206		ADP	33.76392761	-118.2454561
Berth 173		ADP / CTD	33.75645896	-118.2637698

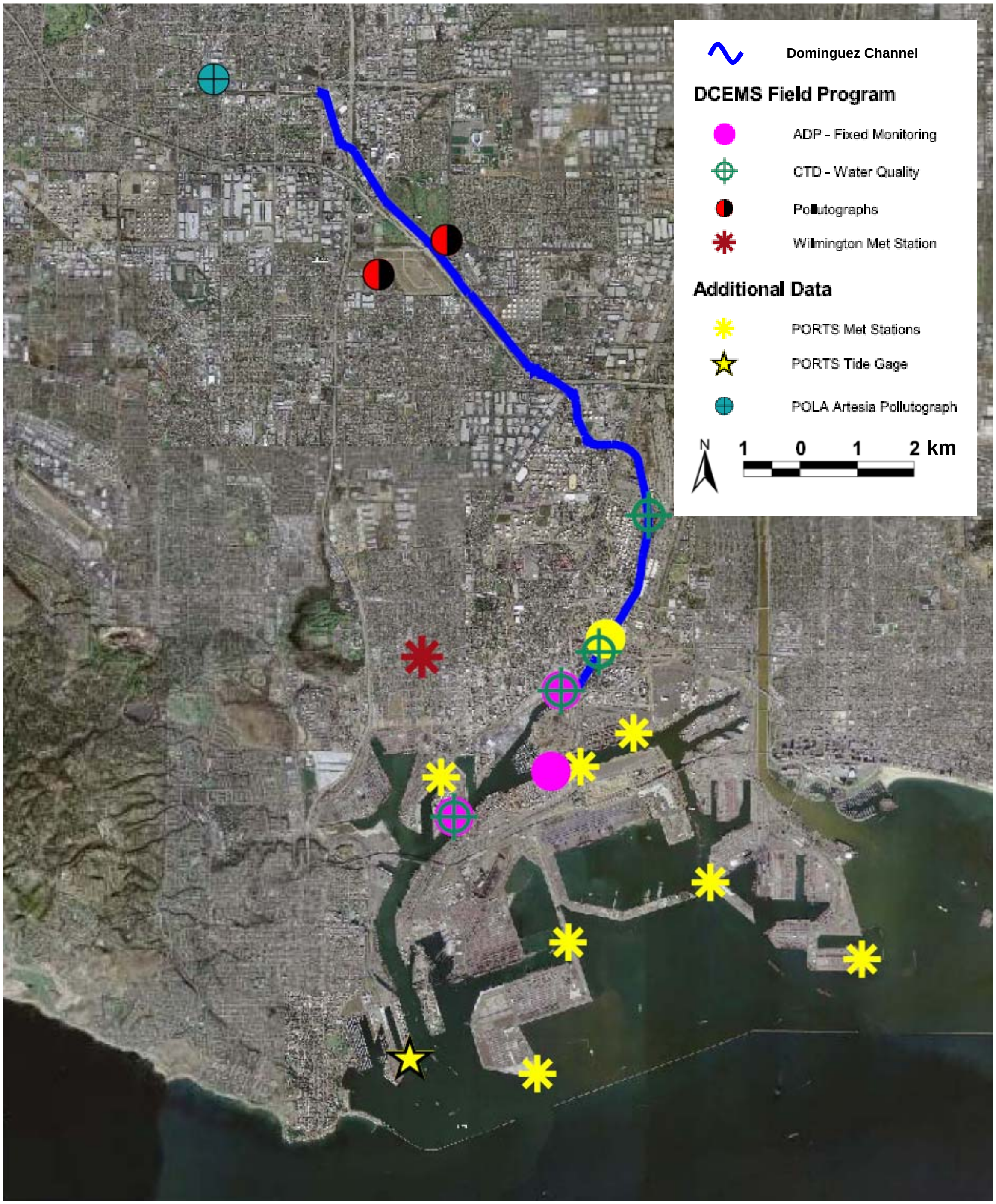

Figure 3.1 Field Data Monitoring Locations

3.2 FIXED MONITORING

Continuous records of pressure, water temperature, and currents were measured at four locations (one channel location and three harbor locations) using Acoustic Doppler Profilers (ADP). These fixed monitoring or ADP locations are shown in Figure 3.2. The ADP at S. Pacific Drive was bottom mounted to measure the vertical velocity profiles near the center of the Dominguez Channel. The other three ADPs at Berth 200G, Berth 206, and Berth 173 were side-mounted to measure cross-channel measurements at a specified depth. For the DCEM calibration, the measured ADP data were processed to obtain the following data:

- Continuous water surface elevations
- Continuous average along-channel velocities
- Vertical velocity profiles in the Dominguez Channel

The ADPs measure the water pressure above the instrument, which is proportional to the water depth. These pressure data were used to calculate the water surface elevations (in meters, MLLW) at the four ADP locations. For the bottom-mounted ADP at S. Pacific Drive, the velocities were measured at uniformly-spaced fixed distances (or bins) above the bottom. Thus, the number of measurements depends on the water depth (i.e., there are more bins during high tide and less bins during low tide). For the three side-mounted ADPs, currents at the depth of the instrument were measured at 10 uniformly-spaced fixed locations (bins) across the channel.

The current measurements consist of the north and east velocity components (i.e., velocity with respect to true north). Since the along-channel velocity allows a better perception of the speed of the water moving through the estuary (i.e., how fast the water is moving through the channel), the velocity data were processed to convert the north-east velocity components to along- and cross- channel velocities for comparison with model predicted velocities. The conversion of the north/east velocity to the along/cross channel velocity for each bin was based on the following vector rotation relationship.

$$\begin{bmatrix} V_{along} \\ V_{cross} \end{bmatrix} = \begin{bmatrix} \cos\theta & \sin\theta \\ -\sin\theta & \cos\theta \end{bmatrix} \cdot \begin{bmatrix} V_E \\ V_N \end{bmatrix}$$

Where,

V_{along}	=	Current velocity in along channel direction
V_{cross}	=	Current velocity in cross channel direction
V_E	=	Current velocity in east direction
V_N	=	Current velocity in north direction
θ	=	Angle between along channel and east direction (measured counterclockwise from positive east direction)

Figure 3.2 ADP Locations

The channel alignments at the ADP locations are listed in Table 3.4. The along channel velocities in each bin were then averaged to obtain a continuous record of the average along channel velocity at each ADP location. A positive velocity indicates flood currents (flow up the estuary) and a negative velocity represents ebb currents (out of the estuary) where the channel is in north-south direction (S. Pacific Drive, Berth 200G, and Berth 173). For the channel in east-west direction at Berth 206 in the Cerritos Channel, positive velocities indicate currents moving east toward the Port of Long Beach and negative velocities indicate currents moving west toward the Port of Los Angeles.

Table 3.4 Channel Alignments for ADP Stations

ADP STATION	CHANNEL ALIGNMENT (DEGREES)
S. Pacific Drive	60.88
Berth 200G	32.75
Berth 206	17.22
Berth 173	49.20

Figure 3.3 shows examples of channel velocities collected at the four ADP locations. As expected, the measured velocities (dark blue lines) are dominated by the tides, with small high-frequency fluctuations on top of the tidal currents (low frequency oscillations). These small high-frequency velocity fluctuations could be caused by passing ships, local eddies, gust winds and many other local effects. Since the DCEM mainly predicts the tidally-dominated channel velocities, these field data were first filtered to remove the high frequency oscillations before comparing with the model predicted velocities.

The raw field data velocities were filtered based on a commonly used spectral analysis (USACE 2002) to remove the high frequency fluctuations within the data. The spectral analysis involved transforming the time series data to the energy spectra in the frequency domain, identifying of the dominant frequencies, selecting and removing (filtering) the high frequencies, and converting the remaining frequencies back into a time series. A Fast Fourier Transform (FFT) technique was used to transform data from the time-domain to a frequency-domain. The FFT technique converts the time series record into a spectrum based on the distribution of energy for various frequencies. The frequency spectra at each ADP site are shown on the left panels next to the time series plots in Figure 3.3. As expected, the energy peaks occur at the two dominant frequencies of approximately 1.16E-5 hertz (Hz) and 2.24E-5 Hz, corresponding to the tidal periods of 23.9 hours and 12.4 hours, respectively. As shown in the figure, a cutoff frequency of 5.0E-5 Hz was selected to eliminate the higher frequencies. A reverse FFT technique converts the filtered spectra back to a time-domain, and these smoothed (i.e., filtered) along channel velocities are shown as the magenta lines in Figure 3.3. The filtered velocities preserve the overall trends

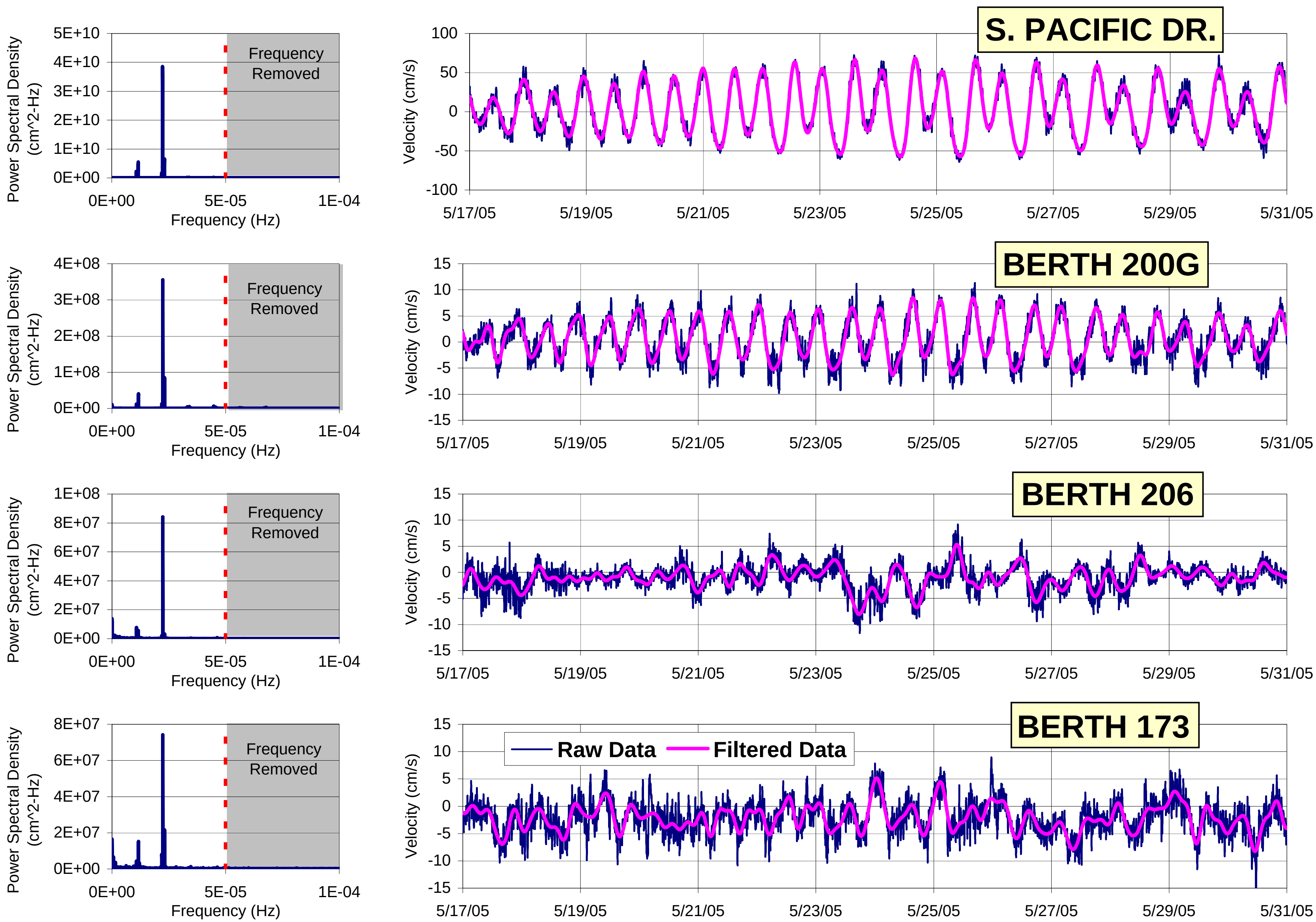

Figure 3.3 Field Measured Velocities and Velocity Spectra

in the original raw time series, while eliminating the high frequency oscillations. As mentioned earlier, these filtered channel velocities will be used for the DCEM calibration.

The vertical velocity profiles in the Dominguez Channel were measured from the bottom-mounted ADP at S. Pacific Drive. As mentioned previously, the velocity vectors were measured at uniformly-spaced vertical bins in the water column. This results in a different number of measurements depending on the water depth. In order to apply the spectral analysis, the bin channel velocities were converted to five velocities equally distributed through the water depth (i.e., velocity profile consisting of five measurements), which results in a uniform number of measurements with at varying water depths. The spectral analysis was then applied to each of the five measurements. The filtered data were then used to determine the vertical velocity profiles at various points in time (e.g., peak flood or ebb tide) for the DCEM calibration.

3.3 VESSEL-BASED SURVEYS

Vessel-based velocity measurements using a downward-looking Acoustic Doppler Current Profiler (ADCP) were taken throughout the lower estuary during one dry weather event and one wet weather event. The ADCP was lowered in the water to obtain a "snapshot" of the currents at all depths and across the navigable channel. The locations of the vessel-based surveys are shown in Figure 3.4. During the dry weather event on May 17, 2005, the velocity direction and magnitude were measured along 10 along and cross channel transects. During the wet weather event on February 27-28, 2006, ADCP measurements were taken at seven locations: one at Berth 200G, three across the channel at Berth 173, and three across the channel at Berth 206.

3.4 SALINITY DISTRIBUTIONS

Spatial distributions of vertical salinity profiles were obtained using a Sea Bird Electronics conductivity, temperature, and depth (CTD) / transmissometer system. CTD measurements include salinity, temperature, density, dissolved oxygen, conductivity, and transmission. Salinity distributions throughout the lower estuary were obtained during one dry and one wet weather event at the locations shown in Figure 3.5. During the May 17, 2005 dry weather event, 21 CTD profiles were taken through the Estuary and included profiles at the same location and different times. The salinity sampling for the wet weather event was expanded to replace the originally-planned wet weather dye study. As such, 42 profiles were measured throughout the Estuary during the February 27-28, 2006 wet weather event. Continuous salinity measurements during the rain event and the two-weeks following were also collected at Berth 200G and Berth 173. Additional data measured during the wet weather event were beam attenuation, colored dissolved organic matter, and chlorophyll fluorescence.

Figure 3.4 Vessel-Based Surveys – ADCP Measurements

Figure 3.5 Salinity Distribution Locations

3.5 ESTUARY WATER QUALITY

Water quality constituents were measured in the Estuary on a monthly basis, as well as during two dry weather events (May 17, 2005 and August 18, 2005) and one wet weather event (February 27-28, 2006). Monthly water quality measurements consisted of vertical CTD profiles and TSS measurements taken at four locations – in the Dominguez Channel at Sepulveda and E. I Street, as well as at Berth 200G and Berth 173. These CTD locations are shown in Figure 3.6. TSS measurements consisted of 10 discrete samples at four locations with varying depths, surface- and bottom-depths for the channel locations and surface-, mid-, and bottom-depths for the other locations. Additional Suite B water quality constituents (see Table 3.2) were measured during the two dry weather events and one wet weather event at the 10 TSS sampling locations. For the wet weather event, 10 discrete samples were taken during rise, peak, and fall of the rainfall.

3.6 POLLUTOGRAPHS

Water quality constituents (TSS and Suite B) were measured at the Del Amo Lateral and Torrance Lateral storm drains during the wet weather event on February 27-28, 2006. The sampling location, as well as the drainage area for each storm drain is shown in Figure 3.7.

3.7 DYE TRACER STUDY

The dry weather dye tracer study was conducted on May 17, 2005. Rhodamine dye was released at the lower end of the Dominguez Channel to evaluate the dispersion and mixing characteristics between the Consolidated Slip and Vincent Thomas Bridge and in the western portion of the Cerritos Channel (Figure 3.8). Three dye patches were also released prior to the channel dye release to capture the complex mixing pattern in the East Basin at the intersection of the Consolidated Slip and Cerritos Channel. Continuous sampling of dye concentrations were made at three locations (Berth 200G, Berth 206, and Berth 173) using an in-situ fluorometer. In addition, automatic ISCO 6712 programmable samplers were used to collect batch samples at 1-hour intervals over 24 hours. Twenty-one vertical dye profiles corresponding to the salinity distribution profiles in the lower estuary were also obtained. Spatial distributions of the dye concentration were also analyzed by periodic aerial photographs.

Figure 3.6 Estuary Water Quality Sampling Locations

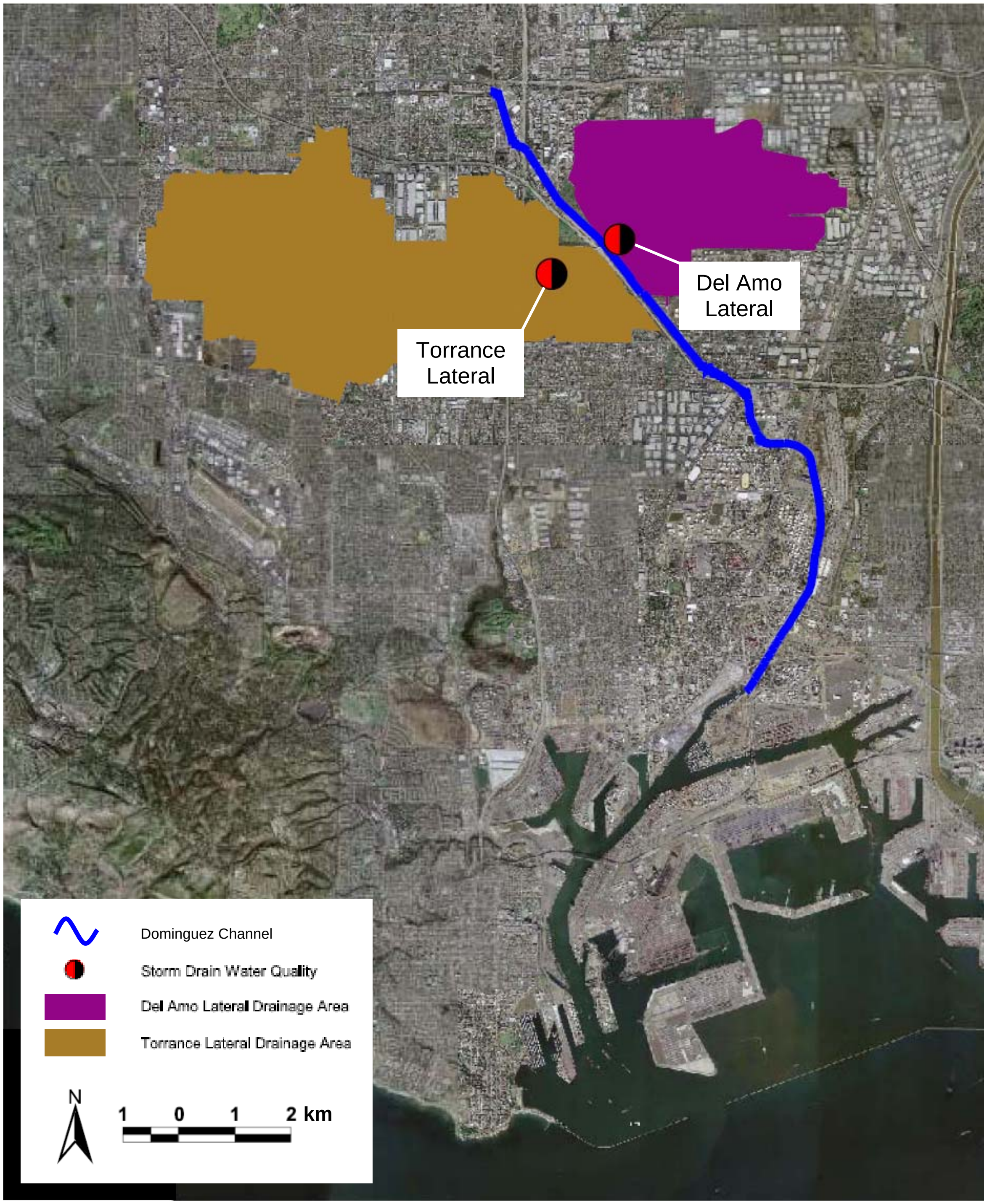

Figure 3.7 Pollutograph Sampling Locations

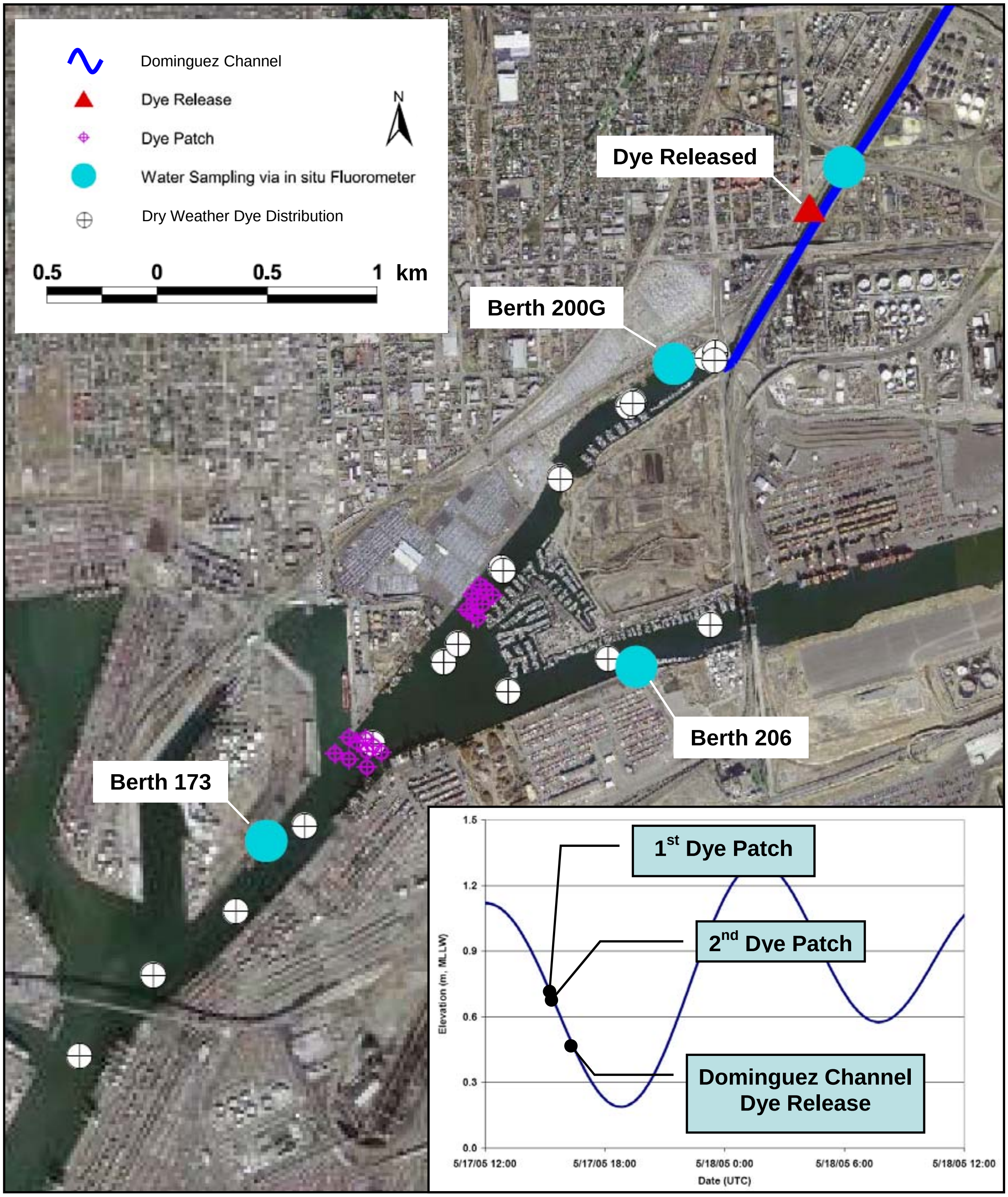

Figure 3.8 Dry Weather Dye Release and Sampling Locations

3.8 METEOROLOGICAL DATA

Meteorological data used for the DCEM calibration were obtained from several gages as part of the Field Program, as well as from on-going monitoring.

As part of the Field Program, a meteorological station was set up in the Wilmington community, above Anaheim Street between Bayview and Neptune. The location of the Wilmington meteorological station is shown in Figure 3.9, together with other wind gage locations in the vicinity of the Study Area. Wind speed, wind direction, wind gust, air temperature, relative humidity, dew point temperature, solar radiation, and barometric pressure were measured continuously between February 26, 2005 and March 22, 2006 at the meteorological station. These data were measured at a 15-minute interval with the exception of the period between February 26 and April 26, 2005, when data were measured at a 1-hour interval.

Additional meteorological data were obtained from the NOAA National Ocean Service (NOS) real-time oceanographic monitoring data. The Physical Oceanographic Real-Time System (PORTS®) measures and disseminates observations and predictions of water levels and meteorological parameters. There are seven meteorological stations and one water level gage within the Harbor Area. The data monitored at each station are summarized in Table 3.5.

Table 3.5 PORTS® Stations

STATION NAME	STATION ID	DATA MONITORED
Angels Gate	m0203	Wind speed, direction, and gust Air temperature and pressure
Badger Avenue Bridge	m0201	Wind speed, direction, and gust
Berth 161	m0202	Wind speed, direction, and gust
Los Angeles (Berth 60)	9410660*	Water level and temperature Air pressure
Pier 400	m0200	Wind speed, direction, and gust
Pier F	m0100	Wind speed, direction, and gust
Pier J	m0102	Wind speed, direction, and gust
Pier S	m0101	Wind speed, direction, and gust

* *NOAA bench mark tide gage*

Figure 3.9 Meteorological Stations

3.9 ARTESIA POLLUTOGRAPH

In addition to the DCEMS Field Program, the Port collected additional water quality and flow data along the Dominguez Channel at Artesia Boulevard during the dry and wet weather sampling events. This sampling location is shown in Figure 3.10. The drainage area at the Artesia sampling location accounts for about one-third of the Dominguez Channel Watershed. These data were used to estimate the loadings (i.e., storm drain sources) from the watershed for the DCEM calibration.

Sampling events were conducted for two dry weather events (May 16-17, 2005 and August 17-18, 2005) and two wet weather events (February 27-28, 2006 and March 17, 2006). Samples were measured for Suite B conventional parameters and metals, total PAHs, total aroclors, detectable DDTs, and other pesticides. Flow data were based on the Los Angeles County Department of Public Works flow gage.

For both dry weather events, 3-hour composite samples were taken over a 24-hour period for a total of 8 composite samples. Each composite sample consisted of 12 draws at a 15-minute interval. For the February 2006 wet weather event, a total of 10 composite samples were collected, two prior to and two after the rain event and six during the rain event. Five composite samples were collected during the March 2006 sampling event, one prior to and one after the rain event and three during the rain event. Each composite consisted of six draws at even intervals, but the time frame for each composite sample varied.

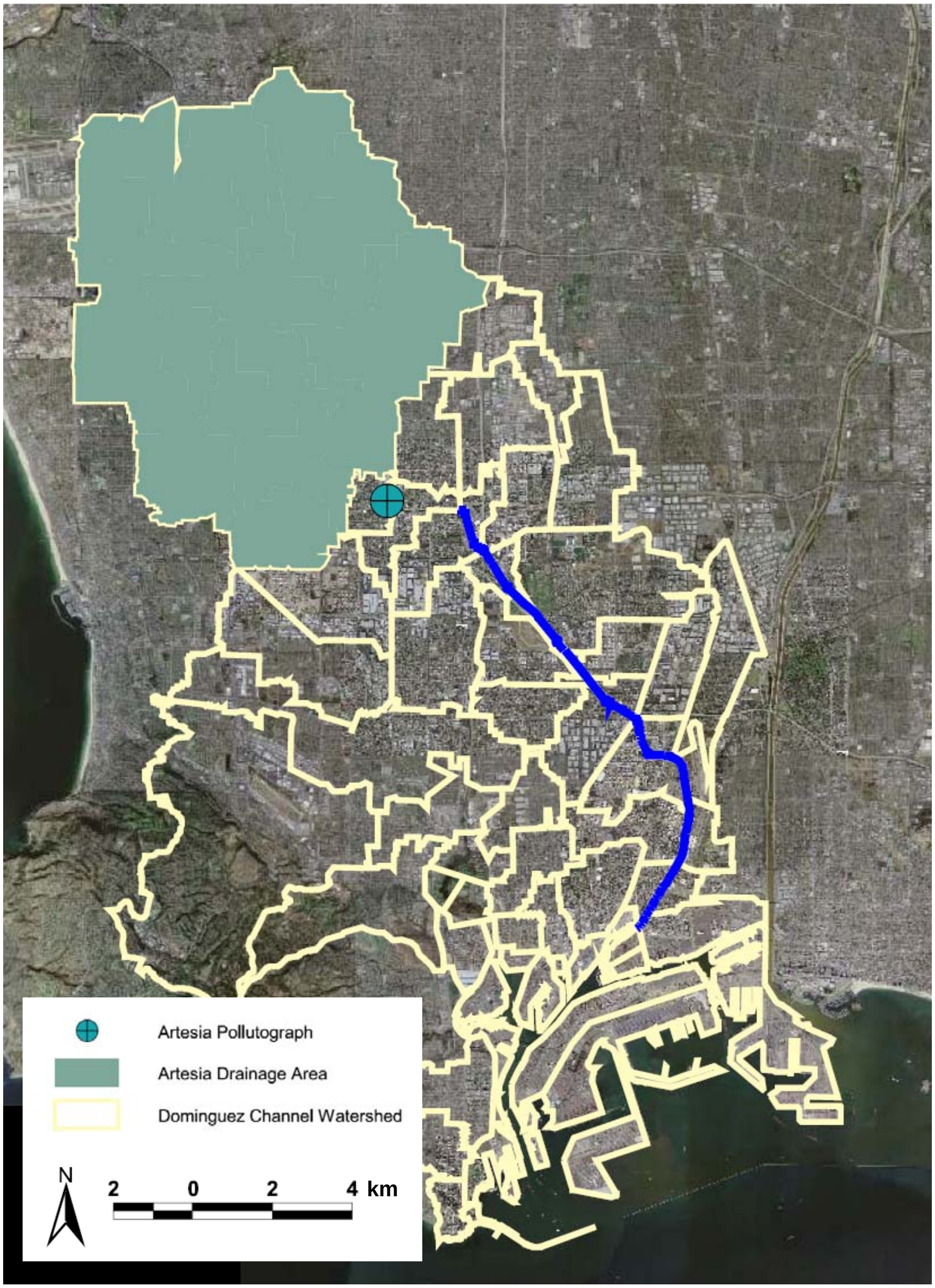

Figure 3.10 Artesia Pollutograph Sampling Location and Drainage Area

4. DRY WEATHER CALIBRATION

4.1 OVERVIEW

The DCEM dry weather calibration involves the selection of the model parameters that will provide the “best” comparison between model predicted hydrodynamics (water elevation and velocity) and water quality (salinity, dye, sediment, and metals) and field measurements. The simulation of hydrodynamics and water quality are inherently linked; for example, hydrodynamics influences salinity, but salinity also influences the hydrodynamics. Hence, the “best” calibrated model for hydrodynamics may not necessary produce the “best” calibrated results for all of the water quality constituents. The calibrated DCEM model is one that produces the overall best results for both the hydrodynamics and water quality for the study area. With the dynamic linkage between hydrodynamic and water quality, a layered approach was used in the calibration procedure, in which an initial “base case” was first developed to evaluate input and boundary conditions, followed by an evaluation of the hydrodynamic model parameters; then the sediment and metal model parameters in an iterative manner.

In summary, the DCEM dry weather calibration began with the selection of the dry weather calibration period and input and boundary conditions for an initial “base case” simulation, which are described in the next section. Next, input tide and wind conditions were evaluated using water surface elevations and velocities, followed by the calibration of the model parameters. Hydrodynamic model parameters (horizontal mixing, vertical mixing, and roughness height) were calibrated first, as they drive the physical processes within the estuary. These parameters were calibrated using velocity, salinity, and dye field data. Salinity and dye were used before the other water quality data since the data covers a more extensive spatial and temporal distribution. After selecting the hydrodynamic model parameters, the DCEM was calibrated for sediment based on TSS measurements and then the metal partition coefficients were adjusted to fit the metal field data. The selection of the final “calibrated” model parameters were based on the best overall fit between the field data and model predictions.

The initial setup for dry weather calibration is provided in Section 4.2, followed by the discussions for the selection of calibration parameters in Section 4.3. The comparison of the final “calibrated” model results with field measurements are provided in Section 4.4.

4.2 DRY WEATHER DCEM CALIBRATION SETUP

4.2.1 Calibration Period Selection

A timeline of the field data, shown in Figure 4.1, was used to determine the most appropriate dry weather calibration period which was selected to include the following:

- Continuous dry weather (i.e., no rainfall)
- Continuous ADP data at all four locations
- May 17, 2005 estuary water quality sampling and dye study for the calibration period
- Sufficient time to capture the seasonal variability of tidal conditions

As shown in the figure, rainfall records from the Los Angeles and Long Beach Airports showed sporadic rainfall in February through the beginning of May, with a continuous dry period between May 9 and September 20, 2005. The mounting depth of the ADP at Berth 200G was adjusted on May 16, 2005 due to a significant reduction in acoustic signal strength, which was suspected to be caused by sedimentation in the middle of the channel. Hence, data collected at Berth 200G prior to May 16, 2005 were not suitable for model calibration. Taking all these factors into consideration, the dry weather calibration period was selected to begin on May 17, 2005 to include the estuary water quality sampling and dye tracer study. A 30-day calibration period was selected since it is long enough to cover the spring and neap tides, as well as requiring a practically reasonable computation time (19 hours and 30 minutes per 60-day simulation that also includes a 30-day spin-up period). A summary of the available field data that were used for the dry weather calibration is provided in Table 4.1.

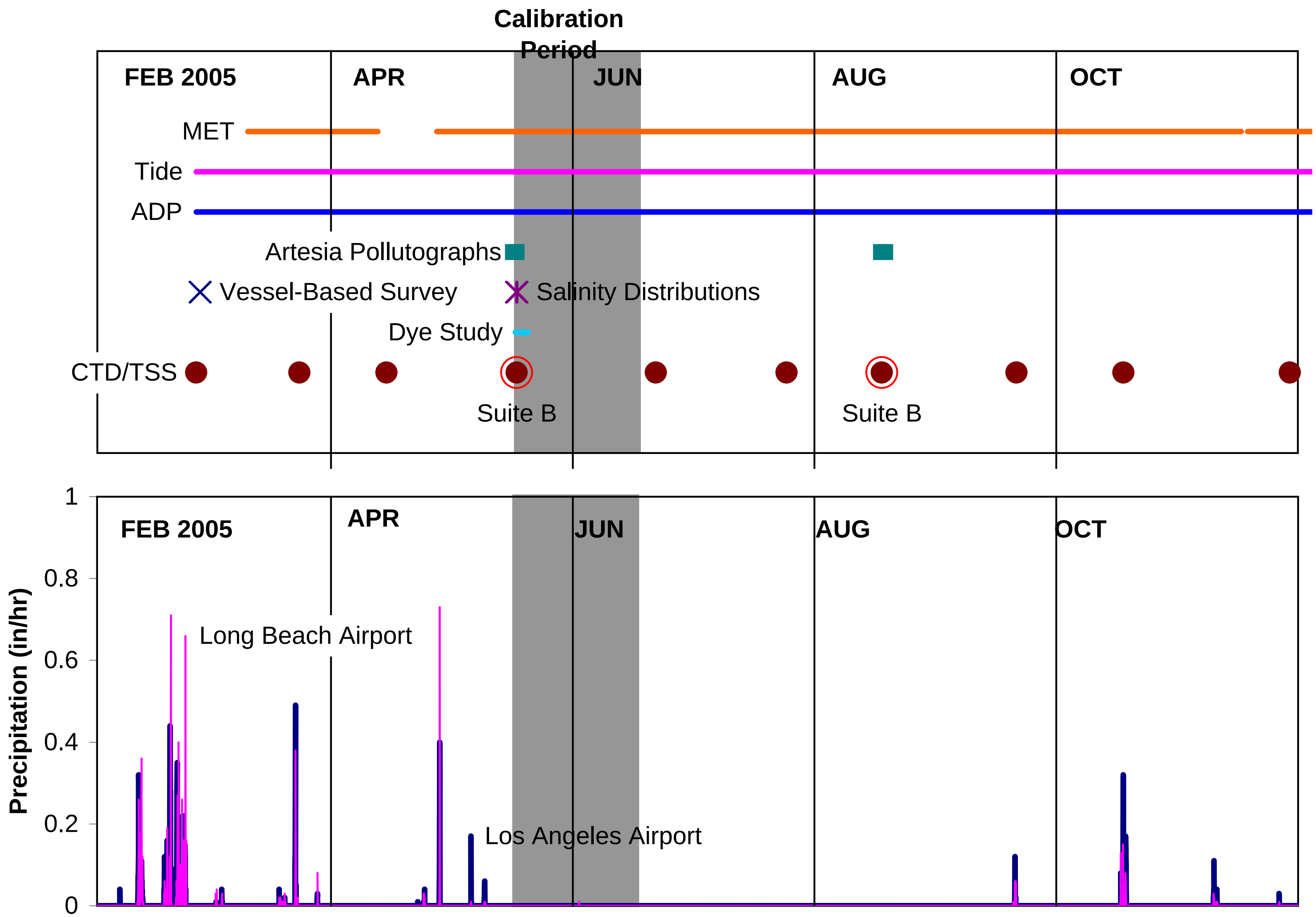

Figure 4.1 Dry Weather Calibration Field Data Timeline

Table 4.1 Dry Weather Calibration Model and Field Data Comparison Summary

MODEL PREDICTIVE PARAMETER	COMPARISON	CHANNEL LOCATIONS	HARBOR LOCATIONS	FIELD DATA
Water Surface Elevation	5/17/05 – 6/17/05	1	3	Fixed ADP
Velocity	5/17/05 – 6/17/05	1	3	Fixed ADP
Velocity Vertical Profile	Peak ebb and flood during neap tide on 5/17/05; Peak ebb and flood during spring tide on 5/24/05	1	0	Fixed ADP
Salinity Vertical Profile	Single measurement on 5/17/05	2	2	Estuary CTD
	Periodically on 5/17/05	0	21	Salinity Distribution
Dye	5/17/05 – 5/20/05	0	3	Dye Study
Dye Vertical Profile	Periodically on 5/17/05	0	21	
Sediment	Single sample on 5/17/05	2 (2 depths)	2 (3 depths)	Estuary Water Quality (TSS and Suite B sampling)
Chromium (Cr)				
Copper (Cu)				
Lead (Pb)				
Zinc (Zn)				

4.2.2 Ocean Boundary Conditions

The selection of the DCEM grid was discussed previously in Section 2.4.1. Figure 4.2 shows this selected model grid, the ocean boundary where a tidal boundary condition is specified, as well as other boundary locations where inflows and pollutant concentrations are specified. The figure also shows the Artesia location where pollutographs were collected to define the dry weather flow, sediment and metal concentrations for model input, the meteorological station setup for the DCEMS to collect site-specific wind data, and the NOAA LA Outer Harbor tide gage.

The tidal water elevations obtained from the NOAA Los Angeles, Outer Harbor gage (9410660) were used to define the water elevations at the ocean boundary shown in Figure 4.2. The tidal datums for this station are shown in Table 4.2. Raw 6-minute tide data were filtered to remove the high frequency noise to produce the water elevation ocean boundary conditions. The raw and filtered tide record during the dry weather calibration period is shown in Figure 4.3. The figure also shows a statistical comparison of the dry weather calibration tide compared to a full one-year tide record to show that the 30-day calibration

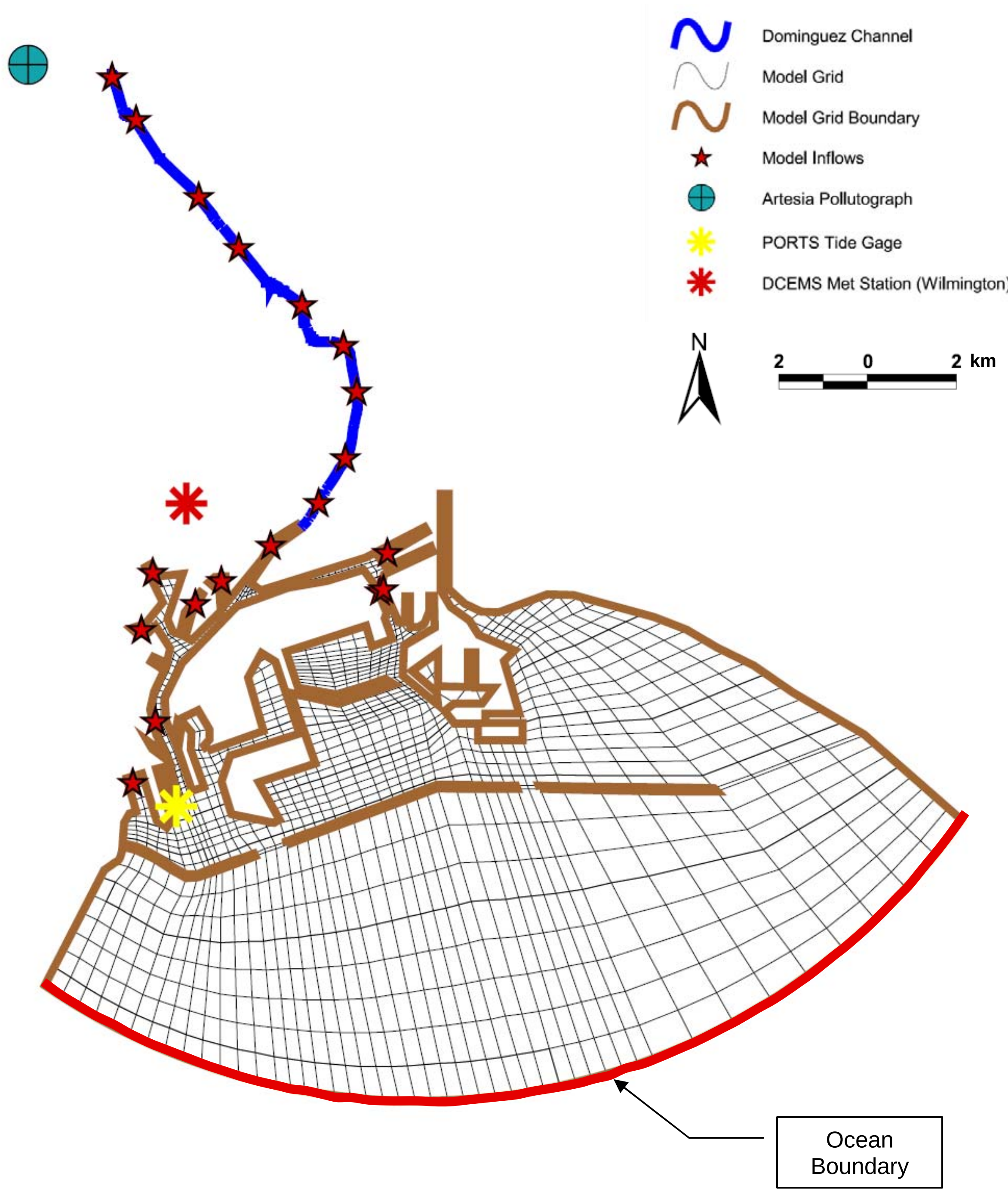

Figure 4.2 DCEM Model Input Locations

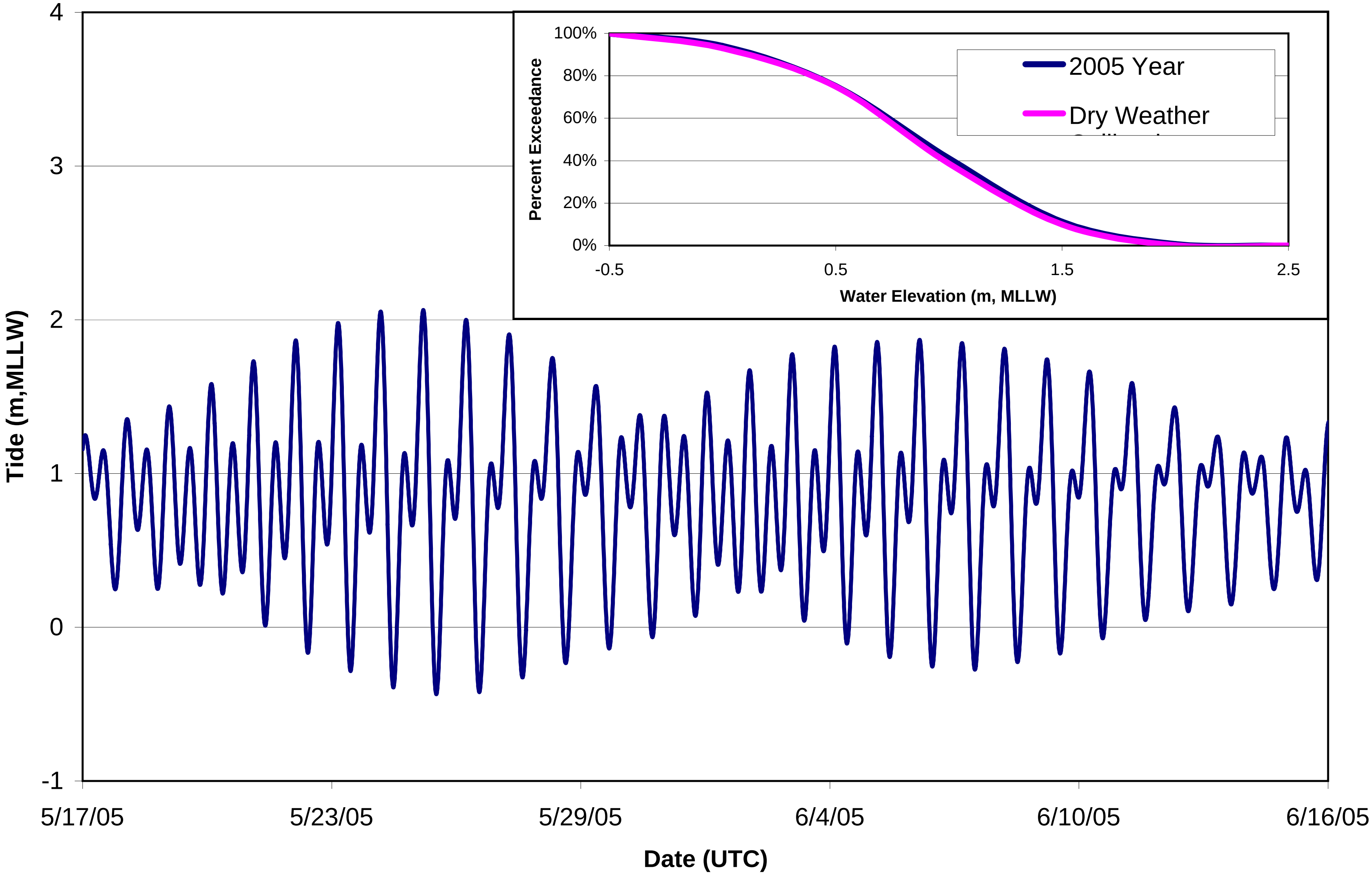

Figure 4.3 Dry Weather Calibration Tide

period was long enough to capture the seasonal tide variability. The tide record during the dry weather calibration period shows a statistically similar distribution compared to the one-year tide record.

Table 4.2 Tidal Datums for Los Angeles, Outer Harbor (Tidal Epoch 1983 – 2001)

TIDAL DATUM	ELEVATION (M, MLLW)
Highest Observed Water Level (01/27/1983)	2.384
Mean Higher High Water (MHHW)	1.674
Mean High Water (MHW)	1.449
Mean Tide Level (MTL)	0.868
Mean Sea Level (MSL)	0.861
Mean Low Water (MLW)	0.287
North American Vertical Datum-1988 (NAVD)	0.062
Mean Lower Low Water (MLLW)	0.000
Lowest Observed Water Level (12/17/1933)	-0.832

Source: NOAA 2003

An initial model simulation was conducted to evaluate whether the tide data from the inner harbor can be used directly as the model ocean boundary without minor adjustment to the tidal amplitudes and phases. This is achieved by comparing the model predicted water surface elevations at the LA Outer Harbor with the measured water elevations at the gage location. A comparison of the LA Outer Harbor gage data with the model predicted water surface elevations at the gage location for the 30-day dry weather calibration period is shown in Figure 4.4. In addition to the time series comparison, the daily tidal peaks (two highs and two lows) were compared. Since the model predicted water elevations match perfectly with the measurements at the gage location, it was determined that the tide ocean boundary condition is suitable and no tidal phasing or amplitude adjustments are necessary.

4.2.3 Flow and Pollutant Inputs

For the DCEM dry weather calibration simulations, fresh water inflow and pollutant concentrations are specified at the 19 input locations shown previously in Figure 4.2. The dry weather inflows are the runoff entering the estuary from storm drains commonly associated with urbanized areas. Dry weather inflows were represented by a constant typical dry weather flow for the region. A relationship between dry weather flow and urban land uses developed by SCCWRP (unpublished data) was used to define the dry weather flows for DCEM. In short, the dry weather flows weather inflow was proportional to the drainage area of each simulated storm drain and listed in Table 4.3. This assumption for dry weather flow is consistent with prior and on-going TMDL developments for Ballona Creek,

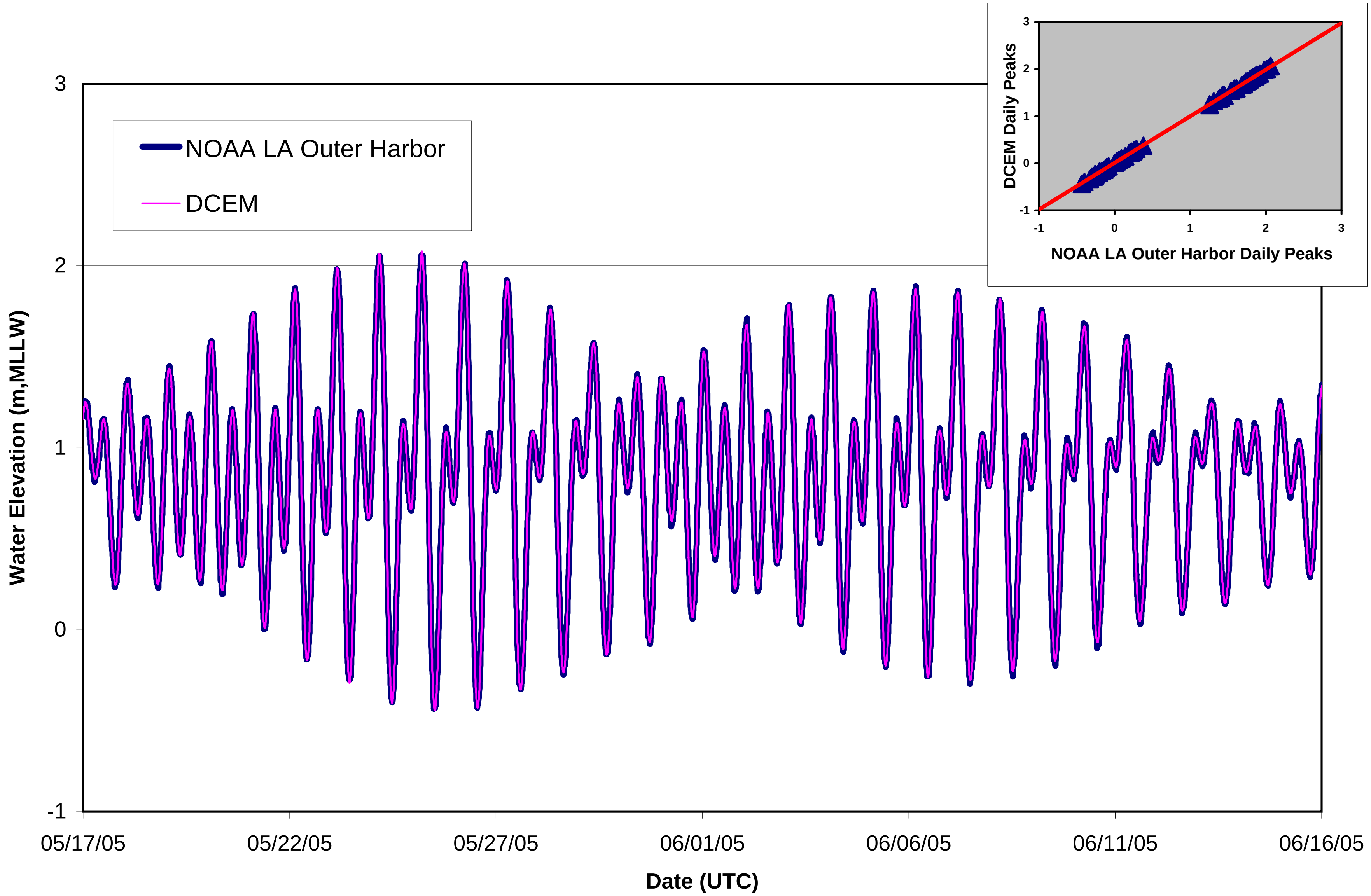

Figure 4.4 Comparison of DCEM Predicted and Measured Water Elevations at LA Outer Harbor

Los Angeles River, San Gabriel River, Los Angeles and Long Beach Harbors, and San Pedro Bay. As mentioned earlier, these dry weather flows are applied to the 19 locations shown in Figure 2.5.

Table 4.3 Dry Weather Inflows

STORM DRAIN	DRAINAGE AREA (km^2)	DRY WEATHER FLOW (m^3/s)
Vermont Avenue	103.36	0.2183
Victoria Street	15.19	0.0320
Gladwick Street	11.77	0.0249
213th Street	30.32	0.0639
223rd Street	8.11	0.0171
Johns Manville Street	5.90	0.0125
Sepulveda	4.34	0.0091
PCH	2.07	0.0043
Anaheim Street	5.14	0.0108
Blinn Avenue	4.60	0.0097
Slip 5	1.60	0.0034
Slip 1	1.46	0.0031
West Basin	66.99	0.1413
Battery Street	15.27	0.0321
Main Channel	1.07	0.0023
West Channel	14.29	0.0302
Channel No. 2	3.34	0.0070
Pier 300 & Pier T	0.71	0.0015
Pier D - J	1.10	0.0023

The dry weather inflows were assumed to be fresh water (e.g., zero salinity) with no dye concentrations. Concentrations of the simulated pollutants associated with the dry weather flows were obtain from field data. Concentrations of cohesive sediment, chromium, copper, lead, and zinc were specified based on the average concentrations from the May 2005 Artesia sampling and are summarized in Table 4.4.

Table 4.4 Dry Weather Calibration Storm Drain Pollutant Concentrations

POLLUTANT	UNITS	CONCENTRATION
Cohesive Sediment	mg/L	1.4
Noncohesive Sediment	mg/L	0.0
Chromium	µg/L	2.6
Copper	µg/L	8.2
Lead	µg/L	0.3
Zinc	µg/L	20.8

4.2.4 Initial and Boundary Concentrations

This section discusses the selection of the initial and boundary concentrations used for salinity, sediments, dye and metals (chromium, copper, lead and zinc) for DCEM calibration.

Salinity

The salinity of the ocean boundary and initial salinity concentrations were selected based on measurements from prior studies for the study area. Two prior studies of the Harbor Area contained vertical salinity profiles measurements conducted in 2000. One sample was located beyond the breakwater, where seven measurements taken between August and December 2000 (ACTA 2001) showed a uniform vertical salinity profile at about 33.5 PSU. This was consistent with other uniform salinity profiles taken at Angels Gate and in the Harbor Area, as well as other harbor measurements from the other study (Port of Long Beach 2002). The salinity data also showed several general trends, 1) salinity variations occurred near the surface, while bottom salinity levels tended to stay relatively constant, 2) bottom salinity concentrations in the Harbor Area were similar to that beyond the breakwater, and 3) salinity profiles in the Harbor Area were more uniform compared to salinity profiles near the Estuary.

The ocean boundary and initial salinity concentrations were specified as 33.5 PSU. However, salinity profiles have spatial, vertical, and temporal variations. The salinity distribution at the start of the calibration period was established by simulating a “spin-up” period prior to the calibration period. The “spin-up” starts with the uniform salinity concentration, as the model simulates the tide and low flows the salinity levels begin to vary vertically. Figure 4.5 shows and example of salinity fluctuations in the Dominguez Channel at Sepulveda over a 60-day simulation period. As shown in the figure, it is determined that a 30-day “spin-up” was sufficient for the salinity to reach a quasi-steady state. For the dry weather calibration, the model simulation was started 30 days before the calibration period using the corresponding data for the wind and tide conditions.

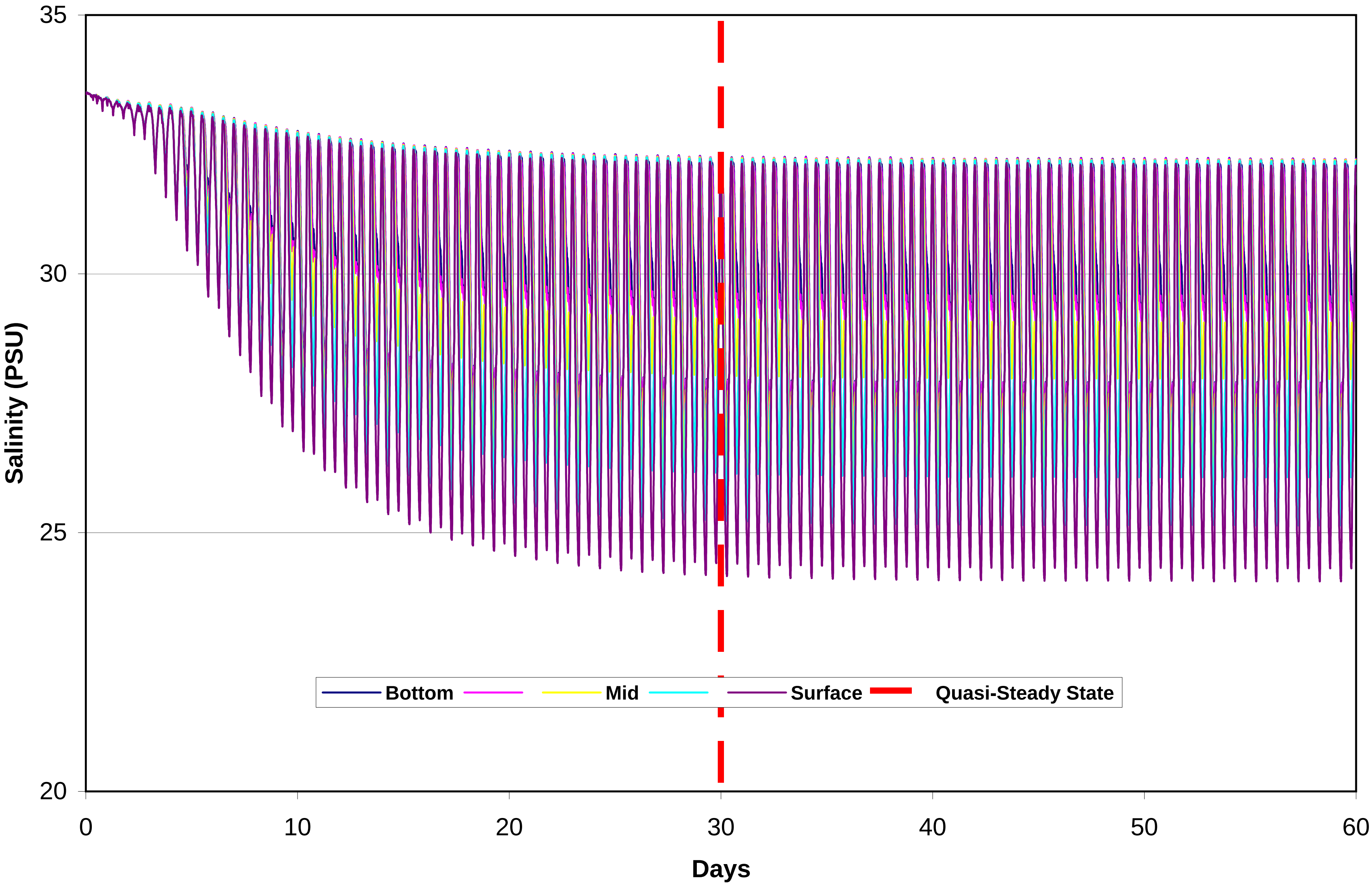

Figure 4.5 Salinity Fluctuations During DCEM Spin-up

Dye

The dry weather dye study consisted of the main dye release in the Dominguez Channel, as well as two dye patches (see Figure 3.8 for these release locations). For the dye release, 47 liters of Rhodamine dye was released over a 24-minute period near E. I Street. The dye was a 20% percent solution by weight with a specific gravity of 1.13 for a total release of 10.62 kg. This dye release was simulated in the model by specifying the inflow and concentration at the release location over a 24-minute period.

For each dye patch, 0.15 liters of dye was released at nine locations (prior to the main dye release) in a 3-by-3 grid for a total of 0.0339 kg. These dye patches were simulated in the model as 18 individual dye releases by specifying an inflow and concentration over a short duration release time.

Cohesive and Noncohesive Sediments

Initial concentrations and boundary conditions for cohesive and noncohesive sediment were required for both the water column and sediment bed. The initial sediment concentrations in the water column were determined in the same methodology as the salinity, where a constant initial concentration was used then allowed to fluctuate during the 30-day “spin-up” period. A constant initial concentration of 3.9 mg/L for cohesive sediment was specified based the average TSS concentration for dry weather monthly TSS measurements in the estuary made in April, May, June, July, August, and November. The constant initial concentration for noncohesive sediment was 0 mg/L since noncohesive sediment was simulated for the sediment bed characteristics. These initial concentrations for cohesive and noncohesive sediment were also used for the ocean boundary conditions.

The sediment bed was specified with four uniform bed layers. For the surface layer of the sediment bed, the initial sediment conditions were specified as sediment fractions (cohesive fraction plus noncohesive fraction equals one). The bed sediment fractions of 70% sands and 30% fines for the Dominguez Channel were based on sediment grain size data taken in 2000 (AMEC 2005), which was the most recent complete set of data including seven sample locations along the channel. The sediment bed in the Consolidated Slip was specified at 10% sands and 90% fines, while the Cerritos Channel was set at 30% sands and 70% fines based on sediment grain size data collected for the Ports of Long Beach and Los Angeles Biological Baseline Study (Port of Long Beach 2002). For the rest of the model domain, the sediment bed surface layer was specified as 100% sands. The remaining three sediment layers were also specified as 100% sands.

Metals

Initial concentrations and boundary conditions for chromium, copper, lead, and zinc were required for both the water column and sediment bed. For the DCEM, these concentrations were specified based on available data. The constant initial total metal concentrations in the water column (at the start of the spin-up period) were taken as the average concentration of data taken in September 2005 and May 2006 from the Port of Los Angeles Enhanced Water Quality Project monitoring stations (27 locations). The respective chromium, copper, lead, and zinc concentrations were 1.8, 1.7, 1.1, and 10.2 µg/L. These concentrations were also used as the ocean boundary conditions.

For the sediment bed, metal concentrations were only specified in the surface bed layer. The initial metal concentrations sediment bed for the Dominguez Channel were specified based on sediment quality data from the Dominguez Channel Sediment Investigation, which contained data from seven channel samples locations taken between 1994 and 2004 (AMEC 2005). The average metal concentrations in mg/kg sediment were then converted to µg/L. The initial metal concentrations in the sediment bed were 67.91, 95.33, 179.25, and 384.06 µg/L for chromium, copper, lead, and zinc, respectively. For the Consolidated Slip, the initial metal concentrations in the sediment bed were based on data from the Consolidated Slip Restoration Project (AMEC 2002). Chromium, copper, and lead concentrations were based on the average sediment quality data. The initial zinc concentration in the sediment bed was from average sediment quality data from 16 locations at various sediment bed depths (AMEC 2003). For the rest of the model domain, the sediment bed was specified with no metal concentrations.

4.2.5 Wind Conditions

A meteorological station was set up in Wilmington as part of the DCEMS Field Program to collect wind data for the project (shown previously in Figure 4.2. A model simulation was conducted applying the wind data collected at this station uniformly over the entire model domain. As shown in Figure 4.6, when comparing the model predicted velocities at the four ADP locations with the field data, it was found that the model results match well with field data for the S. Pacific location along the Dominguez Channel, but did not as well for the other three locations further into the harbor areas. At Berth 206, the field data indicates that there is a net flow towards west (in the figure, positive velocity flows towards east and negative velocity flows towards west) along Cerritos channel during the calibration period, while the model predicts a more or less balanced flow. Similarly, at Berth 173, the field data shows an ebb dominant flow while the model shows a more or less balanced flood and ebb flows.

This initial finding led to a more careful examination of the effect of wind to the flows in the study area. A comparison of the wind conditions (shown as wind roses) at Wilmington with other meteorological stations throughout the Harbor Area is shown in Figure 4.7. As shown in the figure, the dominant wind direction at Wilmington was from northwest or southeast, while the dominant wind directions in the Harbor Area locations were mainly from south-southwest. The wind patterns indicate that during the calibration period, the wind might have generated a counter-clockwise circulation in the Harbor Area, moving water in the

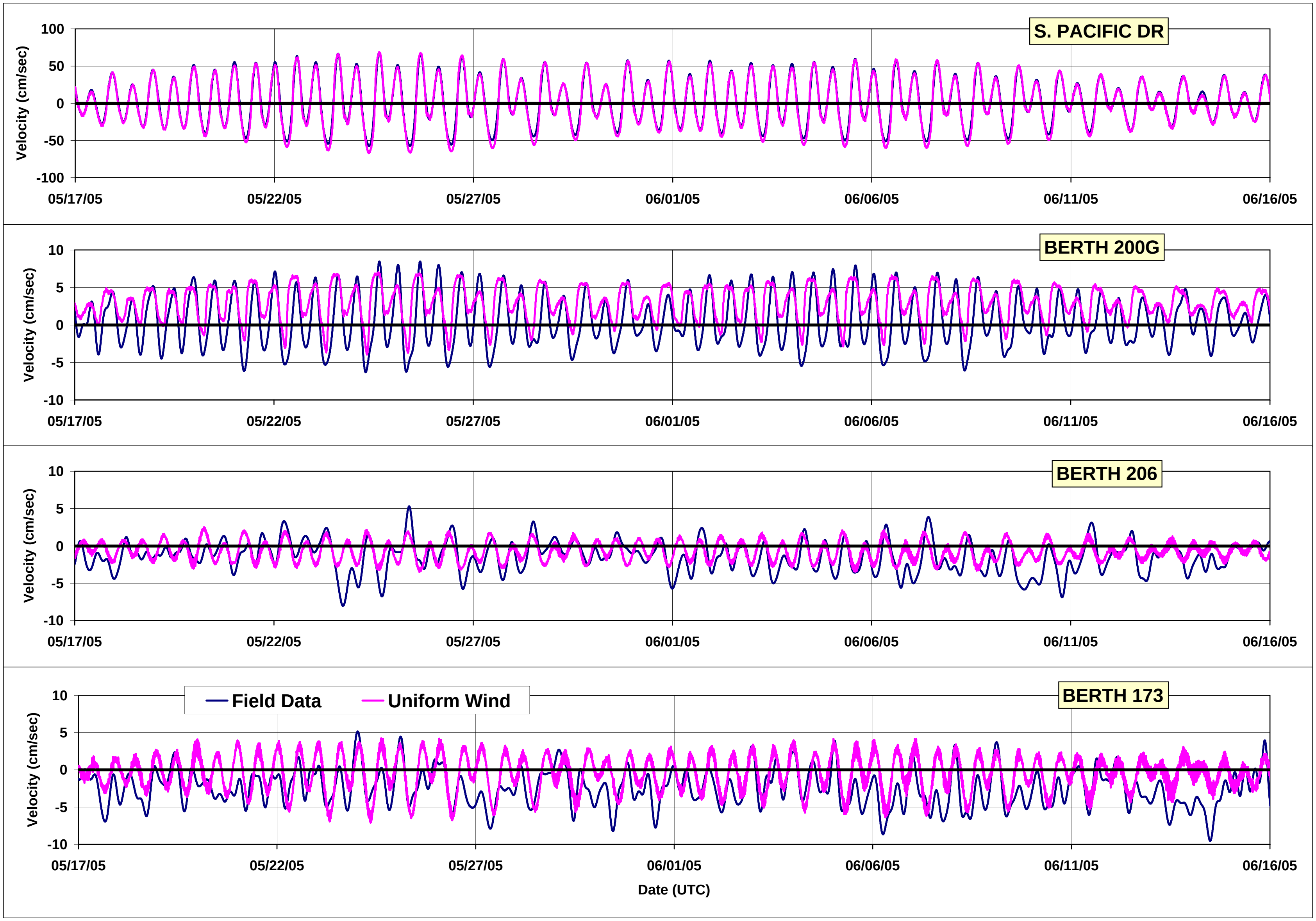

Figure 4.6 Comparison of Field Data and DCEM Predicted Velocities Using Uniform Wind Conditions

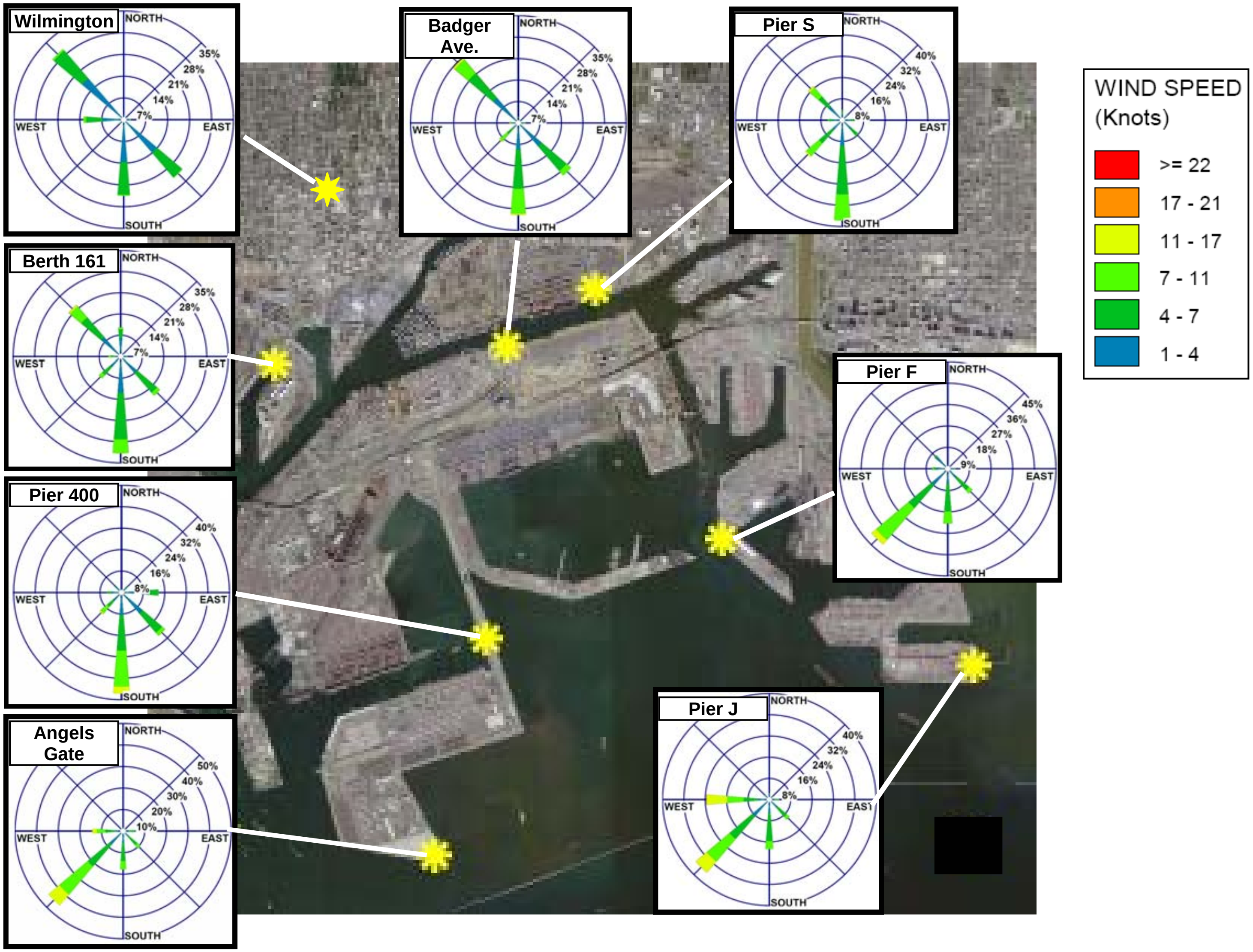

Figure 4.7 Wind Roses (May 17 – June 16, 2005) for Meteorological Stations

Cerritos Channel from east to west, hence causing the ebb-dominant flow observed at Berth 206 and Berth 173.

The impact of the harbor-wide wind pattern on the flow in the Estuary was evaluated by comparing the initial model simulation with uniform wind with a simulation with spatially varying wind conditions. Spatially varying wind conditions were applied based on an inverse distance weighting of the meteorological stations. Wind conditions from each meteorological station were used for the model grid cells located within a 3-km radius of the station or area of influence, which is shown in Figure 4.8. For model grid cells not located within the area of influence for any station, the wind conditions were specified based on the closest meteorological station. A comparison of the model predicted velocities using a uniform and a spatially varying wind conditions, along with the field data velocities, are shown in Figure 4.9. The different wind conditions do not influence the model predicted velocities in the Dominguez Channel at S. Pacific Drive. In addition, the model predicted velocities agree well with the field data at S. Pacific Drive. At Berth 200G, there are minimal difference in the model-predicted velocities between the uniform wind velocities and spatially varying wind conditions. However, the use of a spatially varying wind does however impact the model predicted velocities at Berths 206 and 173. At Berth 206, the model now shows a net flow from east to west, matching with the field data. Similarly, at Berth 173, the model predicted velocities show an ebb dominant flow matching with the field data.

4.3 DCEM PARAMETER CALIBRATION

As mentioned earlier, the calibration of the DCEM involves the selection of the model parameters that provide the “best” comparison between model predictions and field data. The model parameters being evaluated include:

- Horizontal and vertical viscosity/diffusivity,
- Roughness height,
- Cohesive sediment settling velocities, and
- Metal equilibrium partition coefficients

As discussed earlier, an iterative approach was adopted in the calibration process to seek the “best” set of model parameters. Thus, numerous combinations of the model parameter sets have been evaluated. Instead of presenting all the simulation results, the following sections show selective results to illustrate the effects of each of the model parameters listed above.

Figure 4.8 Inverse Distance Weighting for Spatially Varying Wind Conditions

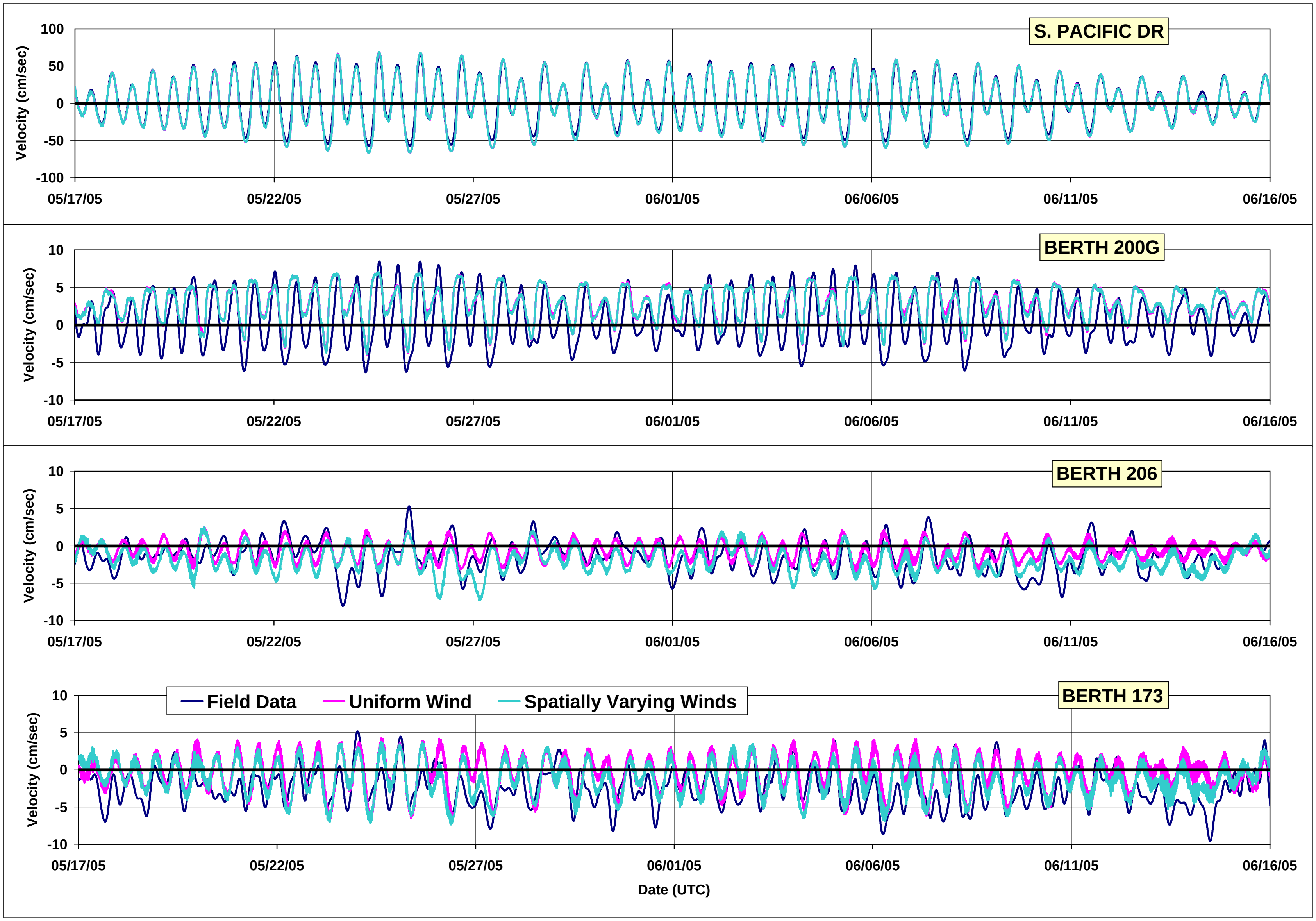

Figure 4.9 Comparison of Field Data and DCEM Predicted Velocities Using Uniform and Spatially Varying Wind Conditions

In the following section, the selection of the initial model parameters is discussed, followed by a discussion of the evaluation of the model parameters in Section 4.3.2. In addition to these physical model parameters, the EFDC model has a numerical model feature, "anti-diffusion" which can be used to suppress numerical diffusion. The effect of whether to turn this feature "on" or "off" is also evaluated and discussed in Section 4.3.3.

4.3.1 Initial Model Parameters

The "base case" simulation was conducted with a set of initial model calibration parameters selected based on site conditions, literature values, and the modeler's experience. These model parameters include the horizontal eddy viscosity, maximum vertical kinematic viscosity and diffusivity, roughness height, cohesive sediment settling velocity, and metal equilibrium partition coefficients.

The horizontal mixing is based on the Algebraic/Smagarinsky model. The model calibration parameter for horizontal mixing of both momentum and mass is the eddy viscosity, which is treated as a constant value used to smooth cell to cell spatial oscillations. Vertical mixing is based on the Mellor-Yamada level 2.5 turbulence closure model. The calibration parameters for vertical mixing are the maximum vertical kinematic viscosity and vertical eddy diffusivity based on a modified Mellor-Yamada turbulence closure model (Mellor and Yamada 1982 and Galperin et al 1988).

The roughness height is the logarithmic boundary layer thickness. This calibration parameter is similar in concept to a friction factor, such that the larger the number the greater the resistance to flow. The roughness height primarily influences the vertical velocity profile, as well as the tidal velocity phasing. This parameter can be used to account for bathymetric irregularities within a model grid cell. In general, the roughness height for natural, river channels range between 0.03 and 0.9 m (USACE 1991). The initial roughness height was specified uniformly at 0.03 m.

Sediment settling velocity for cohesive sediment influences the amount of sediment that stays in suspension in the water column. Due to the limited amount of sediment data for the water column, a constant settling velocity of 1E-5 m/sec was initially selected.

Equilibrium partition coefficients control the fractionation of metals between dissolved and particulate and are dependent on the sediment concentration. Metals with higher equilibrium partition coefficients have a stronger affinity for sediment, resulting in higher particulate concentrations. These coefficients vary for each metal, but in general range between 1E-4 to 0.1 L/mg (based on copper, zinc, cadmium, chromium, lead, and nickel data from 15 rivers) and are typically less in the sediment bed (Chapra 1997). The equilibrium partition coefficients were initially specified based on the estuary water quality sampling data of TSS, dissolved metal, and particulate metal concentrations from both dry weather sampling events. The equilibrium partition coefficients in the sediment bed were set at one-tenth that of the water column.

The selected initial model parameters are summarized in Table 4.5.

Table 4.5 Initial Dry Weather Model Calibration Parameters

INITIAL MODEL PARAMETER	UNITS	VALUE	INFLUENCE
Horizontal Eddy Viscosity	m^2/sec	1E-6	Salinity, dye, sediment, and metals
Maximum Vertical Kinematic Viscosity	m^2/sec	1E-3	Salinity, dye, sediment, and metals
Maximum Vertical Eddy Diffusivity	m^2/sec	1E-3	Salinity, dye, sediment, and metals
Anti-Diffusion Corrections	--	Off	Salinity, dye, sediment, and metals
Roughness Height	m	0.03	Velocity vertical profiles
Sediment Settling Velocity	m/sec	1E-5	Sediment and metals
Equilibrium Partition Coefficient	L/mg	Cr 0.4 Cu 0.1 Pb 1.0 Zn 0.06	Total, dissolved, and particulate metals

4.3.2 Evaluation of Model Parameters

Horizontal and Vertical Mixing

Many simulations were conducted to evaluate the horizontal and vertical mixing characteristics by comparing time series velocities and dye concentrations, as well as vertical velocity, salinity, and dye profiles. The horizontal eddy viscosity, maximum vertical kinematic viscosity and diffusivity, were the model parameters that govern horizontal and vertical mixing. These parameters and the numerical “anti-diffusion” feature cannot be individually calibrated, thus combinations of model parameters were evaluated. The evaluation of “anti-diffusion” is discussed separately in Section 4.3.3.

In evaluating the model parameters, the horizontal eddy viscosity was varied between 1E-4 and 1E-6 m^2/sec. The maximum vertical kinematic viscosity ranged from 1E-3 to 5E-5 m^2/sec and the maximum vertical diffusivity from 1E-5 to 1E-3 m^2/sec. The combinations of model parameters were adjusted to find the “best fit” to all the field data. For example, the combination of parameters that provided the best match to the velocity data did not necessary provides the best match for the salinity and/or dye data.

An example of the effect of the maximum vertical viscosity on velocity and salinity is provided in Figure 4.10. This example compares the model predicted velocities and salinity with the maximum vertical viscosity of 1E-4 and 1E-2 m^2/sec. The results illustrate that the use of different vertical viscosities will result in different model predicted velocities and salinity. In this example, the larger the vertical viscosity (1E-2 m^2/sec) provides a better match with the field measured velocities compared to a smaller vertical viscosity (1E-4 m^2/sec). However, the smaller vertical viscosity provides a better match in salinity than the higher vertical viscosity.

Figure 4.11 provides an example of the effect of the maximum vertical diffusivity on the model predicted salinity profiles. This example compares vertical diffusivities of 1E-4 and 1E-3 m^2/sec. As shown in the figure, a larger vertical diffusivity will produce better vertical mixing, hence, lesser gradients in the salinity profiles.

The evaluation of the horizontal eddy viscosity found insignificant difference in the velocities, salinity, and dye results.

Roughness Height

Model simulations were conducted with various uniform and spatially varying roughness heights. Vertical velocity profiles and velocity phasing were used to evaluate the roughness height. “Snap-shots” of vertical velocity profiles at S. Pacific Drive used for the model and field data comparisons covered different phases of the neap and spring tide when evaluating this parameter. The velocity phasing was also evaluated by comparing the time at which the peak ebb and flood velocities occurred during the spring tide.

Uniform roughness heights were evaluated ranging from 0.01 to 0.05 m. The differences in the velocity profiles among these values were minimal. A higher roughness height slightly increased the velocity gradient by reducing the bottom velocity, and increasing the surface velocity. However it is expected that the roughness height in the Dominguez Channel should be higher compared to the rest of the Harbor Area. Roughness heights in the Dominguez Channel were simulated at 0.03 and 0.04 m, while roughness heights in the rest of the model domain ranged from 0.01 to 0.02 m.

Comparison of the velocity phasing show that the roughness height does not affect the timing of the peak ebb velocity, but does influence the timing of the peak flood velocity. Table 4.6 illustrates the change in the time to peak flood velocity with different roughness heights.

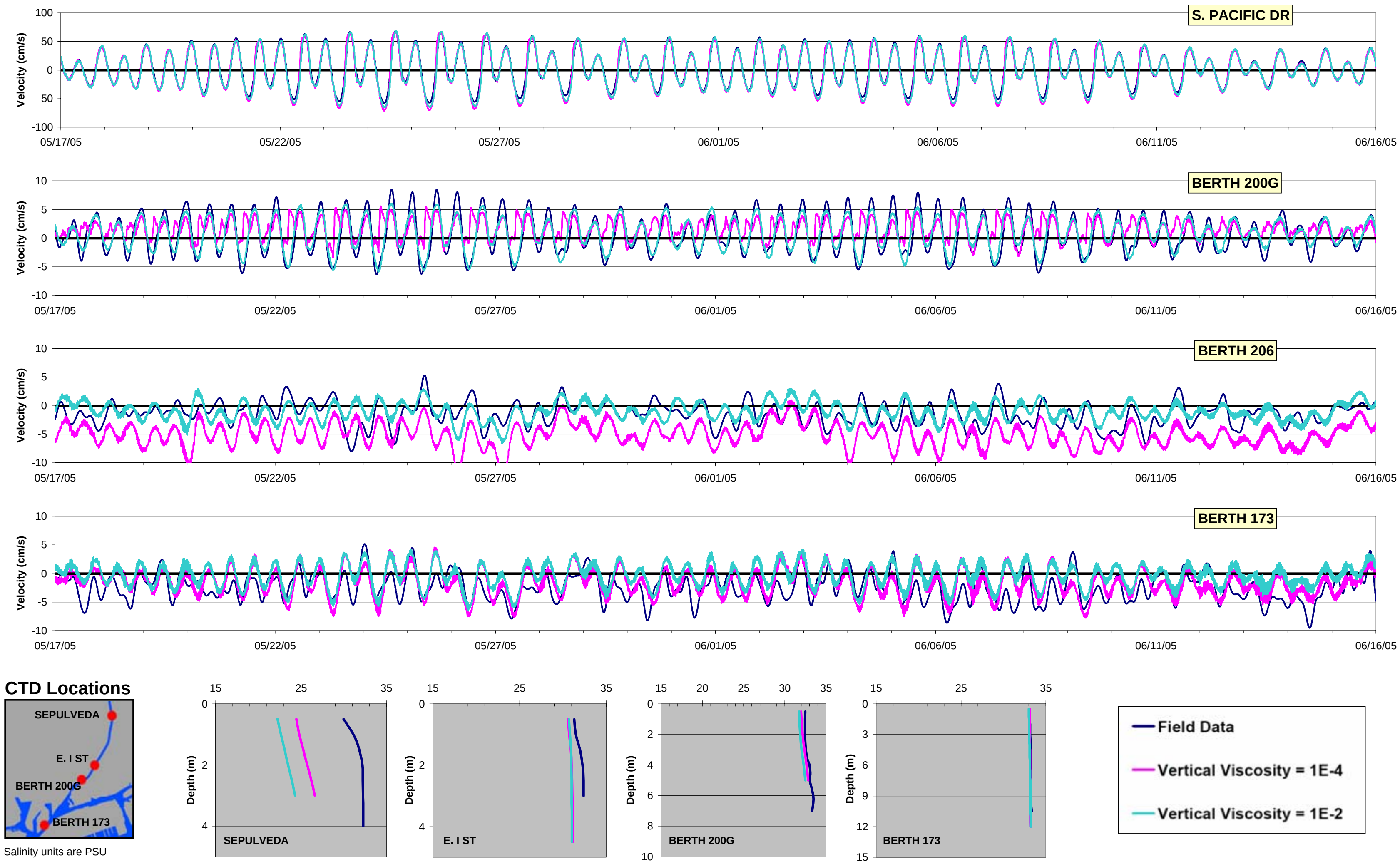

Figure 4.10 Evaluation of Model Parameters - Vertical Viscosity

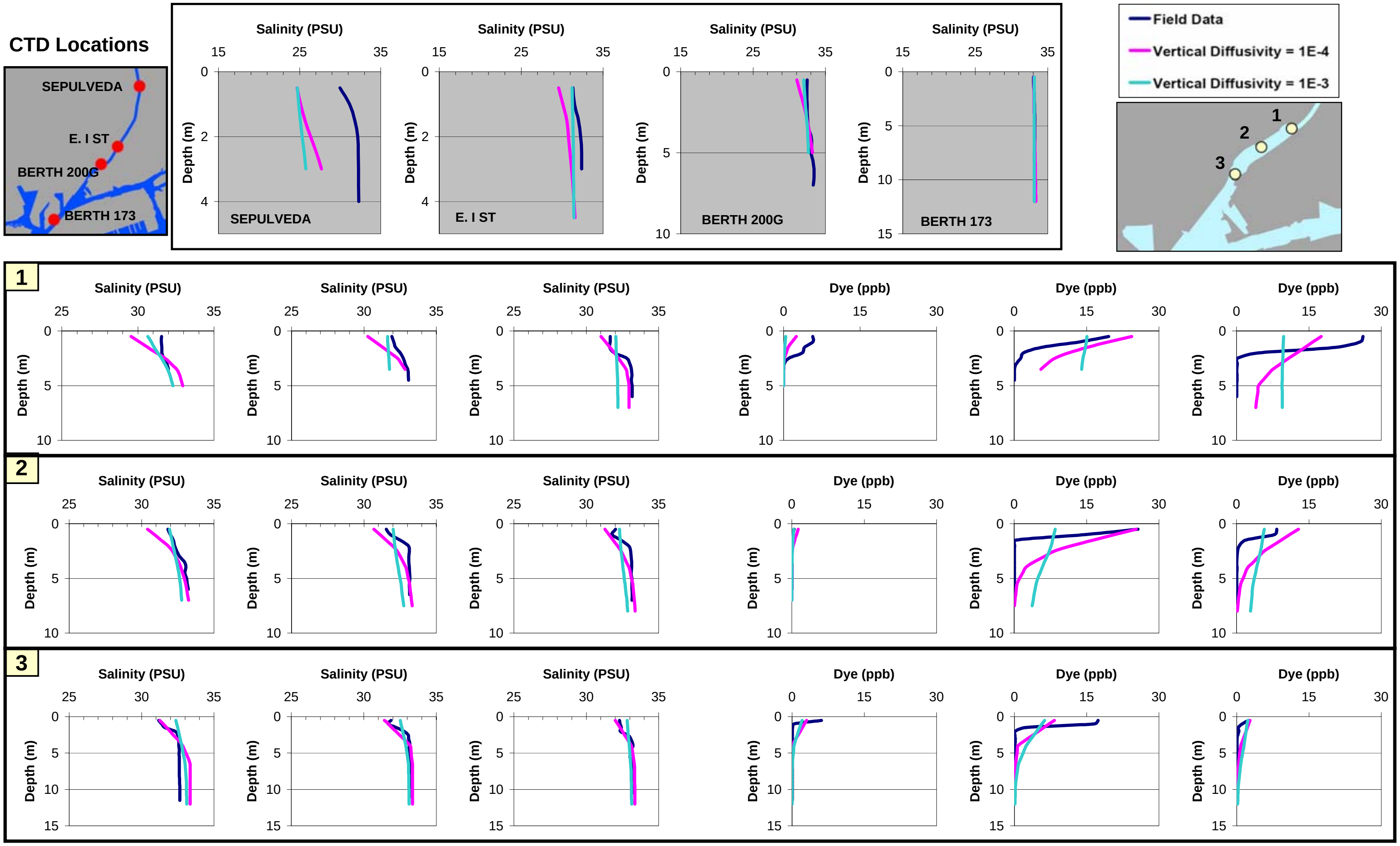

Figure 4.11 Evaluation of Model Parameters - Vertical Diffusivity

Figure 4.12 shows an example of the effect of roughness heights on velocity profiles. In general, the smaller the roughness height, the smoother the boundary, hence the smaller gradient in the velocity profiles.

Table 4.6 Effect of roughness heights on time to peak flood velocity

Roughness Height (m)		Time of Peak Flood Velocity
Channel	Harbor	
0.01	0.01	5/25/05 16:00
0.02	0.02	5/25/05 16:00
0.03	0.03	5/25/05 16:06
0.04	0.04	5/25/05 16:06
0.05	0.05	5/25/05 16:42
0.03	0.01	5/25/05 16:00
0.03	0.02	5/25/05 16:00
0.04	0.01	5/25/05 16:00
0.04	0.02	5/25/05 16:00
Field Data		5/25/05 16:12

Cohesive Sediment Settling Velocity

The TSS data were used to calibrate the cohesive sediment settling velocity. Ten TSS samples were taken at two channel locations at surface- and bottom-depths, along with surface-, mid-, and bottom-depths at two harbor locations. As shown in Table 4.7, half of samples did not detect TSS. For model comparisons, all non-detect samples were specified at the minimum detection level of 0.95 mg/L. All surface-depth samples had non-detected values, as well as the bottom-depth sample for E. I Street.

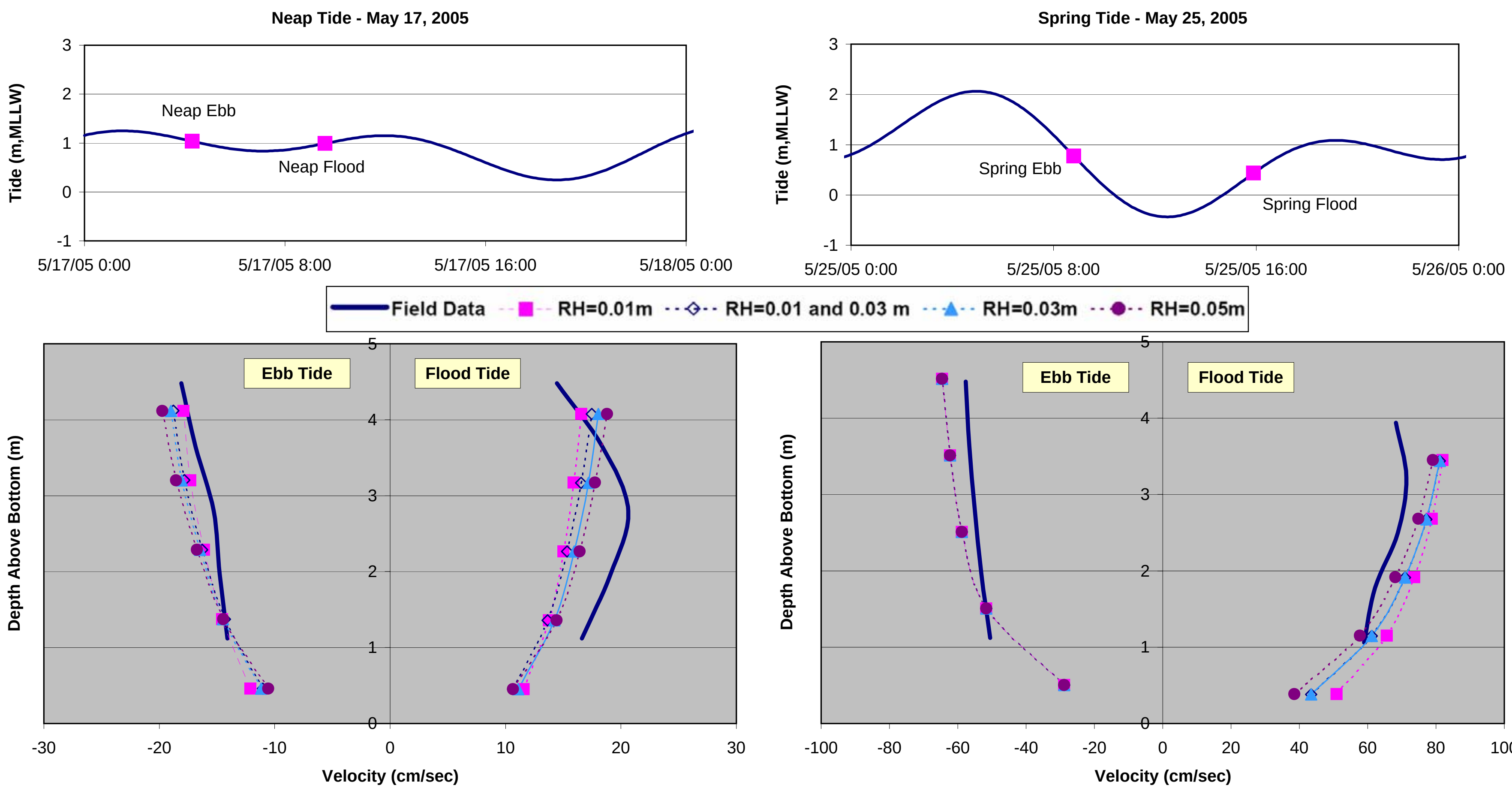

Figure 4.12 Evaluation of Model Parameters - Roughness Height

Table 4.7 Dry Weather Calibration Estuary TSS Field Data

SAMPLE LOCATION	DEPTH	TSS (MG/L)
Sepulveda – Surface	Surface	ND
	Bottom	5.2
E. I Street	Surface	ND
	Bottom	ND
Berth 200G	Surface	ND
	Mid	1
	Bottom	14
Berth 173	Surface	ND
	Mid	9.2
	Bottom	1.2

ND – Non-detect is specified at minimum detection level of 0.95 mg/L for model comparisons

For the dry weather calibration, the cohesive sediment settling velocity was simulated with values ranging between 1E-5 and 1E-7 m/sec. Model predicted cohesive sediment time series concentrations in the water column, as well as vertical cohesive sediment profiles, were compared to the TSS field data. Higher the settling velocity resulted in the lowest cohesive sediment concentrations in the water column, as illustrated in the example shown in Figure 4.13.

Additional sediment parameters were evaluated, but determined to have negligible effects on the model results being calibrated. These sediment parameters were boundary stress for deposition (N/m^2), surface erosion rate (g/m^2-sec), and boundary stress for erosion (N/m^2).

Metal Partition Coefficients

The metal partition coefficients were calibrated based on the dissolved and particulate metals data collected at the same 10 locations as the TSS samples. The field data are summarized in Table 4.8 for chromium, copper, lead, and zinc. The total, dissolved, and particulate metal data were compared to model predicted concentration time series, as well as vertical profiles.

Table 4.8 Dry Weather Calibration Estuary Metals Field Data

Sample Location	Depth	Dissolved (µg/L)	Particulate (µg/L)	Total (µg/L)	Particulate Fraction	Equilibrium Partition Coefficient (L/mg)
Chromium						
Sepulveda	Surface	0.325	0.369	0.694	0.53	1.20
	Bottom	0.325	0.419	0.744	0.56	0.25
E. I St	Surface	0.335	0.349	0.684	0.51	1.10
	Bottom	0.325	0.309	0.634	0.49	1.00
Berth 200G	Surface	0.325	0.269	0.594	0.45	0.87
	Mid	0.275	0.329	0.604	0.55	1.20
	Bottom	0.235	0.689	0.924	0.75	0.21
Berth 173	Surface	0.295	0.119	0.414	0.29	0.43
	Mid	0.305	0.249	0.554	0.45	0.09
	Bottom	0.245	0.259	0.504	0.51	0.88
Copper						
Sepulveda	Surface	1.73	0.248	1.978	0.13	0.15
	Bottom	1.57	0.274	1.844	0.15	0.03
E. I St	Surface	1.71	0.229	1.939	0.12	0.14
	Bottom	1.63	0.249	1.879	0.13	0.16
Berth 200G	Surface	2.10	0.510	2.610	0.20	0.26
	Mid	1.41	0.467	1.877	0.25	0.33
	Bottom	0.67	1.790	2.460	0.73	0.19
Berth 173	Surface	1.43	0.248	1.678	0.15	0.18
	Mid	1.43	0.217	1.647	0.13	0.02
	Bottom	1.29	0.329	1.619	0.20	0.21
Lead						
Sepulveda	Surface	0.698	1.06	1.758	0.60	1.60
	Bottom	0.371	0.581	0.952	0.61	0.30
E. I St	Surface	0.41	0.708	1.118	0.63	1.82
	Bottom	0.348	0.604	0.952	0.63	1.83
Berth 200G	Surface	0.378	0.769	1.147	0.67	2.14
	Mid	0.136	0.540	0.676	0.80	3.97
	Bottom	0.239	1.230	1.469	0.84	0.37
Berth 173	Surface	0.054	0.264	0.318	0.83	5.15
	Mid	0.057	0.183	0.240	0.76	0.35
	Bottom	0.125	0.305	0.430	0.71	2.03
Zinc						
Sepulveda	Surface	13.9	1.41	15.31	0.09	0.11
	Bottom	13.6	1.26	14.86	0.09	0.02
E. I St	Surface	13.0	1.25	14.25	0.09	0.10
	Bottom	12.4	1.4	13.8	0.10	0.12
Berth 200G	Surface	15.6	3.5	19.1	0.18	0.24
	Mid	10.3	1.74	12.04	0.15	0.17
	Bottom	8.2	4.77	12.97	0.37	0.04
Berth 173	Surface	5.89	1.04	6.93	0.15	0.19
	Mid	6.18	0.69	6.865	0.10	0.01
	Bottom	7.18	0.817	7.997	0.10	0.10

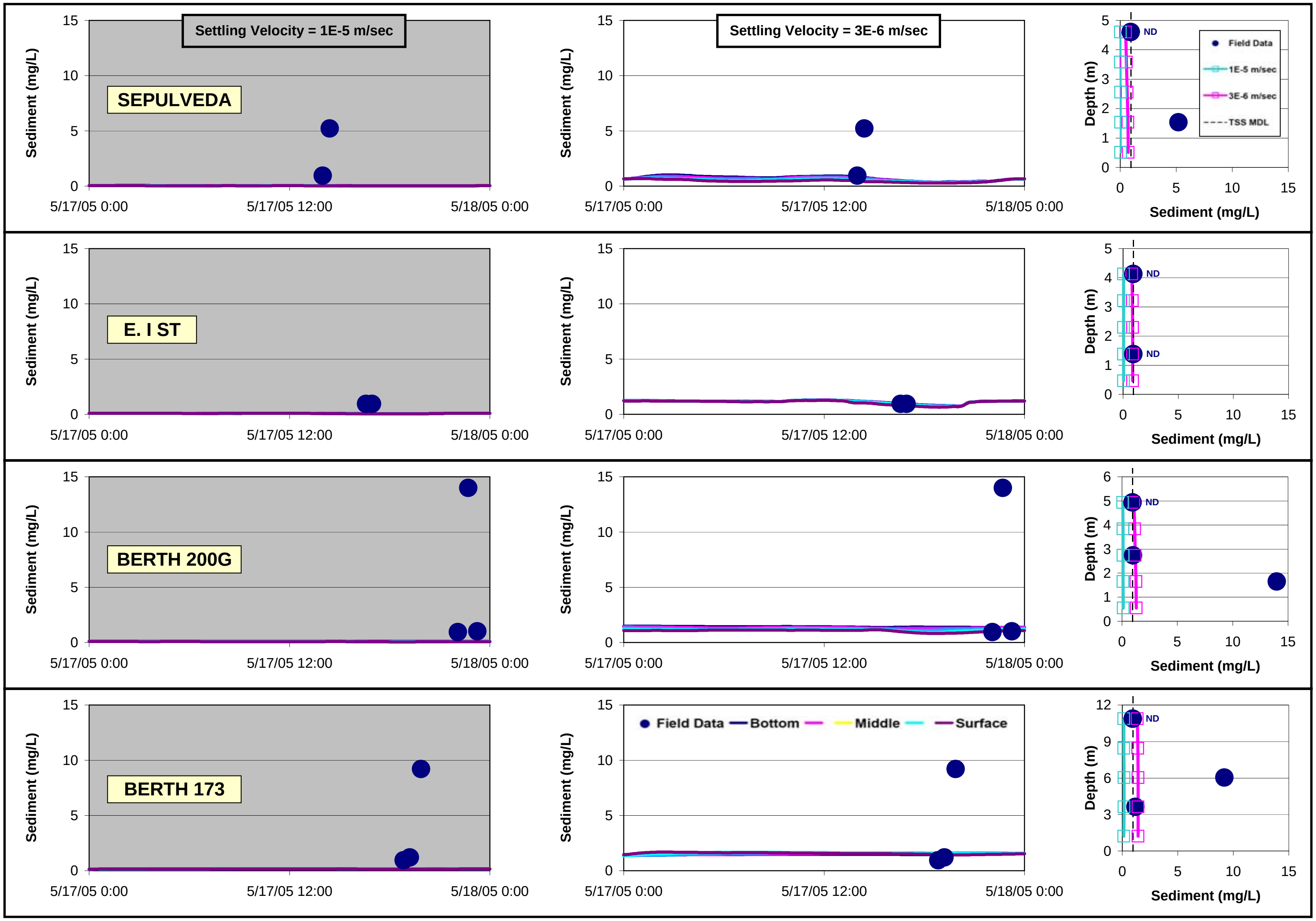

Figure 4.13 Evaluation of Model Parameters - Cohesive Sediment Settling Velocity

Chromium - The chromium field data showed on average, a 50/50 split between the dissolved and particulate fraction. The equilibrium partition coefficient of the field data ranged between 0.09 and 1.2 L/mg. For dry weather calibration, the chromium equilibrium partition coefficient was varied between 0.4 L/mg to 1.0 L/mg.

Copper - In general, the copper field data had a higher dissolved fraction of about 80%. The equilibrium partition coefficient of the field data had an average value of 0.17 L/mg. For the dry weather calibration, the copper equilibrium partition coefficient was evaluated between 0.1 and 2.0 L/mg.

Lead - From the May 2005 field data, lead results showed a higher particulate fraction of an average about 70% and an equilibrium partition coefficient of 2.0 L/mg. The lead equilibrium partition coefficient varied between 1.0 and 3.0 L/mg for the calibration of the lead equilibrium partition coefficient.

Zinc - Compared to the other metals, zinc concentrations were higher. The data also showed zinc having a higher dissolved fraction of about 85% and the equilibrium partition coefficient ranging between 0.24 and 0.01 L/mg. The zinc equilibrium partition coefficient was varied from 0.06 to a maximum value of 0.2 L/mg.

Figure 4.14 use the calibration for chromium as an example. In the figure, partition coefficients of 0.4 and 1.0 are shown. As expected, the higher partition coefficient results in a higher concentration of particulate chromium relative to the dissolved fraction even there is very small change in the total concentration.

4.3.3 Anti-Diffusion

As discussed earlier, EFDC has a numerical “anti-diffusion” feature that can be used to suppress numerical diffusion. Applying the anti-diffusion correction would increase the vertical gradients and peak concentrations. Figure 4.15 illustrates the change in model predicted salinity and dye concentrations with the “anti-diffusion” on or off.

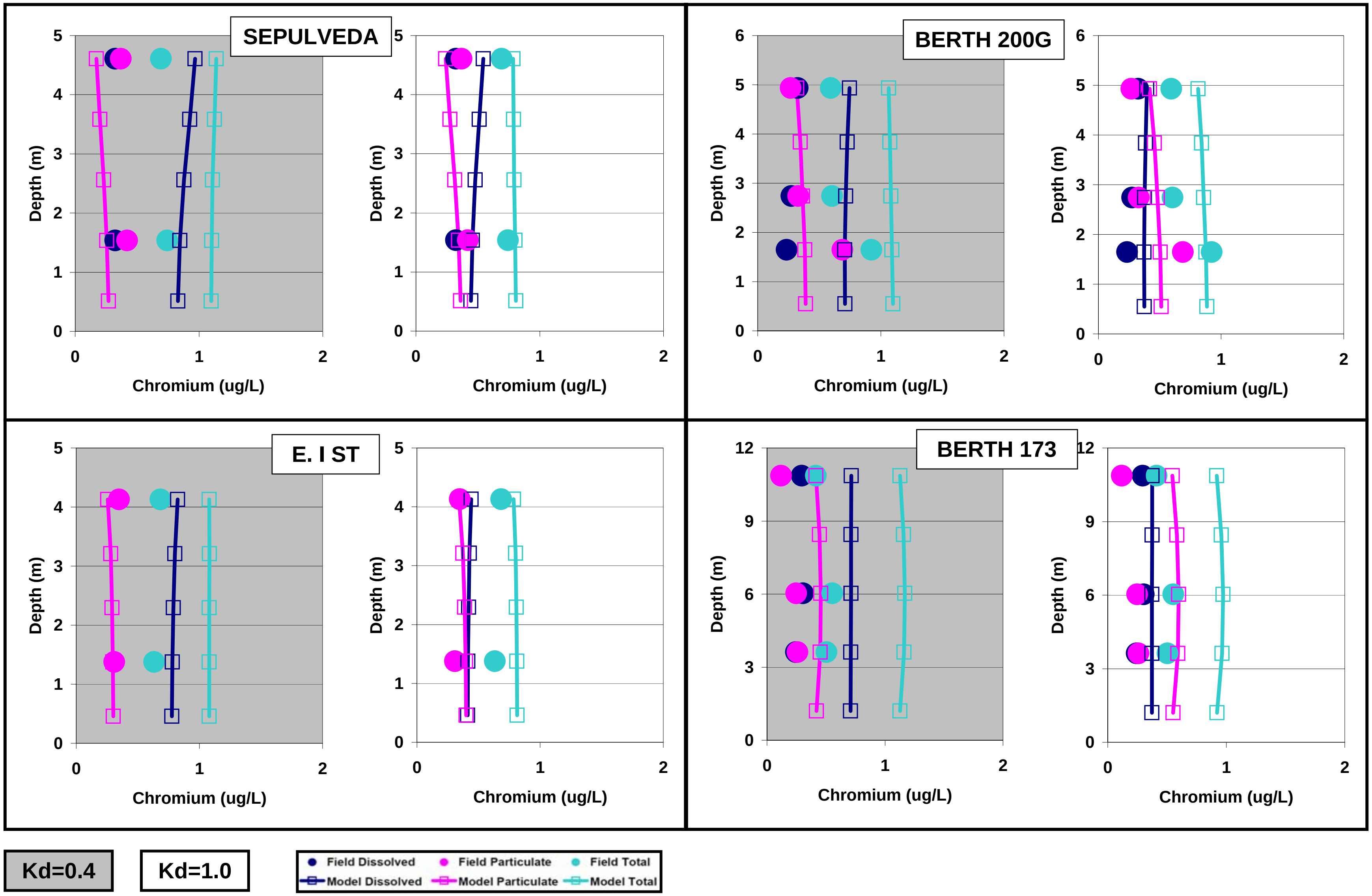

Figure 4.14 Evaluation of Model Parameters - Equilibrium Partition Coefficient for Chromium

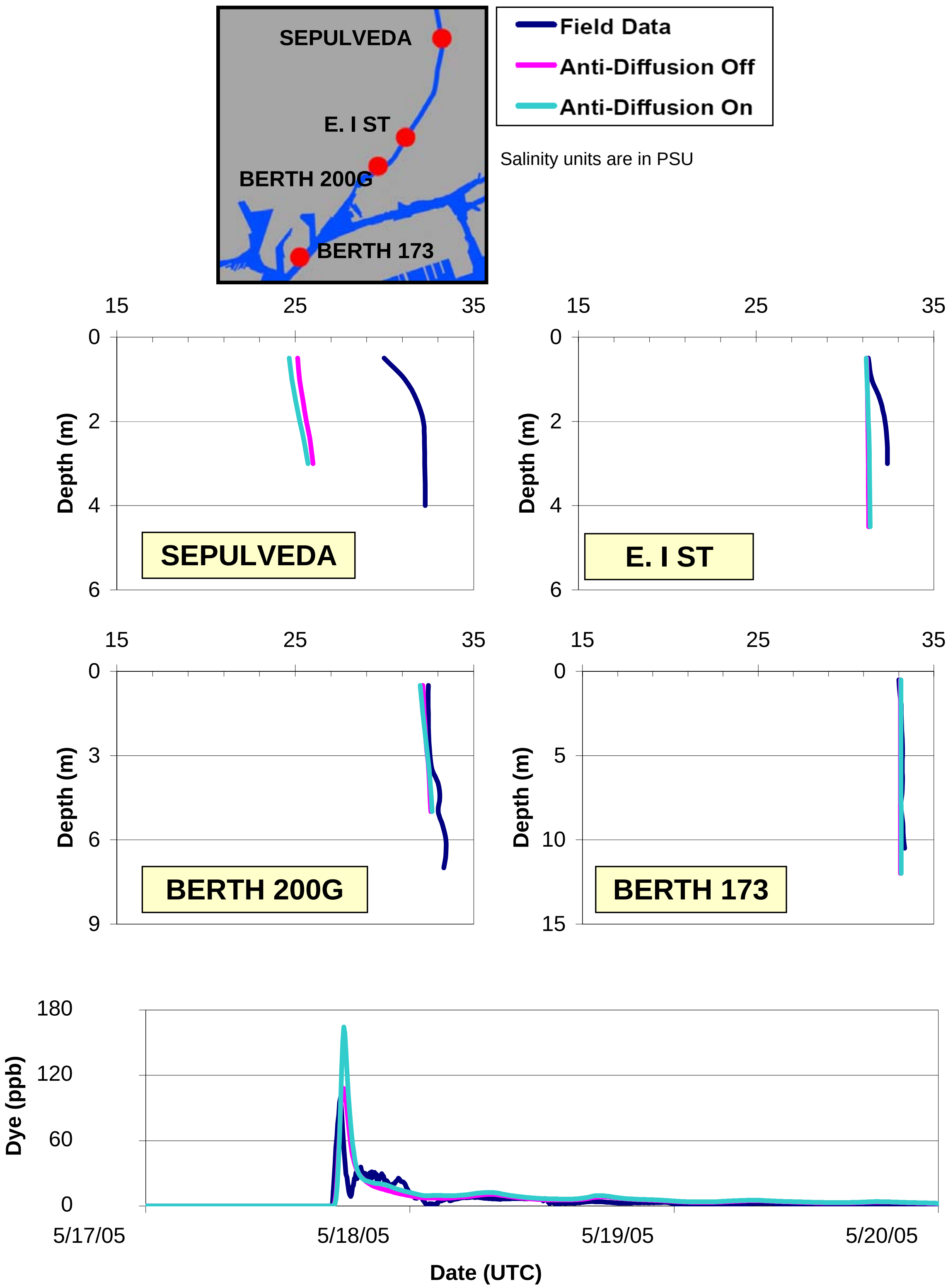

Figure 4.15 Evaluation of Model Parameters - Anti-Diffusion

4.4 DRY WEATHER CALIBRATION RESULTS

A summary of the selected dry weather calibration parameters is provided in Table 4.9. A spatially varying roughness height was selected as 0.03 m in the Dominguez Channel and 0.02 m in the harbor and ocean areas. The horizontal eddy viscosity was selected to be 1E-6 m^2/sec, while the maximum vertical kinematic viscosity and diffusivity were calibrated to 2E-3 and 1E-4 m^2/sec, respectively. Anti-diffusion corrections were used only for cohesive sediment and metals. The sediment settling velocity was calibrated to be 3E-6 m/sec. The dry weather metal equilibrium partition coefficients were determined to be 0.9, 0.18, 2.5, and 0.13 L/mg for chromium, copper, lead, and zinc, respectively.

Table 4.9 Selected DCEM Dry Weather Calibrated Parameters

MODEL PARAMETER	UNITS	VALUE
Roughness Height – Dominguez Channel	m	0.03
Roughness Height – Harbor and Ocean	m	0.02
Horizontal Eddy Viscosity	m^2/sec	1E-6
Maximum Vertical Kinematic Viscosity	m^2/sec	2E-3
Maximum Vertical Eddy Diffusivity	m^2/sec	1E-4
Anti-Diffusion Correction for Hydrodynamics	--	Off
Anti-Diffusion Correction for Salinity	--	Off
Anti-Diffusion Correction for Dye	--	Off
Anti-Diffusion Correction for Cohesive Sediment	--	On
Anti-Diffusion Correction for Noncohesive Sediment	--	On
Anti-Diffusion Correction for Metals	--	On
Sediment Settling Velocity	m/sec	3E-6
Equilibrium Partition Coefficient	L/mg	Cr 0.9 Cu 0.18 Pb 2.5 Zn 0.13

The dry weather calibration results compares the model predicted results with field data for water surface elevations, velocities, velocity profiles, salinity profiles, dye, dye profiles, TSS, chromium, copper, lead, and zinc.

4.4.1 Water Surface Elevations and Velocities

The calibrated DCEM water surface elevations compared to the field data at the four ADP locations are shown in Figure 4.16. The field data is represented by a navy blue line and

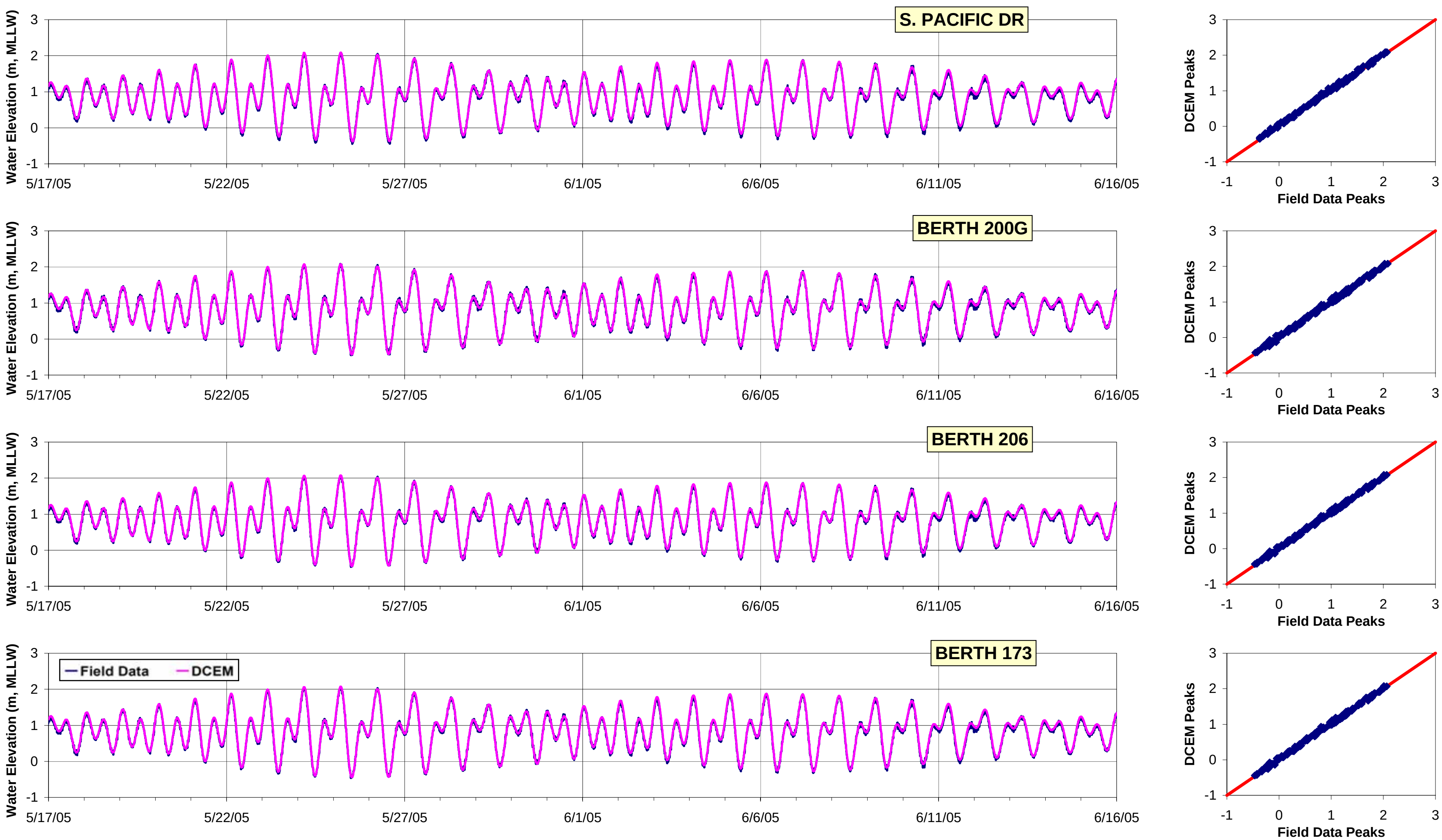

Figure 4.16 Dry Weather Calibrated Water Surface Elevations

model predicted results in magenta. As shown in the figure, the DCEM water surface elevations are in good agreement with the field data over the 30-day dry weather calibration period. Statistical comparisons of model predicted and field data daily highs – HHW and HW and daily lows – LLW and LW at each ADP location are also shown in the figure.

The dry weather calibrated velocities at the ADP locations along with scatter plot comparisons of the peak ebb and flood velocities are shown in Figure 4.17. In the figure, velocities are shown in units of cm/sec with the velocities for S. Pacific Drive on a larger vertical scale than the other three locations. Positive values indicate flood tides, while negative values indicate ebb tides for S. Pacific Drive, Berth 200G, and Berth 173. For Berth 206, positive velocities indicate flow to the east, while negative values indicate flow is west towards Berth 173.

In general, the DCEM velocities over the 30-day dry weather calibration period agrees well with the field data and show similar trends such as dominant velocity direction and tidal variations (e.g., higher velocities during spring tide). The best model-field comparison occurred at S. Pacific Drive, which shows nearly the same velocity magnitude and phasing within the Dominguez Channel. The scatter plot comparison of peak ebb and flood velocities also shows a good model prediction at S. Pacific Drive. Model predicted velocities at Berth 200G show an under estimation of the peak ebb and flood velocities, generally ranging between 1 and 3 cm/sec. However, there is a relatively good match of the phasing of the peak ebb and flood velocities. Compared to S. Pacific Dr. and Berth 200G, there is a greater deviation between the model predicted and field data velocities at Berths 206 and 173. However, the model velocity predictions show similar trends to the field data. Field data for Berth 206 shows a dominant current west towards Berth 173 (negative velocity), which is also apparent from the model predicted velocities. For Berth 173, both the field data and model shows a dominant flood velocity. The peak velocity scatter plot comparisons for Berths 206 and 173 show reasonable agreement with the field data. Differences in the model predicted and field data velocities may be attributed to the vertical averaging of the model predicted velocities, accuracy of the model bathymetry, and localized velocity fluctuations.

The neap and spring tide vertical velocity profiles at S. Pacific Drive are shown in Figure 4.18. Field and DCEM comparisons are made for eight velocity profiles, which are color-coded based on the tide condition shown at the top of the figure. Field data are shown as a solid navy blue line and the DCEM profiles shown in magenta. The DCEM velocity profiles compare well with the field data and capture both magnitude and shape.

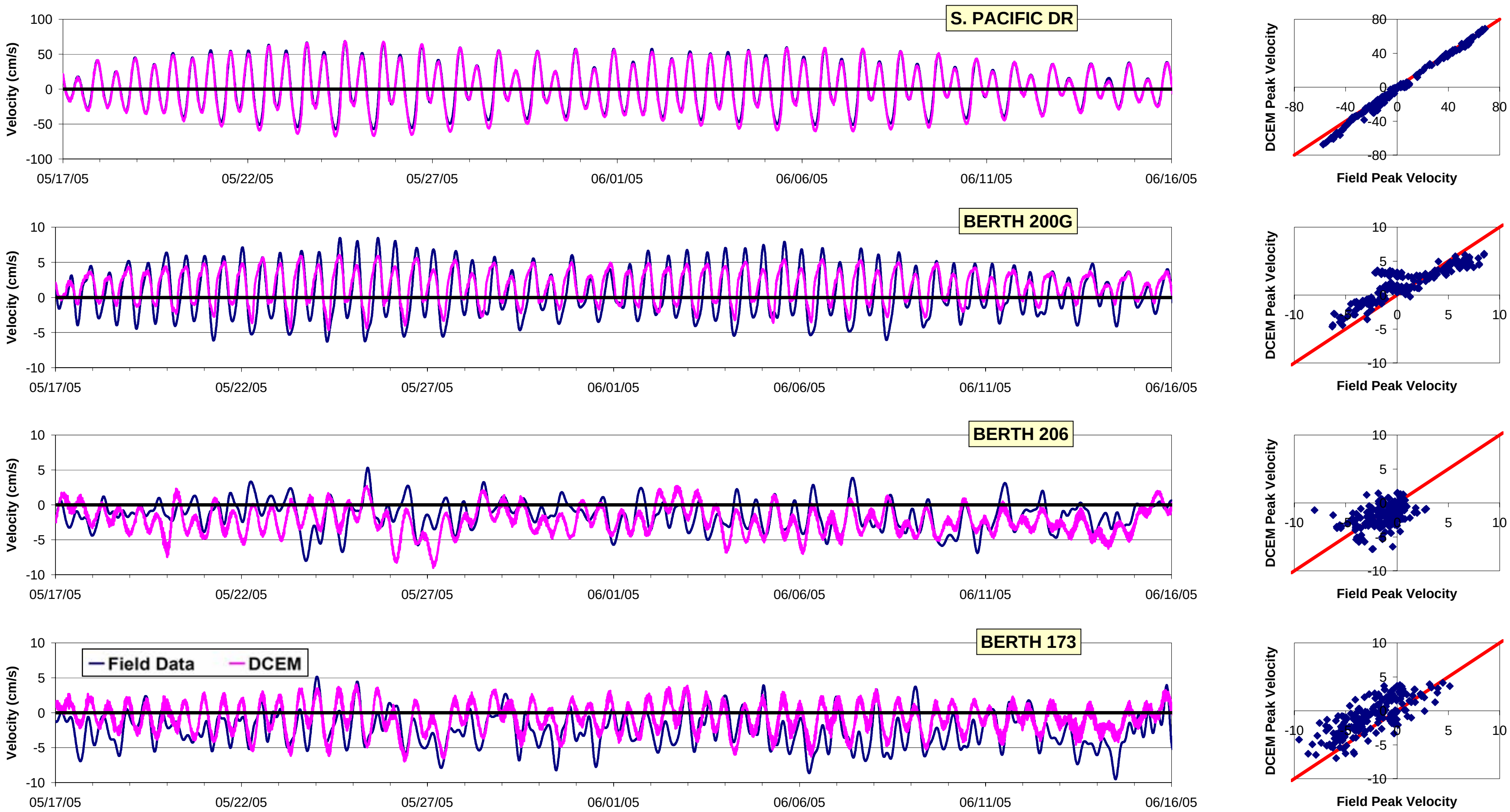

Figure 4.17 Dry Weather Calibrated Velocities

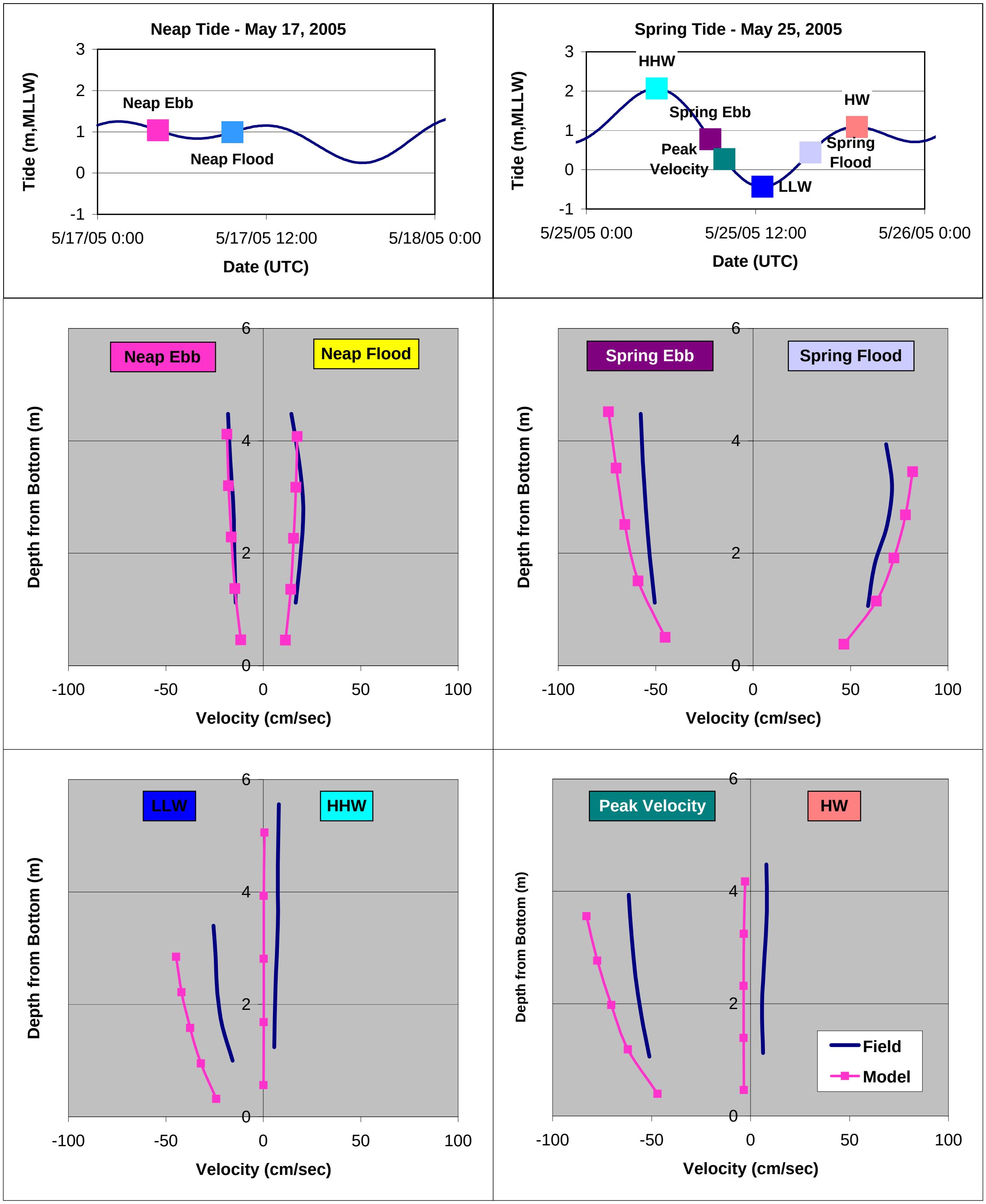

Figure 4.18 Dry Weather Calibrated Velocity Profiles

4.4.2 Salinity and Dye

The measured salinity profiles during the May 2005 dry weather event are compared with DCEM results in Figure 4.19. The salinity profiles are grouped by locations - Dominguez Channel, Consolidated Slip, Cerritos Channel, and Main Channel. Each profile shows the field data in navy blue and the model predicted salinity profile in magenta. Salinity profiles from the monthly CTD data are indicated by a shaded gray chart, the rest of the profiles are from the dry weather salinity distribution. Overall, the DCEM salinity profiles match both in shape and magnitude to the field data, as illustrated by the scatter plot comparison of the model and field data surface salinity also shown in the figure. The one exception is the salinity profile prediction at Sepulveda, where the DCEM predicted lower salinity levels (about 5 PSU lower) than the field data. The lower salinity levels may be attributed to the estimation of the dry weather inflows, which would have a greater influence on salinity levels in the Dominguez Channel compared to the Harbor Area. Both the DCEM salinity results and field data show two general trends: 1) channel locations with shallower water depths have a greater vertical variation compared to the deeper harbor locations and 2) vertical profiles vary with the tide condition, increasing with larger tide ranges (e.g., spring tide), especially during ebb tide.

A time series of dye concentrations taken during the dry weather dye study and DCEM results at Berths 200G, 206, and 173 are shown in Figure 4.20. The dye concentrations are shown in units of parts per billion (ppb) and results for Berth 200G are shown on a different vertical scale. The DCEM dye concentrations at Berth 200G show the same general shape as the field data, with a slightly higher peak dye concentrations. The higher dye concentration may be attributed to the model grid setup where the three grid cells defining the Dominguez Channel are directly connected to the three grid cells of the Consolidated Slip while in the field the gage was a little bit sheltered. Results at Berths 206 and 173 also compared well with the field data.

The DCEM predicted and field measured dye profile distributions in the Consolidated Slip, Cerritos Channel, and Main Channel are compared in Figure 4.21. In the figure, the horizontal scale for the Consolidated Slip locations is different than the dye profiles from the Cerritos and Main Channels. The figure also shows a comparison of the predicted and measured near-surface salinities. In general, the DCEM dye profiles follow same trends as the field data. Model-field dye comparisons were also made using the dye study aerial photos, which are shown in Figure 4.22. The figures shows “snap-shot” comparisons of the DCEM surface dye concentrations compared to the aerial photos. The times of each comparison indicates the time (hour:minute) after the dye release. The DCEM shows the same trends as the aerial photos – 1) dye concentrates at the marina near the Berth 200G, 2) the dye primarily stays in and around the marina, which also corresponds to field observations, and 3) the dye dissipates slowly.

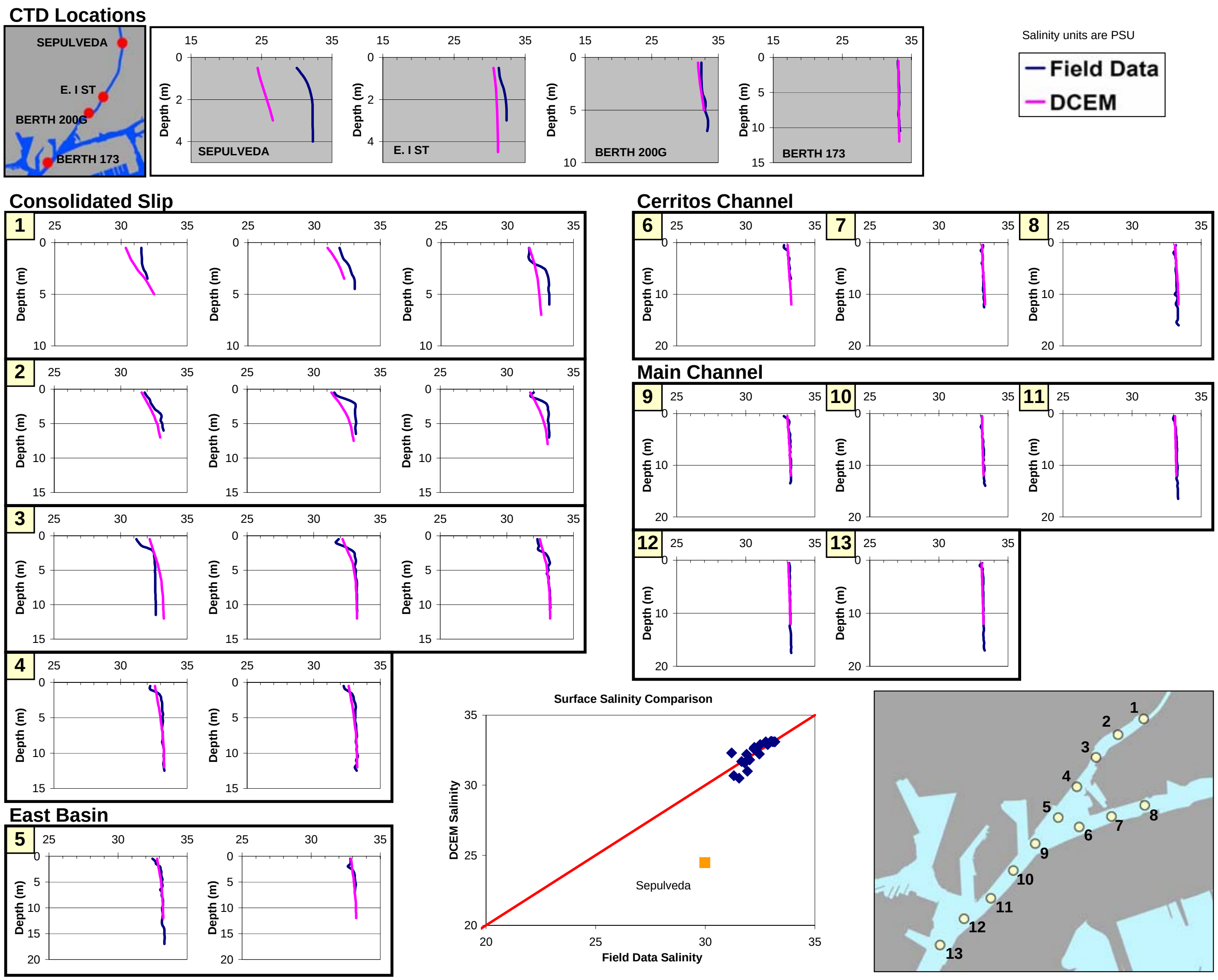

Figure 4.19 Dry Weather Calibrated Salinity Profiles

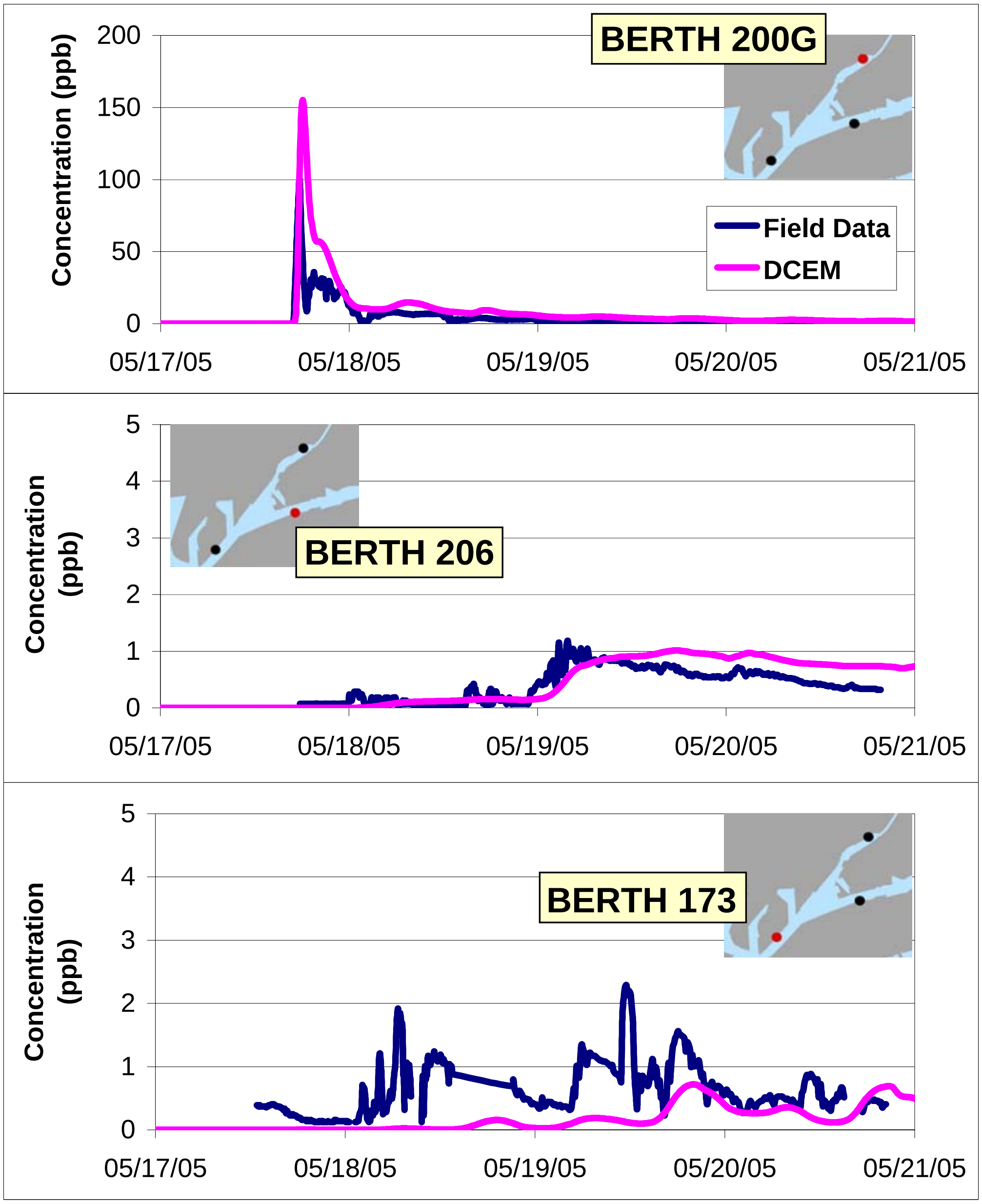

Figure 4.20 Dry Weather Calibrated Dye

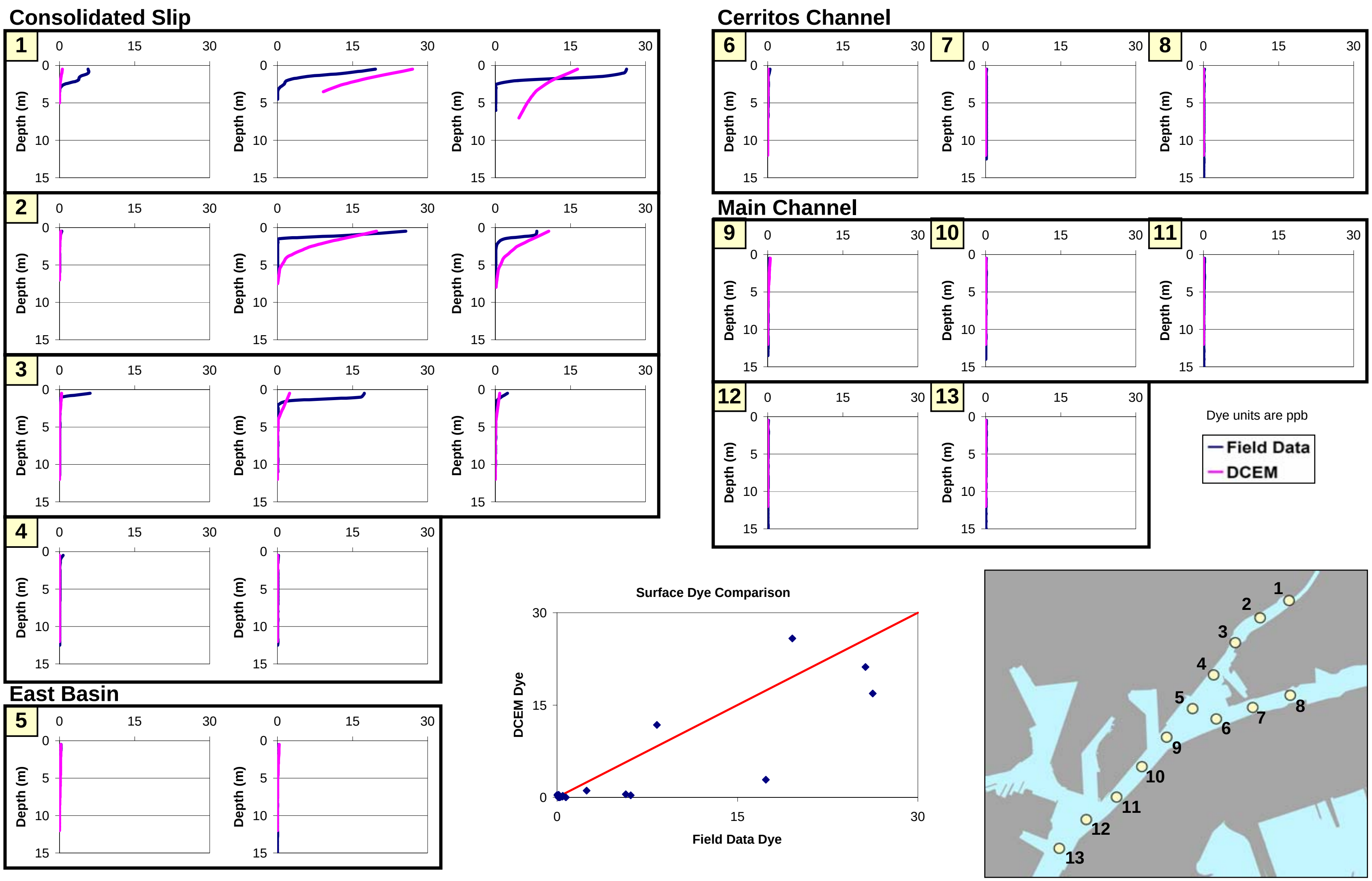

Figure 4.21 Dry Weather Calibrated Dye Profiles

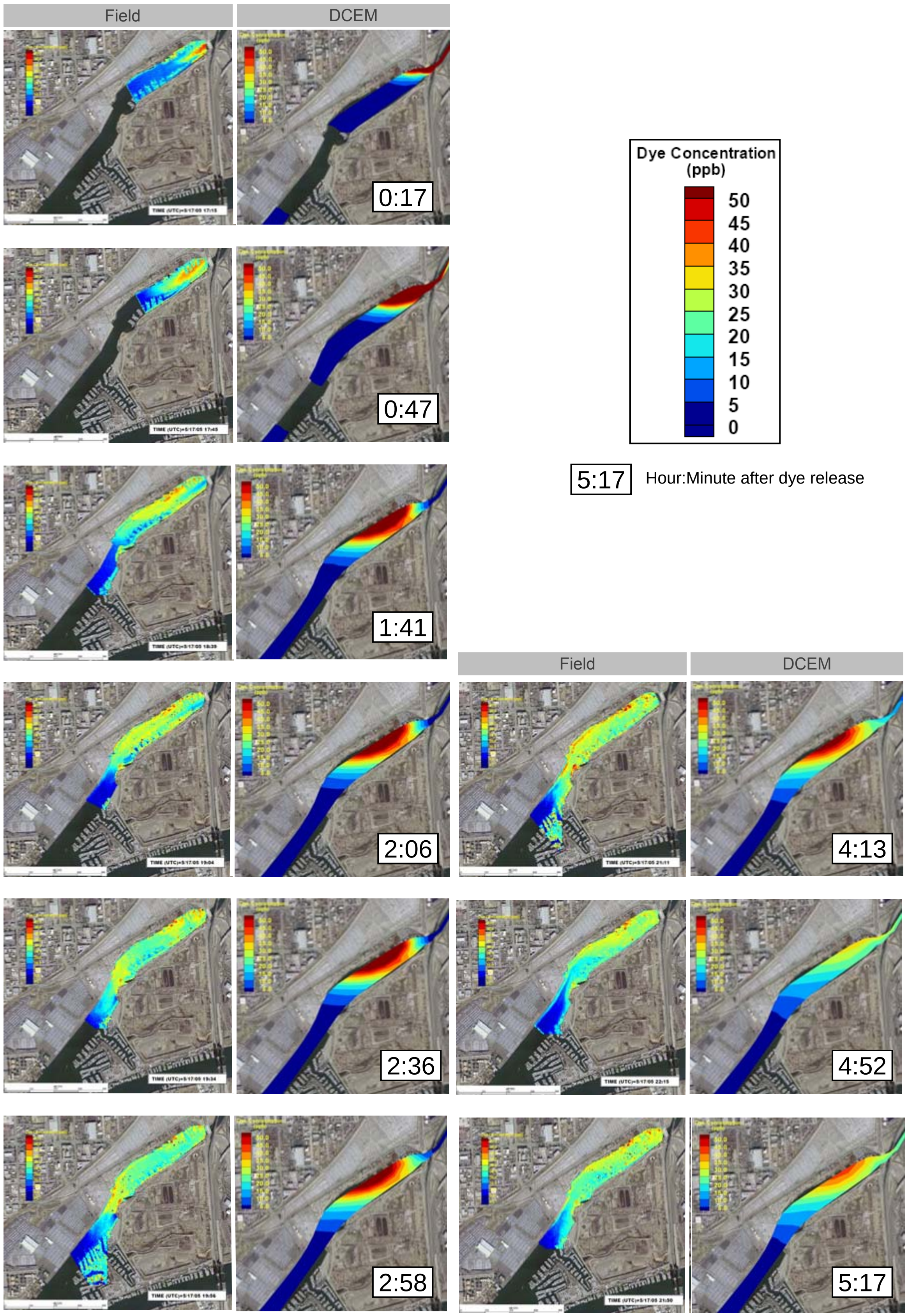

Figure 4.22 Dry Weather Calibrated Dye Distributions

4.4.3 TSS and Metals

The DCEM cohesive sediment concentrations are compared to the field TSS measurements in Figure 4.23. The results are shown as both time series and vertical profiles. The DCEM time series on May 17, 2005, in the left-side panels, show the cohesive sediment concentration in the five vertical layers, as well as the field data TSS measurements shown by solid circles. The DCEM time series results show that overall the model results match with the field data. The time series show some vertical variations with a greater variation during the second half of the day when the tide range is higher. The vertical variations also tend to increase during ebb tide. The cohesive sediment vertical profiles are also compared to the TSS measurements, which included two depths at Sepulveda and E. I St. and three depths at Berth 200G and Berth 173. The vertical scales of the profiles vary due to differences in the water depth at each location. The minimum detection limit (MDL) is also indicated on the vertical profiles with a dashed-line since the five non-detect samples were specified at the MDL for model comparisons.

Chromium, copper, lead, and zinc results are shown as time series and vertical profiles, in the same manner as the TSS results. DCEM and field data comparisons for chromium are shown in Figure 4.24. For each of the four sampling locations, time series results for total, dissolved, and particulate chromium are shown in the top three panels, followed by the vertical profiles for total, dissolved, and particulate chromium, which are distinguished by color. In the figure, field data are indicated by solid circles. The chromium results show similar concentrations to the field data, which were under 1 µg/L. The DCEM results also indicate little vertical stratification.

DCEM and field data comparisons for copper are shown in Figure 4.25. The DCEM copper results show a higher dissolved copper concentration compared to particulate copper, replicating the same trend as the field data. The higher dissolved copper fraction also results in a greater vertical variation that oscillates with the tide in a similar manner as salinity and also has a greater variation at the channel locations versus the harbor locations. The DCEM vertical profiles also show a good comparison to the field data in shape and magnitude, especially at E. I Street.

Lead results are shown in Figure 4.26 and show similar trends as the field data, which indicates higher particulate concentrations than dissolved lead. The higher particulate fraction also results in less vertical variations similar to the chromium results.

Compared to the other metals, zinc concentrations were higher, as shown in the results in Figure 4.27. DCEM zinc results showed a higher dissolved concentration than particulate concentration, which is also apparent in the field data. The zinc results follow the same trends as the copper results.

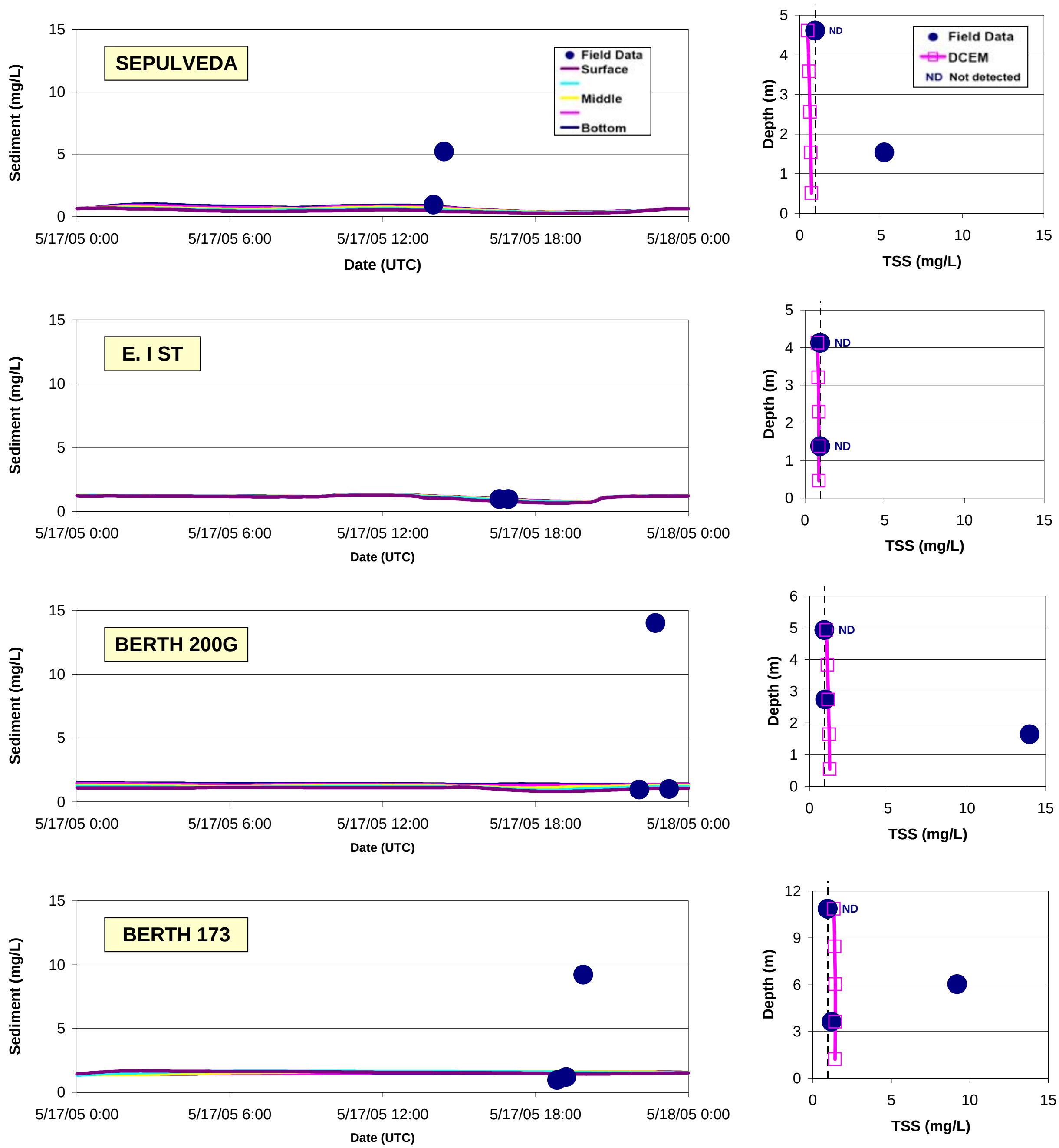

Figure 4.23 Dry Weather Calibrated TSS

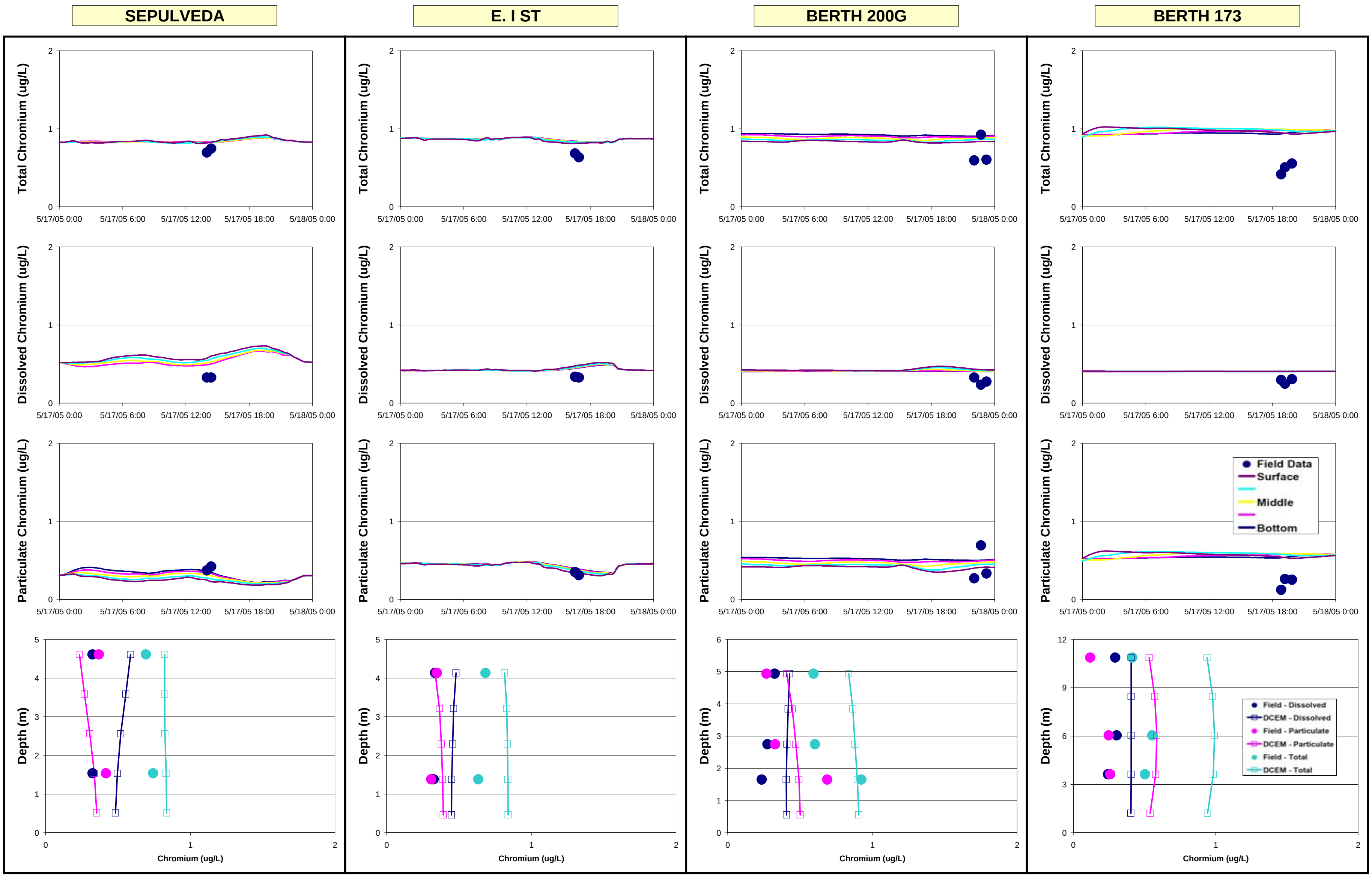

Figure 4.24 Dry Weather Calibrated Chromium

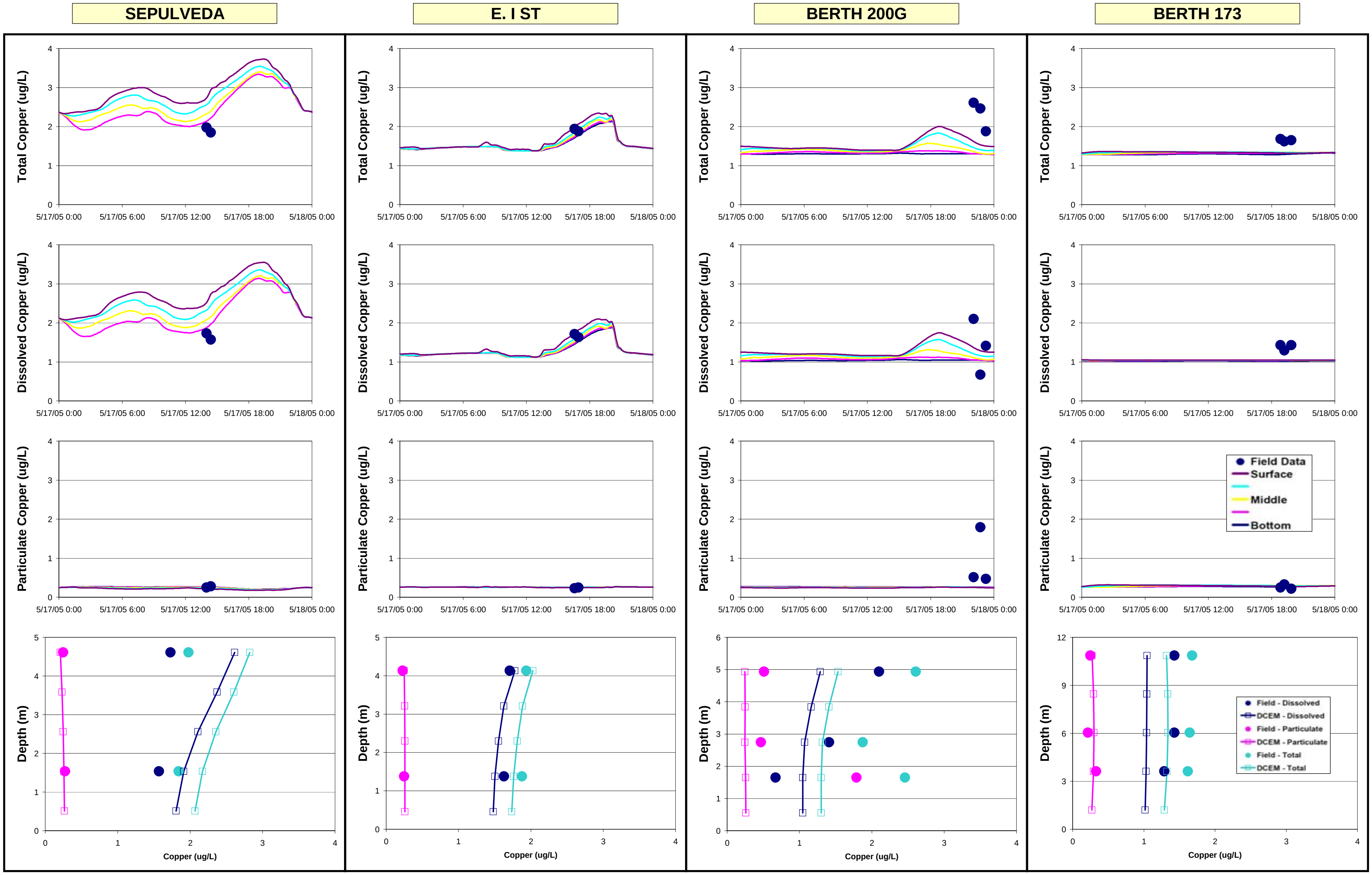

Figure 4.25 Dry Weather Calibrated Copper

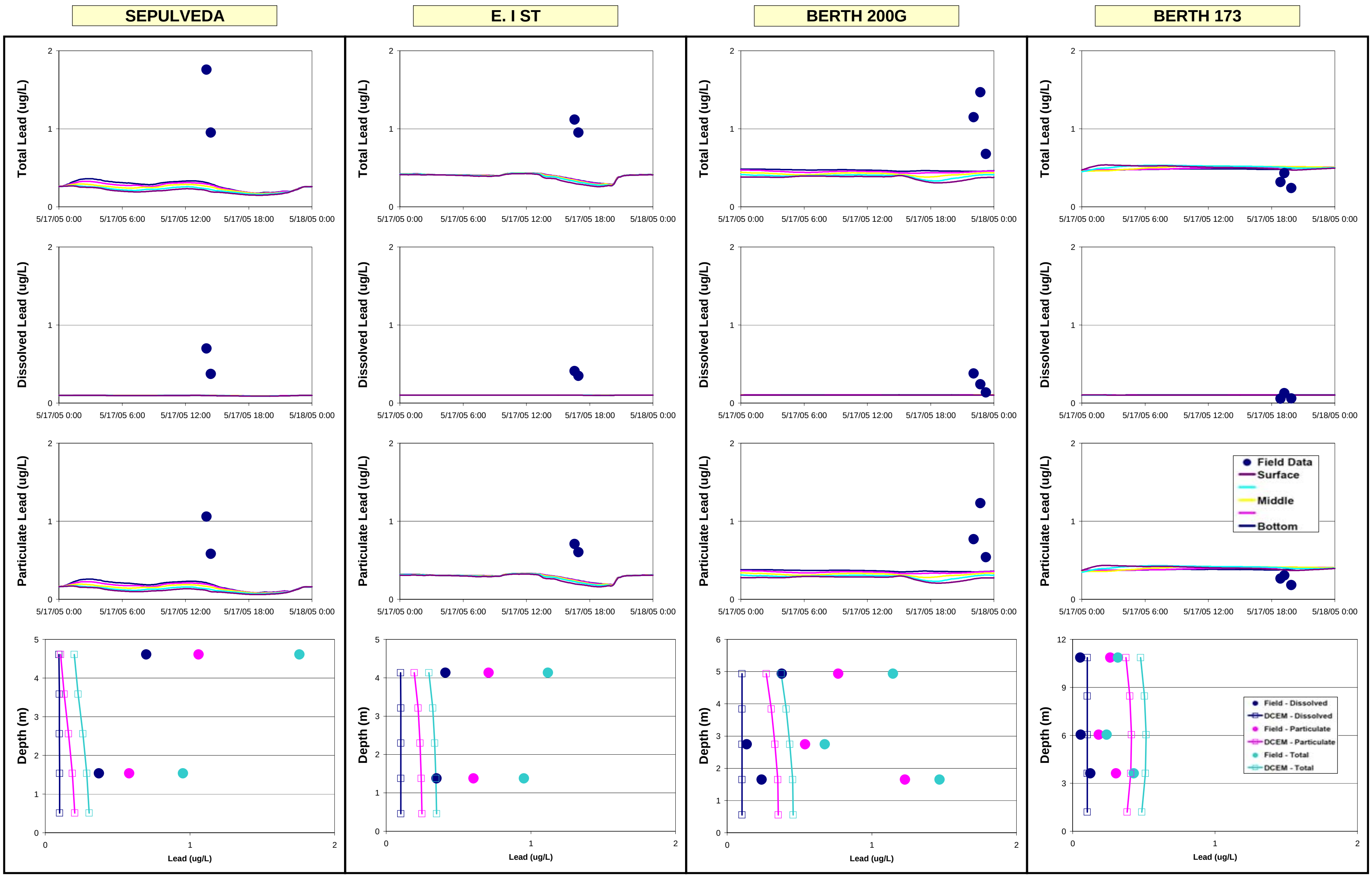

Figure 4.26 Dry Weather Calibrated Lead

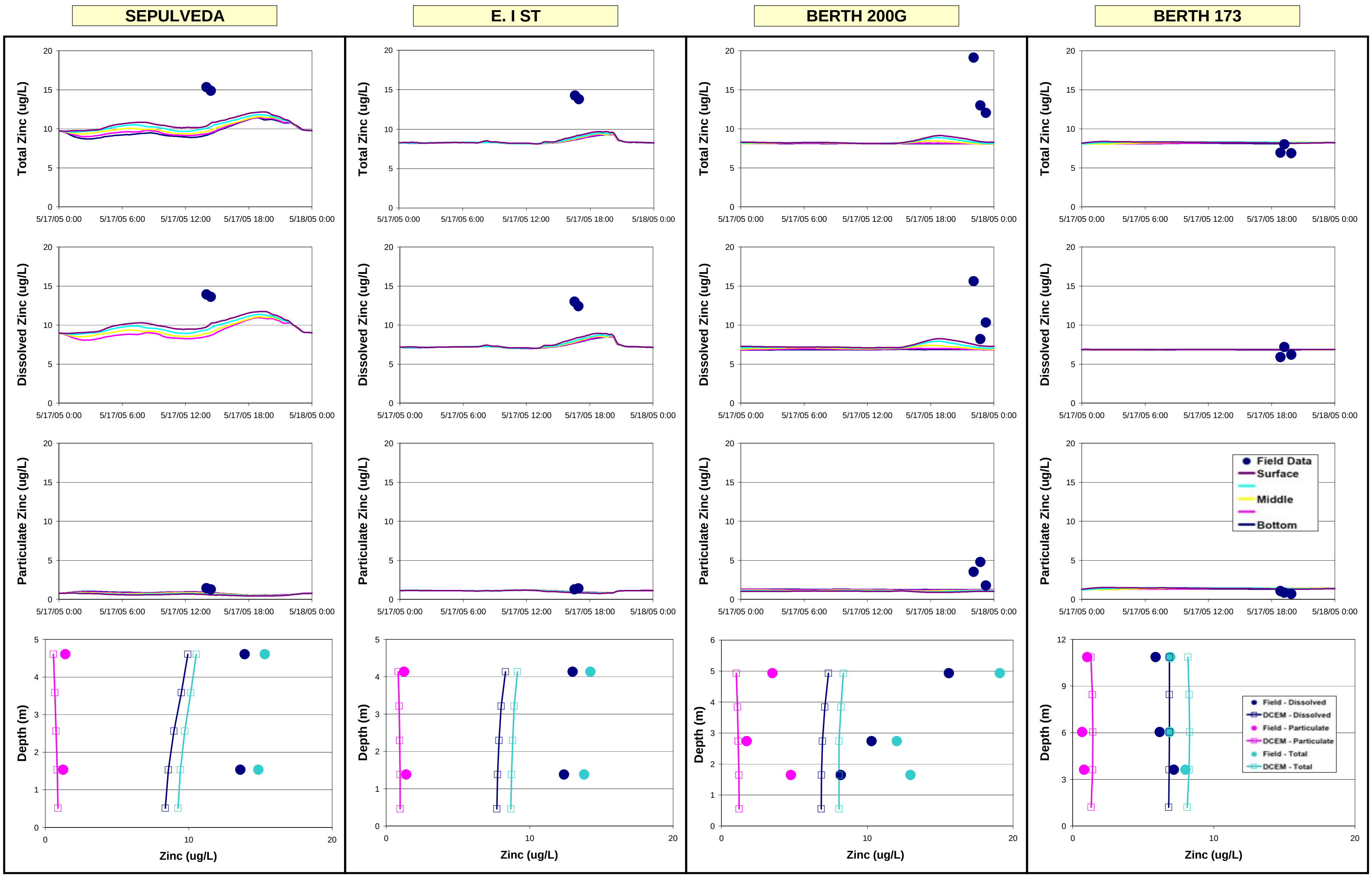

Figure 4.27 Dry Weather Calibrated Zinc

A statistical comparison of DCEM and field data metals was done based on a scatter plot of the particulate fractions of the 10 samples and is shown in Figure 4.28 for the four metals. The red square indicates the average particulate fraction for the 10 samples. In general, the DCEM particulate fractions compare relatively well to the field data.

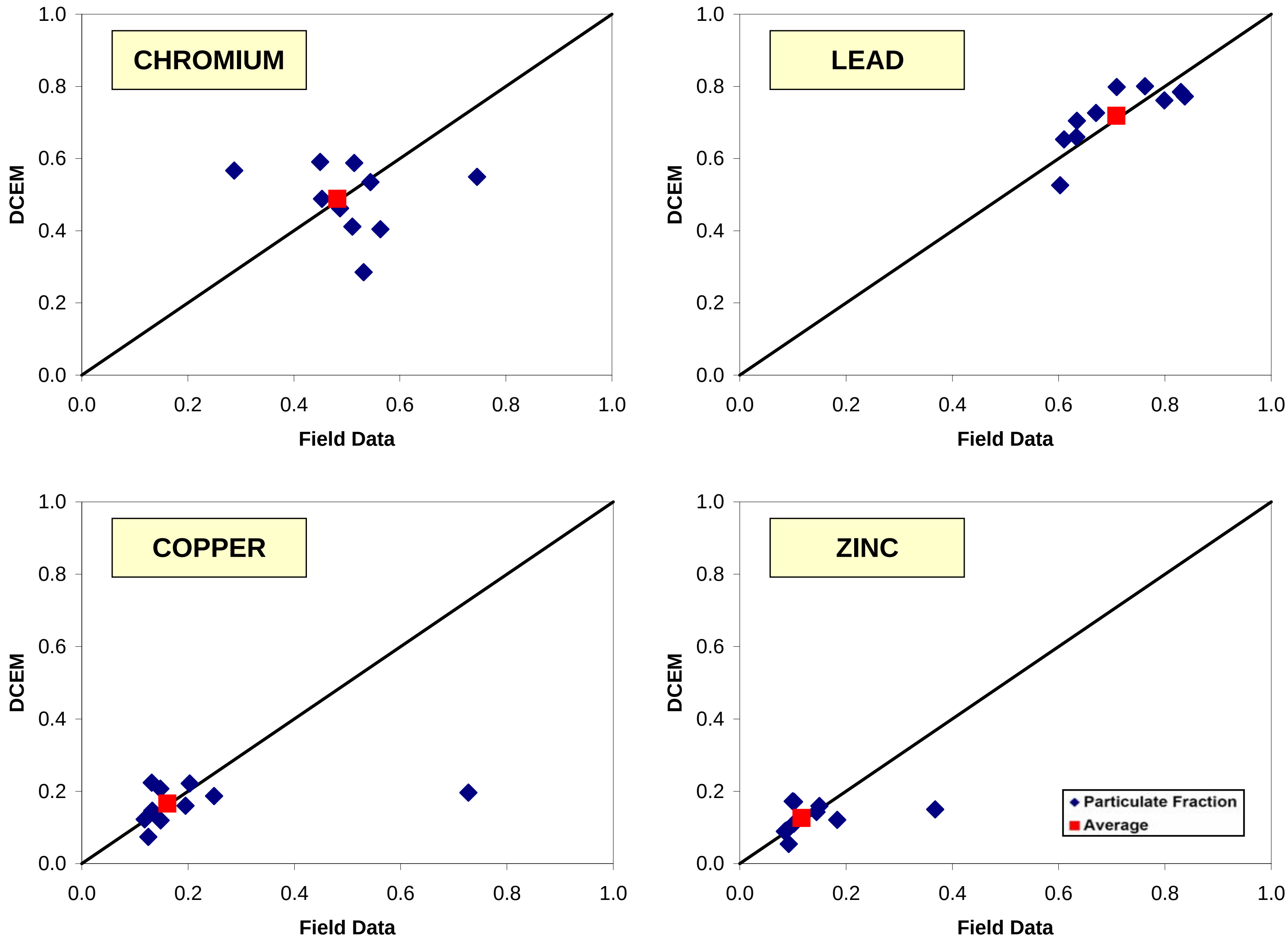

Figure 4.28 Comparison of Dry Weather Calibrated Particulate Fractions with Field Data

5. DRY WEATHER VERIFICATION

5.1 OVERVIEW

Similar to the dry weather calibration period selection, a 30-day verification period starting on August 18, 2005 and ending on September 18, 2005 was selected. A timeline showing the dry weather verification period and the field data collected during dry weather is shown in Figure 5.1. The dry weather verification was selected to start at the day of the second dry weather sampling event, indicated by the gray-shaded area in the figure.

The initial concentrations and a 30-day spin-up period were simulated in the same manner as the dry weather calibration except that dye was not simulated. Similarly, the ocean boundary was specified based on the tide data from the Los Angeles Outer Harbor gage and spatially-varying wind conditions were based on data from the eight meteorological stations. The same calibrated parameters selected for the dry weather calibration period (shown previously in Table 4.9) were used for simulating the hydrodynamics and water quality for the dry weather verification period.

Sediment and metal loadings from the storm drains were specified based on the average concentrations from the August 2005 pollutographs measured at Artesia. These concentrations are summarized in Table 5.1. The measured metal concentrations used for model comparison (Suite B samples) are provided in Table 5.2. Non-detect values for particulate lead samples were specified at the minimum detection level for the model comparison and calculation of the equilibrium partition coefficients.

Table 5.1 Dry Weather Verification Storm Drain Pollutant Concentrations

POLLUTANT	UNITS	CONCENTRATION
Cohesive Sediment	mg/L	5.0
Noncohesive Sediment	mg/L	0.0
Chromium	µg/L	1.6
Copper	µg/L	14.9
Lead	µg/L	1.3
Zinc	µg/L	20.8

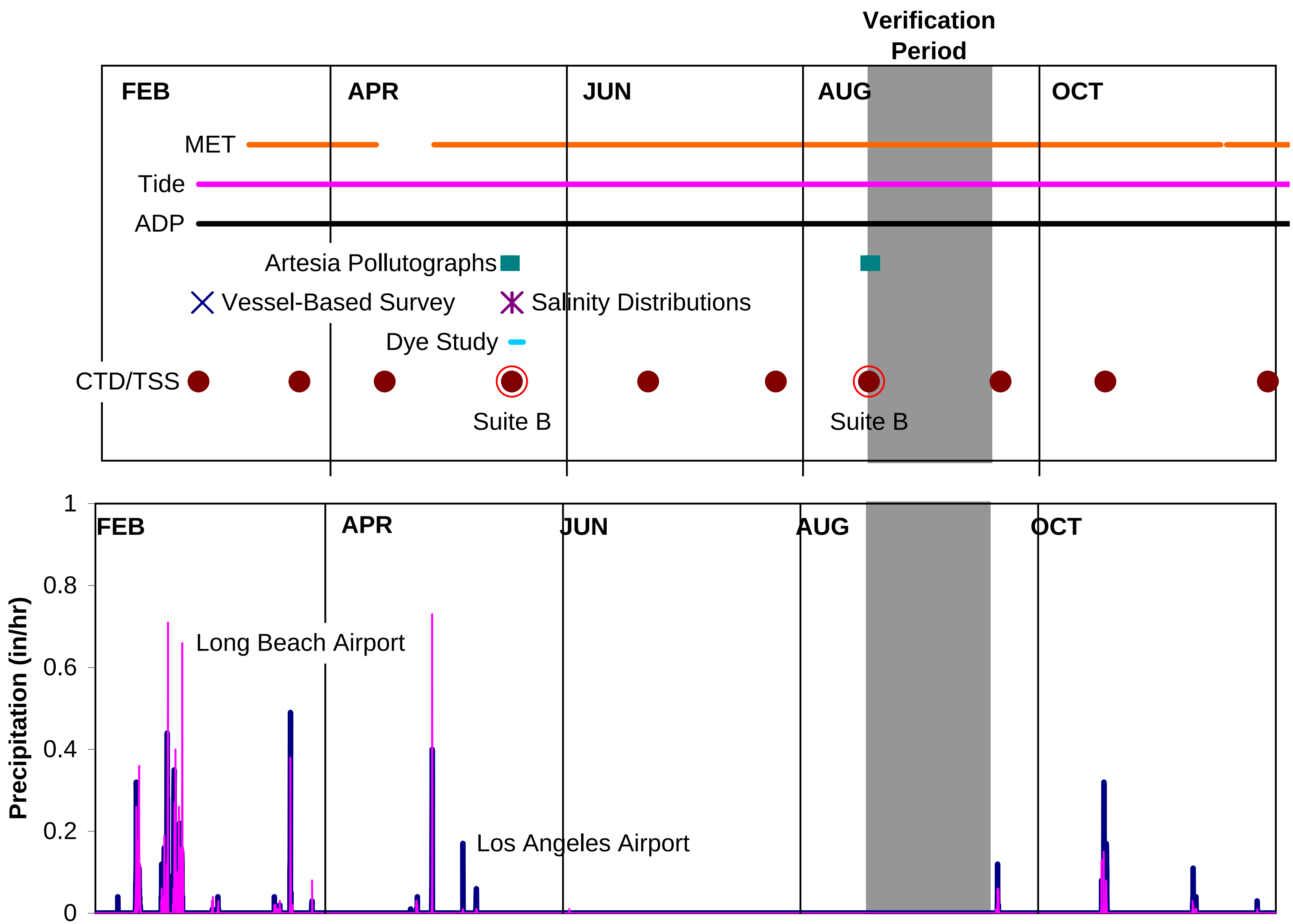

Figure 5.1 Dry Weather Verification Field Data Timeline

Table 5.2 Dry Weather Verification Estuary Metals Field Data

Sample Location	Depth	Dissolved (µg/L)	Particulate (µg/L)	Total (µg/L)	Particulate Fraction	Equilibrium Partition Coefficient (L/mg)
Chromium						
Sepulveda	Surface	0.48	0.07	0.55	0.13	0.08
	Bottom	0.24	0.08	0.32	0.25	0.30
E. I St	Surface	0.24	0.04	0.28	0.14	0.17
	Bottom	0.26	0.04	0.30	0.13	0.16
Berth 200G	Surface	0.28	0.05	0.33	0.15	0.19
	Mid	0.24	0.06	0.30	0.20	0.09
	Bottom	0.29	0.83	1.12	0.74	0.05
Berth 173	Surface	0.24	0.03	0.27	0.11	0.13
	Mid	0.23	0.06	0.29	0.21	0.10
	Bottom	0.22	0.05	0.27	0.19	0.16
Copper						
Sepulveda	Surface	1.48	0.05	1.53	0.03	0.02
	Bottom	1.21	0.06	1.27	0.05	0.05
E. I St	Surface	1.21	0.04	1.25	0.03	0.03
	Bottom	1.22	0.04	1.26	0.03	0.03
Berth 200G	Surface	1.66	0.03	1.69	0.02	0.02
	Mid	1.05	0.06	1.11	0.05	0.02
	Bottom	1.48	1.89	3.37	0.56	0.02
Berth 173	Surface	1.74	0.03	1.77	0.02	0.02
	Mid	1.53	0.03	1.56	0.02	0.01
	Bottom	1.12	0.10	1.22	0.08	0.06
Lead						
Sepulveda	Surface	0.453	ND	0.478	0.05	0.03
	Bottom	0.316	ND	0.341	0.07	0.07
E. I St	Surface	0.316	ND	0.341	0.07	0.01
	Bottom	3.090	ND	3.115	0.01	0.08
Berth 200G	Surface	0.802	ND	0.827	0.03	0.03
	Mid	0.110	ND	0.135	0.19	0.08
	Bottom	0.754	0.80	1.554	0.52	0.02
Berth 173	Surface	0.111	ND	0.136	0.18	0.24
	Mid	0.095	ND	0.120	0.21	0.10
	Bottom	0.249	ND	0.274	0.09	0.07
Zinc						
Sepulveda	Surface	10.4	0.19	10.59	0.18	0.01
	Bottom	10.2	0.22	10.42	0.02	0.02
E. I St	Surface	10.2	0.32	10.52	0.03	0.03
	Bottom	18.9	0.26	19.16	0.01	0.01
Berth 200G	Surface	11.5	0.12	11.62	0.01	0.01
	Mid	5.68	0.14	5.82	0.02	0.01
	Bottom	10.2	4.62	14.82	0.31	0.01
Berth 173	Surface	7.36	0.09	7.45	0.01	0.01
	Mid	5.54	0.09	5.63	0.02	0.01
	Bottom	5.45	0.16	5.61	0.03	0.02

ND – Non-detect is specified at minimum detection level of 0.025 µg/L for model comparisons

5.2 DRY WEATHER VERIFICATION RESULTS

The DCEM predicted results for water surface elevations, velocities, velocity profiles, salinity profiles, TSS, chromium, copper, lead, and zinc are compared with field measurements in this section.

5.2.1 Water Elevations and Velocities

The dry weather verified water surface elevations and velocities at the ADP locations are compared with field data in Figure 5.2 and Figure 5.3, respectively. As shown in Figure 5.2, the model predicted water surface elevations match very well with field measurements at all the four ADP locations. Also shown in the figure are the scatter plot comparisons of the daily water surface elevation peaks (HHW, HW, LW, and LLW), which show very good agreement between the DCEM and field data. Similar to the dry weather calibration results, the model predicted velocities, shown in Figure 5.3, generally compare well with the field data. The predicted and measured velocity profiles at S. Pacific Drive are compared at peak ebb and flood tide conditions during a spring and mean tide in Figure 5.4. Overall, the DCEM velocity profiles match the field data in both magnitude and shape.

5.2.2 Salinity

The DCEM dry weather verification water quality results for salinity are compared with field measurements in Figure 5.5. Except for the Sepulveda salinity profile, the DCEM salinity profiles compare well with the field data. As explained earlier, the DCEM under-predicts salinity at Sepulveda because, while the model specifies constant fresh water inflow near that location, the actual fresh water inflow could be sporadic and might not be present during the field measurement.

5.2.3 TSS and Metals

The DCEM-predicted and field-measured TSS are compared in Figure 5.6. The DCEM predicted cohesive sediment concentrations are within 2 mg/L of the field measurements, which were consistent with the May 2005 samples and included three non-detect samples. An exception occurred for the near-bottom TSS sample at Berth 200G with a high concentration of 62 mg/L. This sample was substantially higher than all other TSS field data collected and could have been an anomaly in the field data. Overall, the dry weather verification TSS concentrations were similar to the dry weather calibration results in magnitude and vertical variation.

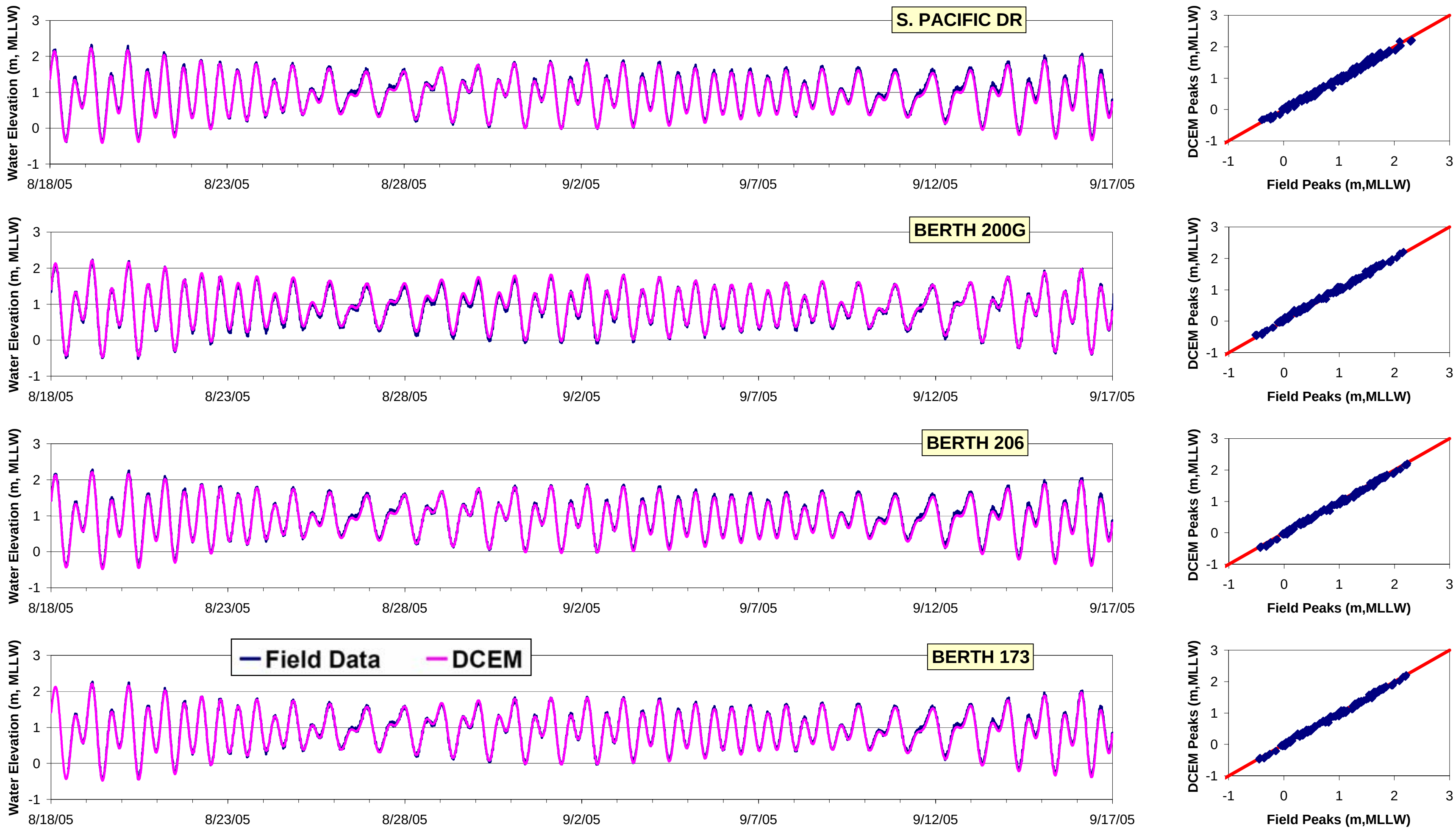

Figure 5.2 Dry Weather Verified Water Surface Elevations

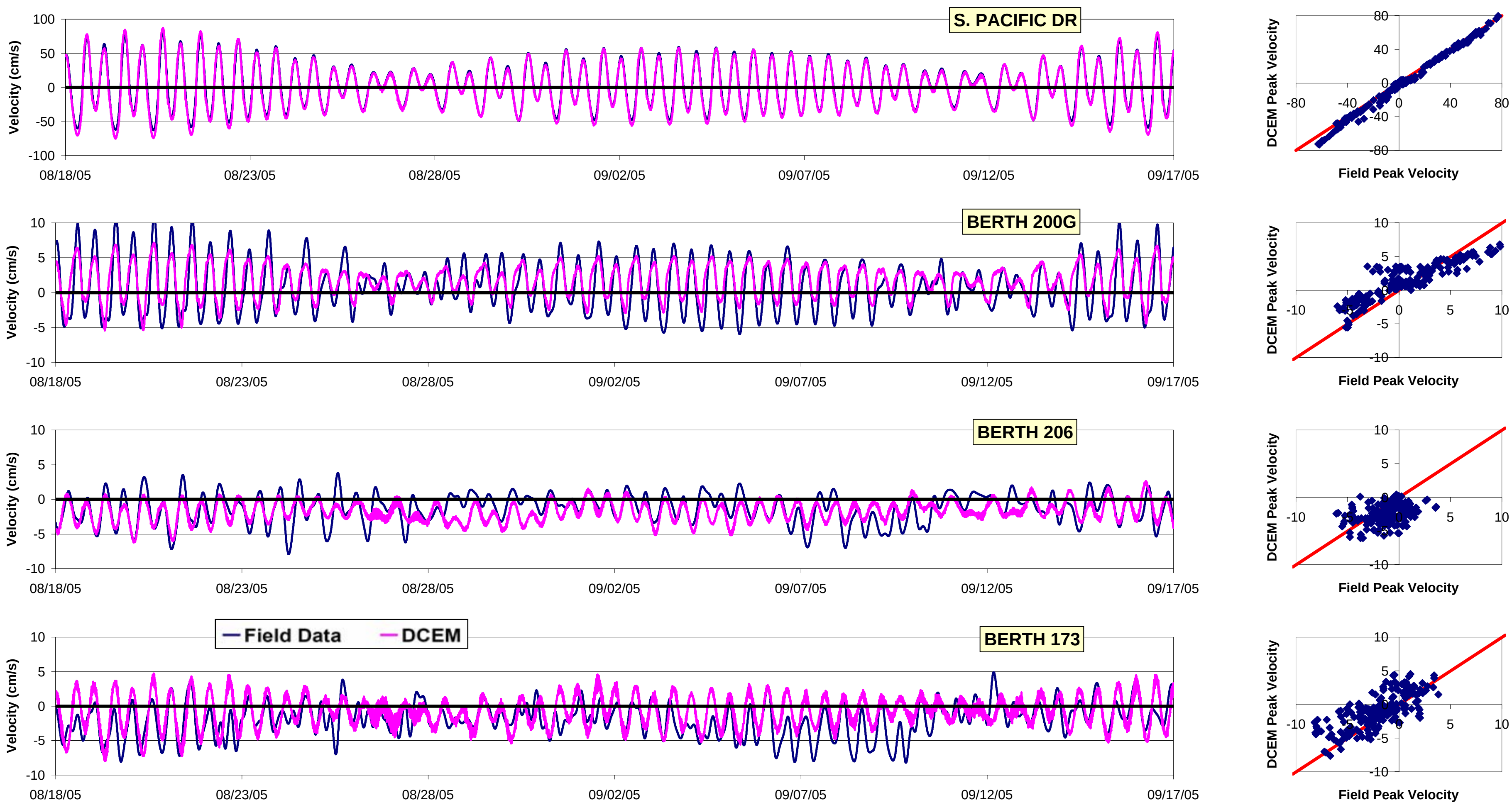

Figure 5.3 Dry Weather Verified Velocities

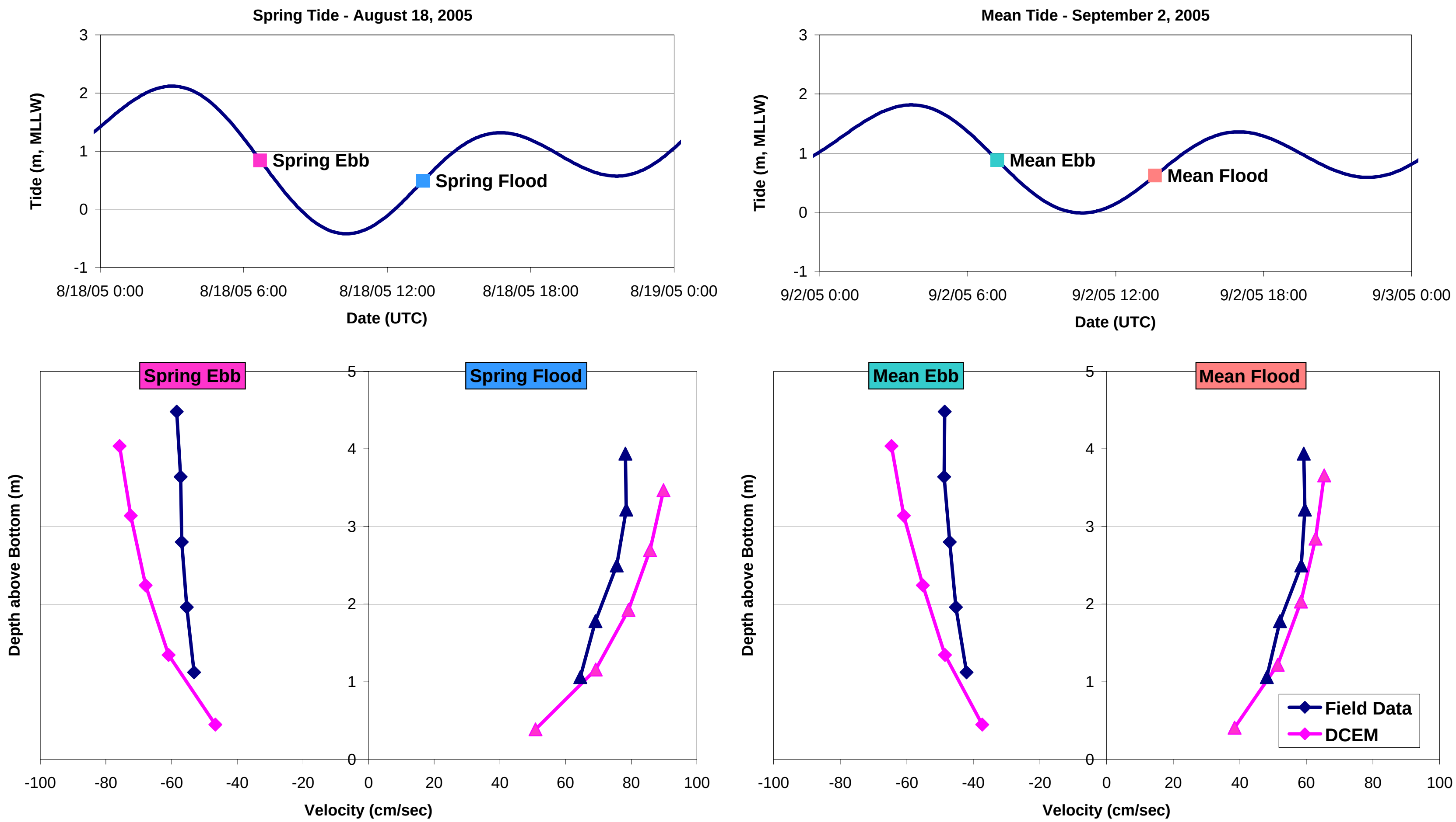

Figure 5.4 Dry Weather Verified Velocity Profiles

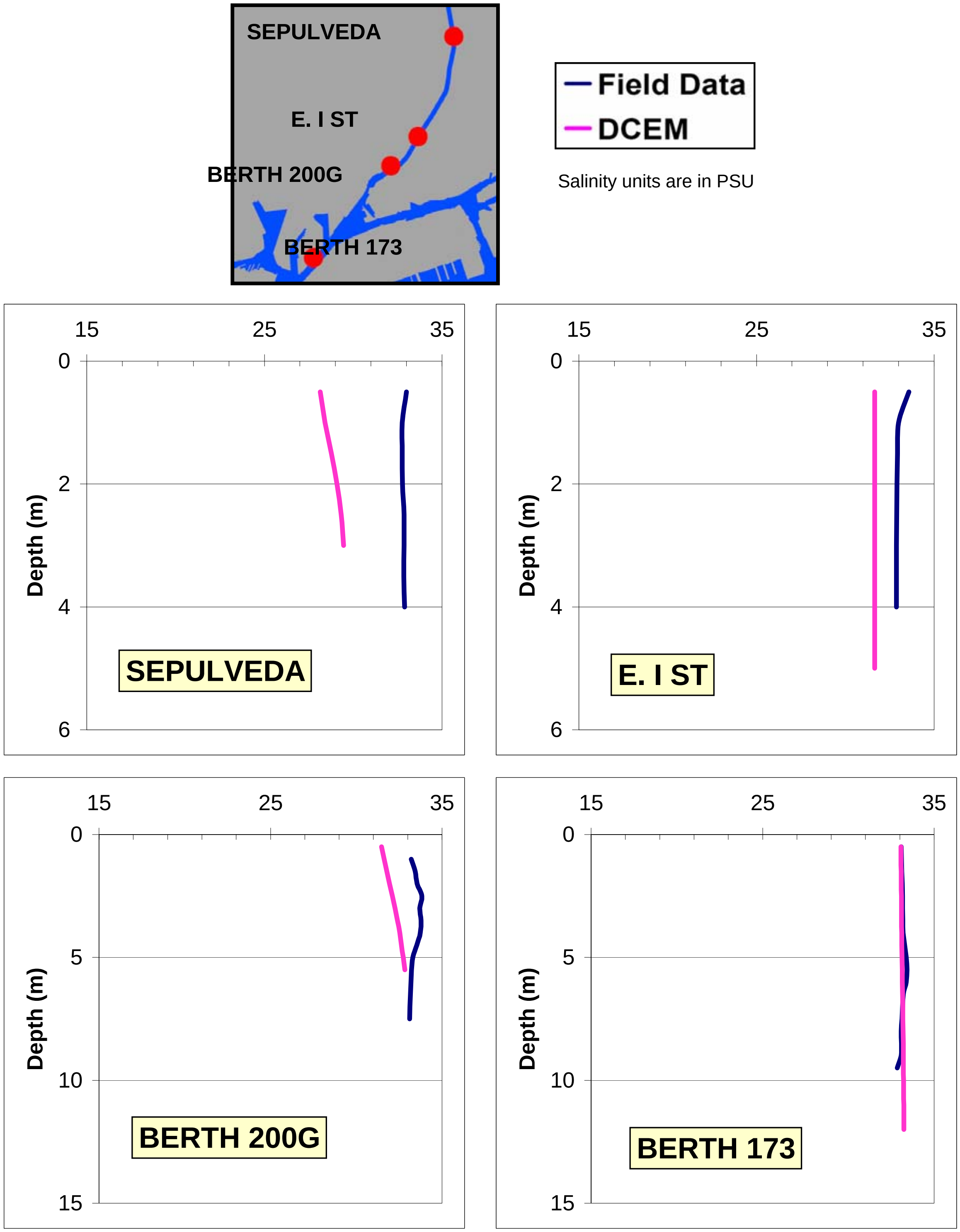

Figure 5.5 Dry Weather Verified Salinity Profiles

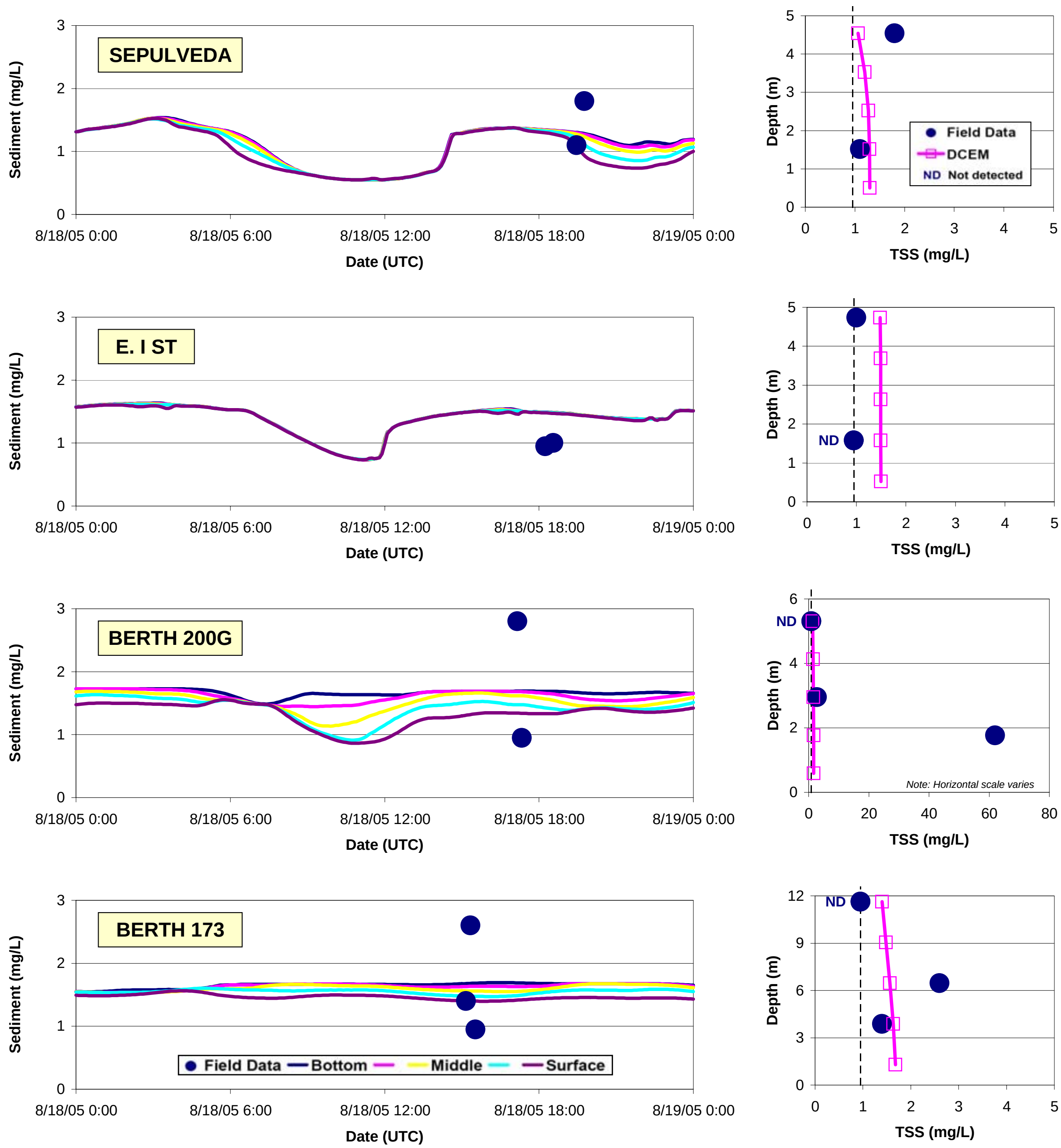

Figure 5.6 Dry Weather Verified TSS

The DCEM-predicted and field-measured chromium, copper, lead, and zinc time series concentrations and vertical profiles are compared in Figure 5.7 through Figure 5.10, respectively. In general, the DCEM metal concentrations were within the same order of magnitude as the field data. The vertical variations of the metal concentration time series, along with the magnitude of the total metal concentrations, were similar to those of the dry weather calibrated results.

The DCEM-predicted dissolved and particulate fractions, however, varied substantially from the field data, as shown by the scatter plot of the particulate fractions in Figure 5.11. The DCEM over predicted the particulate fractions, especially for chromium and lead, compared to the field data. These differences are most likely due to the variability in the field data collected for the dry weather calibration (May 2005) and dry weather verification (August 2005). While the verification field data showed similar total metal concentrations as the calibration field data, the particulate fractions were consistently lower resulting in proportionally higher dissolved metal concentrations and lower equilibrium partition coefficients. Table 5.3 compares the equilibrium partition coefficients for the May and August sampling events, as well as the corresponding average and standard deviations. As shown in the table, the August data for the verification event shows consistently lower equilibrium partition coefficients compared to the May data for the calibration event. The DCEM over-predicted the metal particulate concentrations since the equilibrium partition coefficients were calibrated based on the May field data. For chromium, the May field data showed an even distribution between dissolved and particulate chromium, while the August field data indicates a higher dissolved concentration. The May field data for lead indicated a larger particulate concentration which was switched to a larger dissolved concentration in the August field data. The copper and zinc particulate fractions did not differ as much since the May field data showed a higher dissolved proportion, which was lower in the August field data.

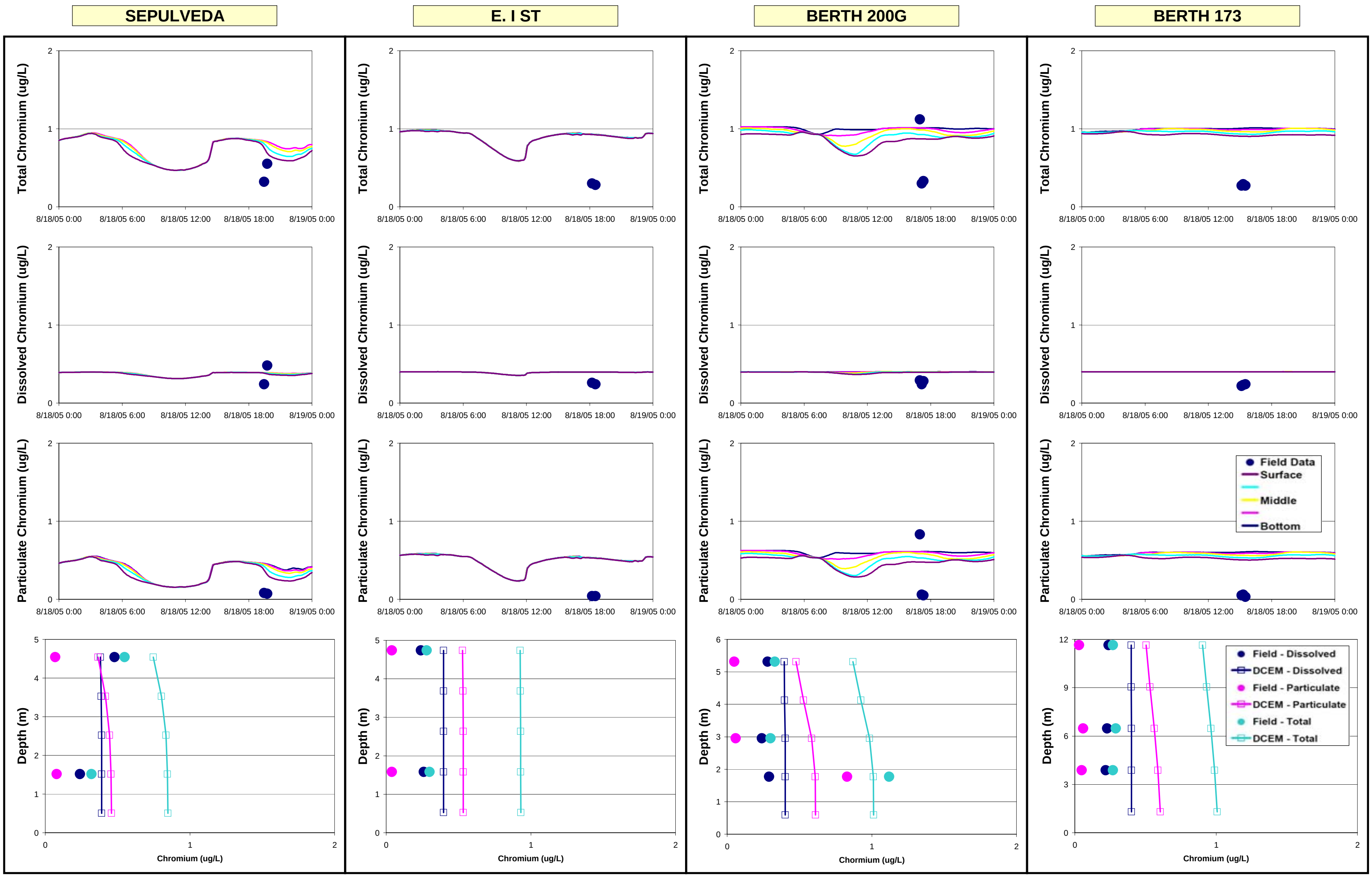

Figure 5.7 Dry Weather Verified Chromium

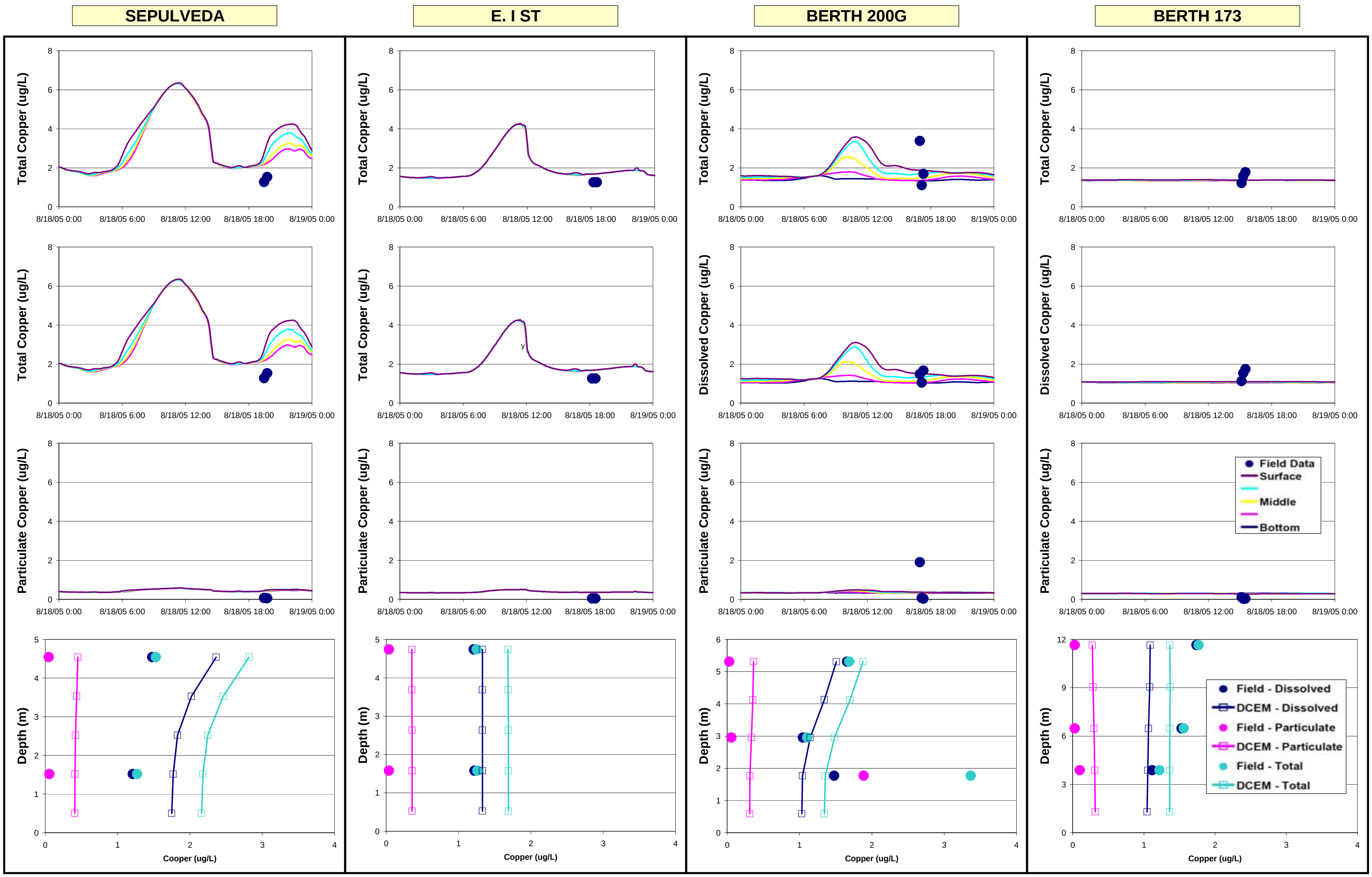

Figure 5.8 Dry Weather Verified Copper

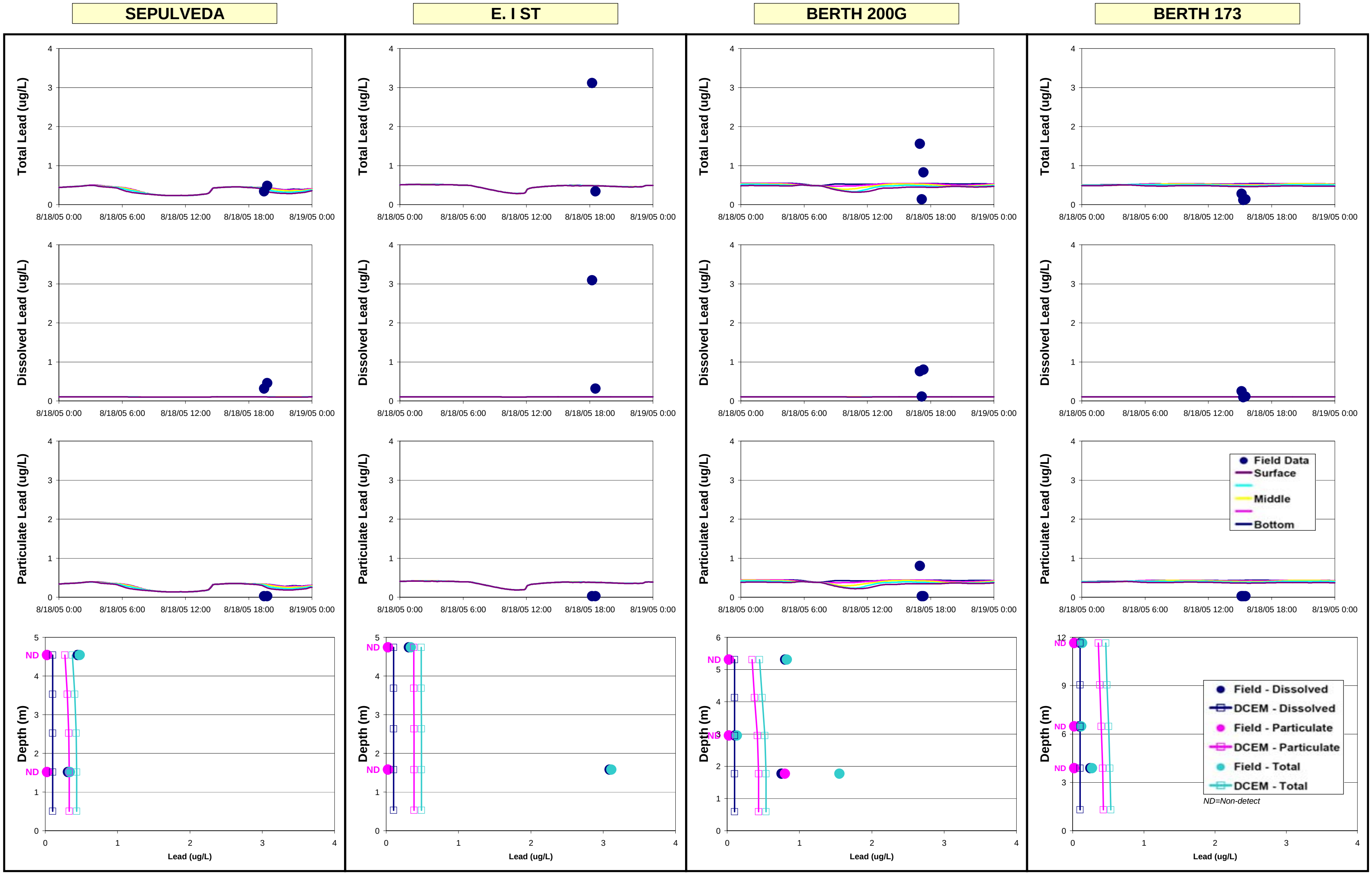

Figure 5.9 Dry Weather Verified Lead

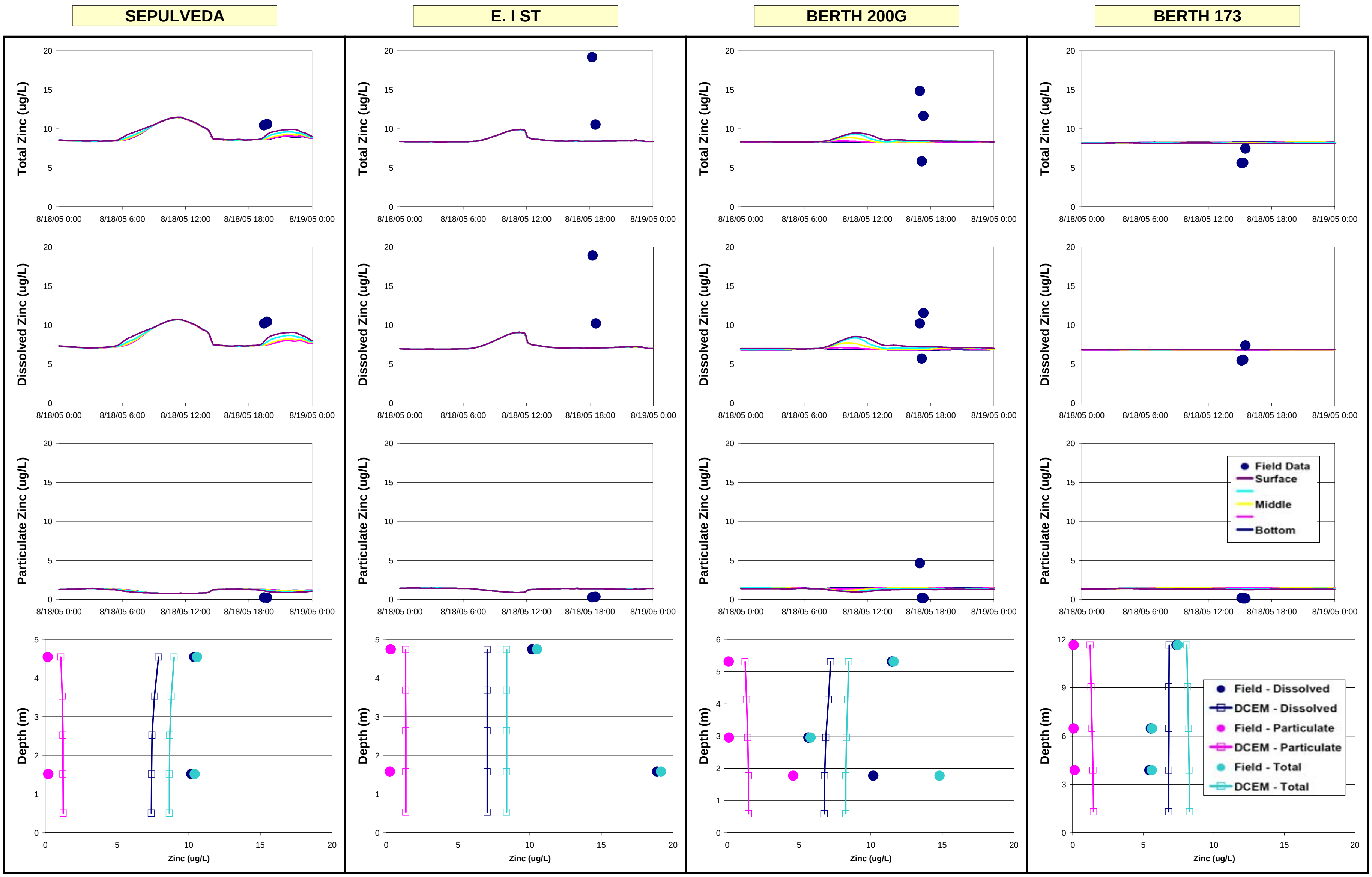

Figure 5.10 Dry Weather Verified Zinc

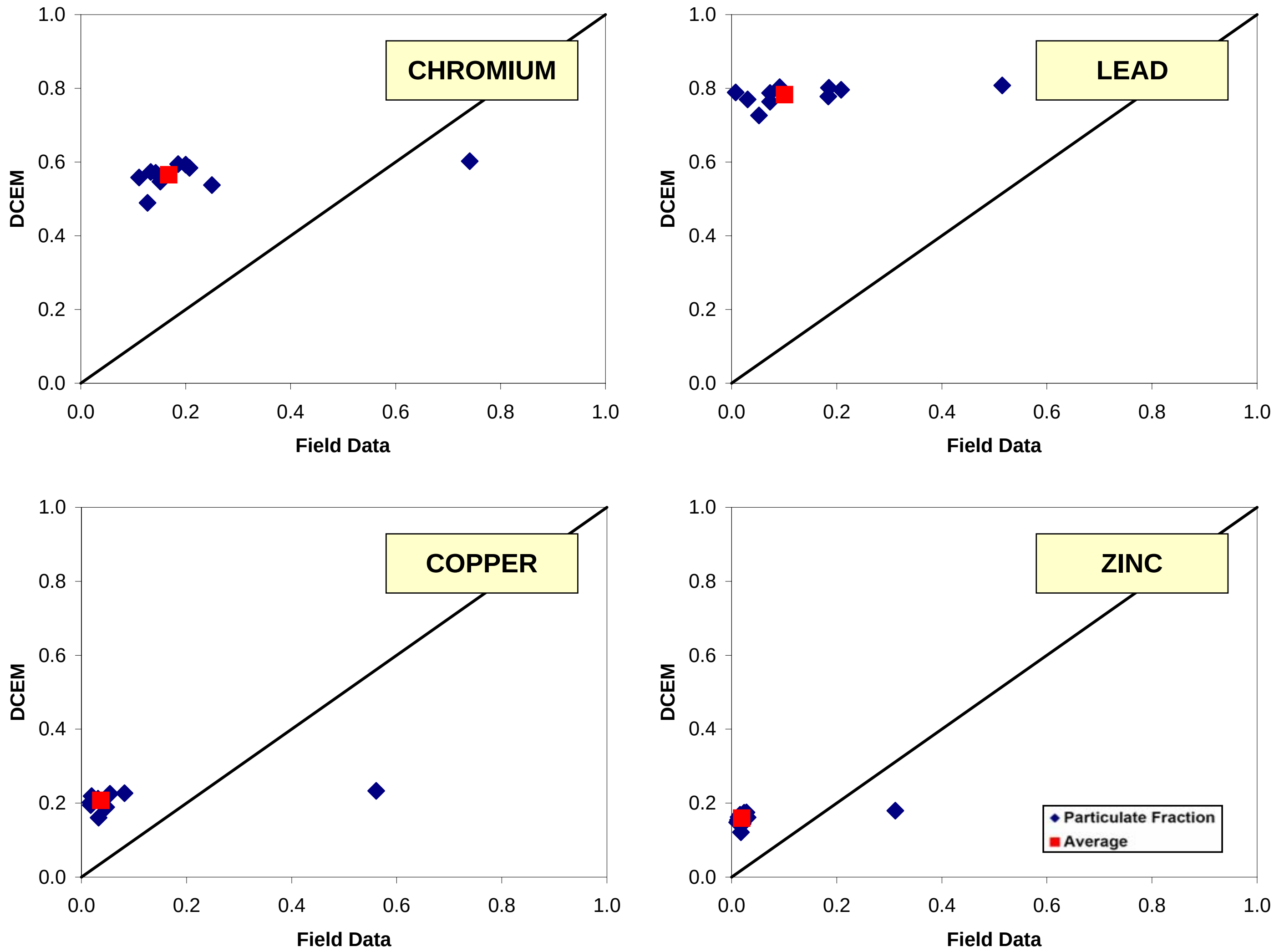

Figure 5.11 Comparison of Dry Weather Verified ParticulateFractions with Field Data

Table 5.3 Dry Weather Equilibrium Partition Coefficient Comparisons

Location	Chromium		Copper		Lead		Zinc	
	May	August	May	August	May	August	May	August
Sepulveda Bottom	0.25	0.30	0.03	0.05	0.30	0.07	0.02	0.02
Sepulveda Surface	1.20	0.08	0.15	0.02	1.60	0.03	0.11	0.01
E. I St Bottom	1.00	0.16	0.16	0.04	1.83	0.01	0.12	0.01
E. I St Surface	1.10	0.17	0.14	0.03	1.82	0.08	0.10	0.03
200G Bottom	0.21	0.05	0.19	0.02	0.37	0.02	0.04	0.01
200G Mid	1.20	0.09	0.33	0.02	3.97	0.08	0.17	0.01
200G Surface	0.87	0.19	0.26	0.02	2.14	0.03	0.24	0.01
173 Bottom	0.88	0.16	0.21	0.06	2.03	0.07	0.10	0.02
173 Mid	0.09	0.10	0.02	0.01	0.35	0.10	0.01	0.01
173 Surface	0.42	0.13	0.18	0.02	5.15	0.24	0.19	0.01
Average	0.72	0.14	0.17	0.03	1.96	0.07	0.11	0.01
Standard Deviation	0.41	0.07	0.09	0.02	1.49	0.06	0.07	0.01

6. WET WEATHER CALIBRATION

6.1 OVERVIEW

The DCEM wet weather calibration compared field data with model predictions of hydrodynamics and water quality constituents, in which hydrodynamics, salinity, cohesive sediment, noncohesive sediment, chromium, copper, lead, and zinc were simulated for a rain event. Field data used for model comparisons were continuous hydrodynamic conditions, spatial and temporal salinity profiles, and single-sample sediment and metal concentrations at multiple locations.

Similar to the layered and iterative approach of the dry weather calibration, the wet weather calibration procedure began with the calibrated dry weather conditions, followed by an evaluation of the mixing model parameters and then the metal model parameters. Parameters that were not contingent upon dry or wet weather conditions such as the tide boundary and wind conditions were not changed. The DCEM wet weather calibration procedure was conducted in the following steps:

- Select wet weather calibration period
- Select physical input conditions, boundary conditions, and model parameters
- Calibrate vertical mixing (velocity, salinity, and vertical profiles)
- Evaluate anti-diffusion corrections (velocity, salinity, and vertical profiles)
- Calibrate metal equilibrium partition coefficients (total, particulate, and dissolved metals)

The wet weather calibration started with the selection of the calibration period, then the input and boundary conditions. The model parameters were initially specified as the calibrated dry weather parameters; then model parameters that could vary between dry and wet weather conditions were evaluated.

6.2 WET WEATHER CALIBRATION SETUP

6.2.1 Calibration Period Selection

The wet weather calibration period was selected based on the wet weather field data collection in February 2006. This wet weather event lasted approximately 18-hours on February 27-28, 2006 (UTC). A timeline of the field data that were collected for this wet weather event, as well as the rainfall records in the area are shown in Figure 6.1. In the

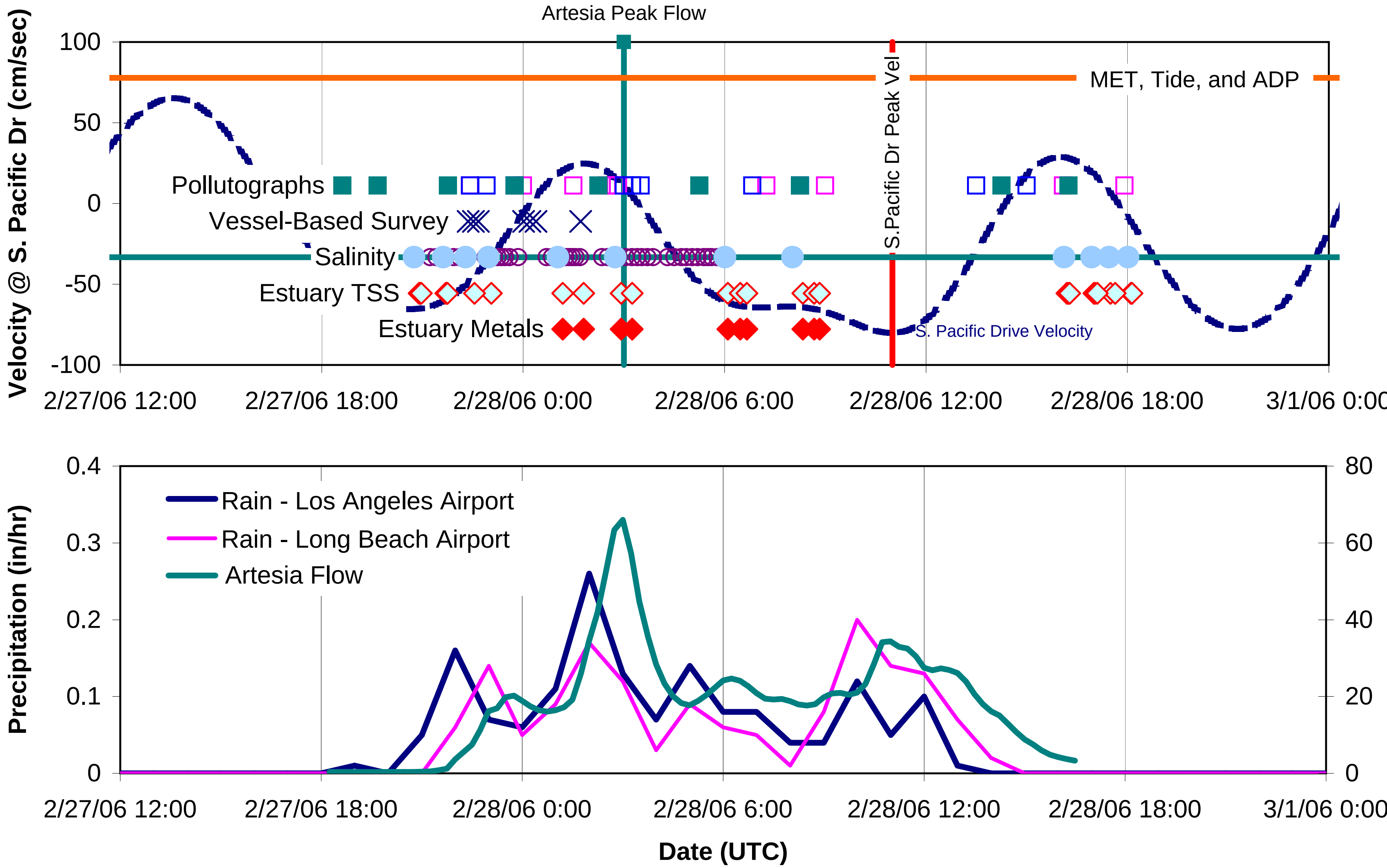

Figure 6.1 Wet Weather Calibration Field Data Timeline

figure, the lower panel shows the rainfall records for the Los Angeles and Long Beach Airports, as well as the flow data measured at Artesia. It can be seen that the peak of the flow hydrograph measured at Artesia had a lag time of a couple of hours behind the peak of the rainfall intensities.

The peak of the Artesia flow measurements is also indicated by the vertical green line on the upper panel of Figure 6.1. In this panel, the average velocity measured at S. Pacific Drive and the timing of the field measurements including meteorological, tide, ADP, pollutographs, vessel-based ADCP, salinity, TSS, and metals are shown. Also shown on this panel is the timing of the peak velocity at S. Pacific Drive indicated with a red line. The peak velocity corresponds to the peak flow at S. Pacific Drive. The peak flow into the Consolidated Slip would have occurred sometime after the peak arrival time at S. Pacific Drive.

The wet weather field samplings followed the rise, peak and fall of the rainfall event. Hence, as illustrated in Figure 6.1, with the time lags between the peak rainfall and the arrival of the peak flow to S. Pacific Drive (and subsequently the Consolidated Slip), most of the wet weather samples in the estuary were collected prior to substantial fresh water inflows to the sampling locations. Nevertheless, the bottom-mounted ADP at S. Pacific Drive captured the fresh water flow through the Dominguez Channel very well and provided the necessary velocity data to calibrate the hydrodynamics of DCEM. The most valuable data for wet weather calibration was the expanded salinity program designed to replace the originally planned wet weather dye study. As shown in Figure 6.2, the salinity sampling continued beyond the rain event for another two weeks, providing valuable data for calibrating the DCEM for both the rain event fresh water flows at the sampling locations, as well as the salinity recovery from the rain event. The figure also shows the two other rain events that occurred during this recovery time on March 3 and 6, 2006.

The wet weather calibration period was selected to start on February 27, 2006 and end March 15, 2006, which would capture the initial rain event as well as the salinity recovery period. However, the subsequent rain events on March 3 and 6, 2006 were not simulated since no flow or other samplings were performed for those two rain events.

A summary of the field data used for model comparisons is provided in Table 6.1.

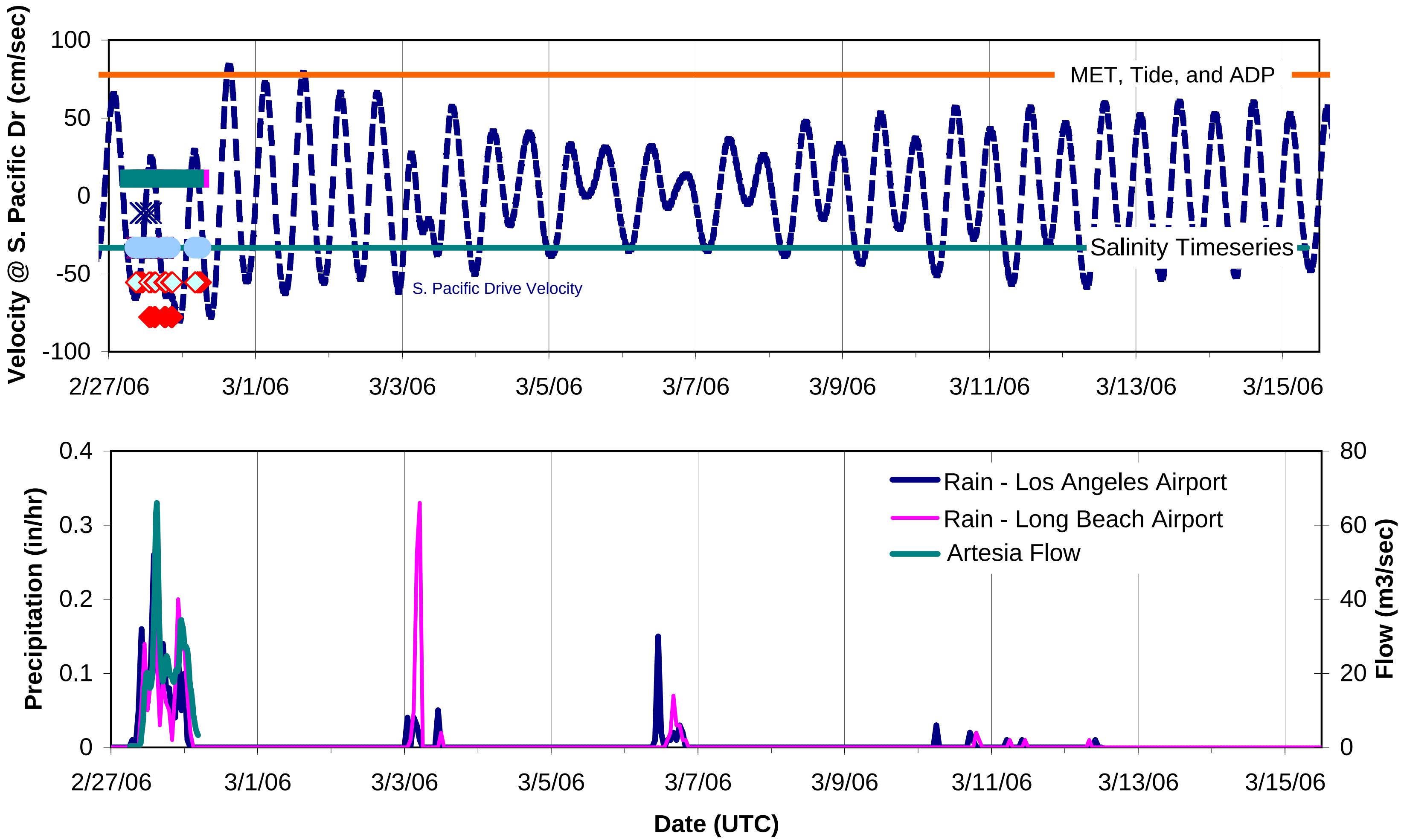

Figure 6.2 Wet Weather Calibration Salinity Recovery Timeline

Table 6.1 Wet Weather Calibration Model and Field Data Comparison Summary

<table>
<tr><th>MODEL PREDICTIVE PARAMETER</th><th>COMPARISON</th><th>CHANNEL LOCATIONS</th><th>HARBOR LOCATIONS</th><th>FIELD DATA</th></tr>
<tr><td>Water Surface Elevation</td><td>2/27 – 3/15/06</td><td>1</td><td>3</td><td>Fixed ADP</td></tr>
<tr><td>Velocity</td><td>Peak channel velocity</td><td>1</td><td>3</td><td>Fixed ADP</td></tr>
<tr><td>Velocity Vertical Profiles</td><td>2/27 – 6/28/06</td><td>1</td><td>0</td><td>Fixed ADP</td></tr>
<tr><td>Salinity</td><td>2/27 – 3/15/06</td><td>0</td><td>2</td><td>Continuous Salinity</td></tr>
<tr><td rowspan="2">Salinity Vertical Profile</td><td>Three measurements on 2/27 – 2/28/06</td><td>2</td><td>2</td><td>Estuary CTD</td></tr>
<tr><td>Periodically on 2/27 – 2/28/06</td><td>0</td><td>42</td><td>Salinity Distribution</td></tr>
<tr><td>Sediment</td><td>Three samples on 2/27 – 2/28/06</td><td>2 (2 depths)</td><td>2 (3 depths)</td><td>TSS sampling</td></tr>
<tr><td>Chromium (Cr)</td><td rowspan="4">Three samples on 2/27 – 2/28/06</td><td rowspan="4">2 (2 depths)</td><td rowspan="4">2 (3 depths)</td><td rowspan="4">Estuary Water Quality Suite B</td></tr>
<tr><td>Copper (Cu)</td></tr>
<tr><td>Lead (Pb)</td></tr>
<tr><td>Zinc (Zn)</td></tr>
</table>

6.2.2 Input and Model Boundary Conditions

This section summarizes the wet weather calibration input and boundary conditions that were different from the dry weather calibration, specifically the wet weather inflows and pollutant concentrations. Tide and wind data were obtained and used in the same manner as for the dry weather calibration. Initial salinity, cohesive sediment, noncohesive sediment, chromium, copper, lead, and zinc concentrations were also the same as those used for the dry weather calibration. Similar to the dry weather calibration, the wet weather calibration included a 30-day model “spin-up” time prior to the wet weather calibration period.

<u>Wet Weather Inflows and Concentrations</u>

The wet weather inflows from storms drains were estimated based on the measured flow at Artesia. Since the drainage area above Artesia accounts for only approximately 83% of the 103-km^2 Vermont drainage area, the wet weather hydrograph for the Vermont inflow was first scaled up to account for the larger drainage area, then shifted in time based on the estimated travel time of the flow between Artesia and Vermont. The travel time was estimated based on the average flow velocity in the channel during the rain event. A comparison of the Artesia flow data and the estimated flow hydrograph at Vermont is shown in Figure 6.3. The Vermont hydrograph was then used for estimating the other storm drain inflows based on a scaling factor calculated as the ratio of the respective drainage areas.

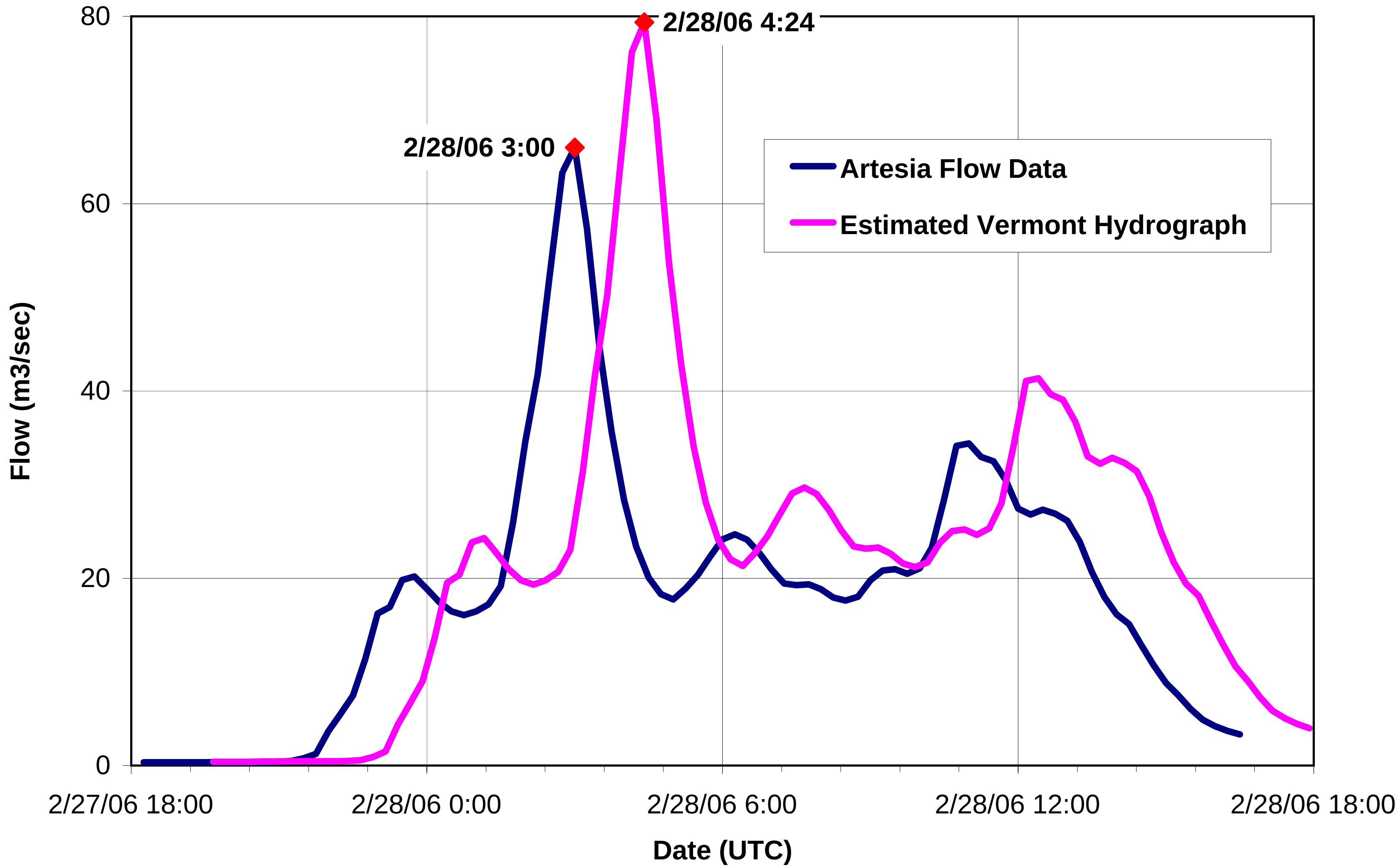

Figure 6.3 Wet Weather Artesia Flow and Estimated Vermont Hydrograph

The sediment and metals concentrations specified for wet weather calibrations at the 19 storm drain inflows considered by the DCEM were estimated based on field measurements taken at Artesia, Del Amo Lateral, and Torrance Lateral, which are shown in Figure 6.4. The sediment, chromium, copper, lead, and zinc concentrations for the Vermont inflow were assumed to be the same as those at the Artesia inflow, which have peak concentrations about three hours prior to the peak flow. The concentrations measured at Torrance Lateral were used for the 213th Street inflow, and the Del Amo concentrations were used for all the other storm drains.

Initial Model Calibration Parameters

Only parameters that might possibly vary from dry weather conditions were calibrated for wet weather conditions. These parameters include: mixing for maximum vertical kinematic viscosity and diffusivity, and the equilibrium partition coefficients of the four metals since these coefficients are dependent on salinity. The differences between fresh and salt water equilibrium partition coefficients were apparent based on the field data taken during the two dry weather events. During the dry weather events, the equilibrium partition coefficients for the fresh water samples taken at Artesia were substantially lower than the equilibrium partition coefficients of the estuary (saline) samples. This indicates that drops in salinity levels affect the fractionation between the dissolved and particulate metal concentrations. The dry weather calibrated model parameters that were used for the initial wet weather simulation are summarized in Table 6.2.

Table 6.2 Initial Parameters used for DCEM Wet Weather Calibration

MODEL PARAMETER	UNITS	VALUE
Maximum Vertical Kinematic Viscosity	m^2/sec	2E-3
Maximum Vertical Eddy Diffusivity	m^2/sec	1E-4
Equilibrium Partition Coefficient	L/mg	Cr 0.9 Cu 0.18 Pb 2.5 Zn 0.13

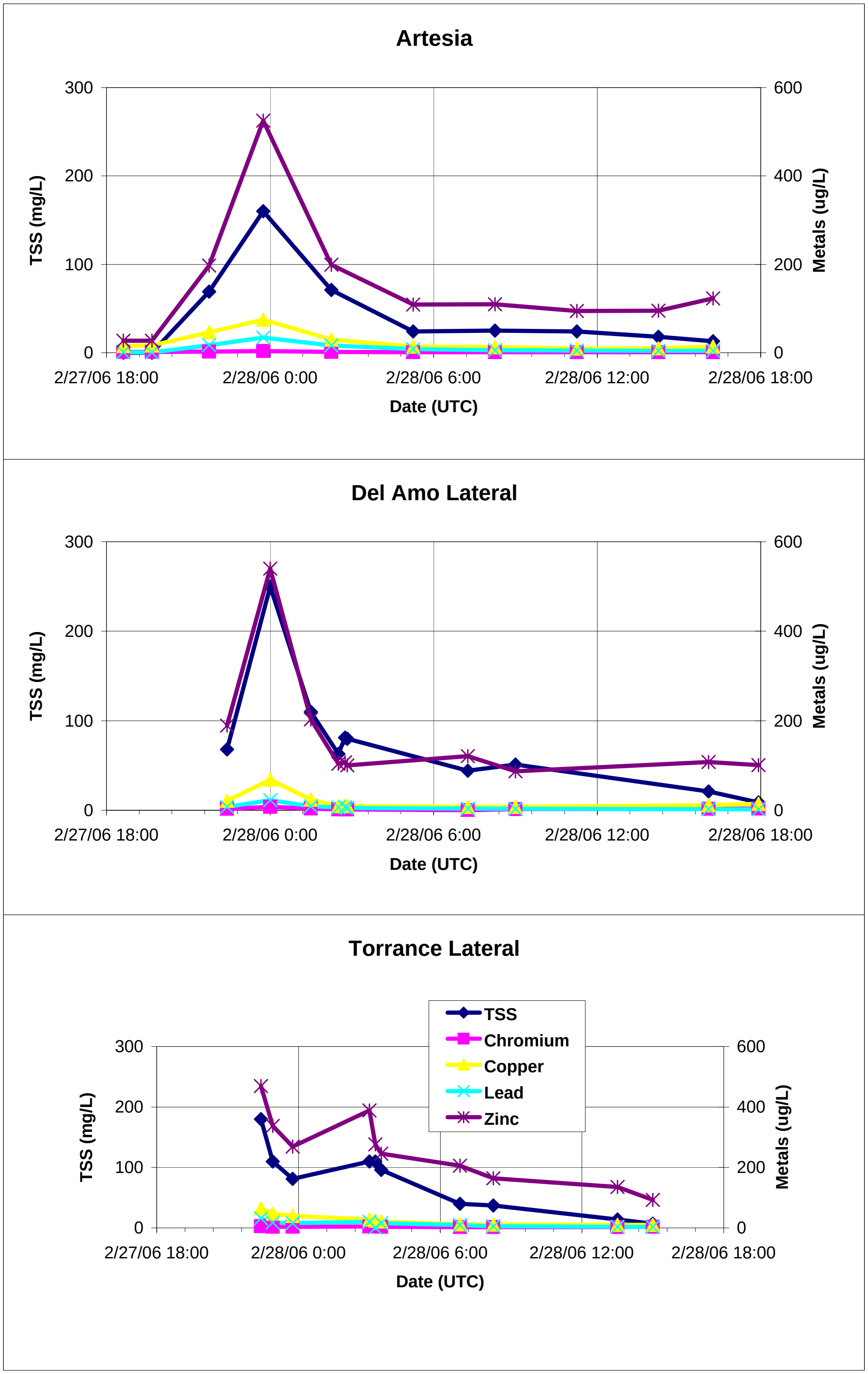

Figure 6.4 Wet Weather Concentrations

6.3 DCEM Parameter Calibration

6.3.1 Vertical Mixing

The vertical mixing characteristics were evaluated under wet weather conditions by comparing profiles and time series of velocity and salinity. TSS data, which are listed in Table 6.3, were also used to evaluate the mixing characteristics. Various combinations of the maximum vertical kinematic viscosity and diffusivity were simulated with values ranging from 1E-2 to 1E-5 m^2/sec.

Table 6.3 Estuary TSS Field Data used for Wet Weather Calibration

Sample Location	Depth	Rise TSS (mg/L)	Peak TSS (mg/L)	Fall TSS (mg/L)
Sepulveda – Surface	Surface	4.9	35	28
	Bottom	--	13	26
E. I St	Surface	3.8	9.1	26
	Bottom	--	2.8	4.2
Berth 200G	Surface	3.9	17	5.4
	Mid	4.8	13	6.2
	Bottom	3.6	3.3	16
Berth 173	Surface	ND	3.5	13
	Mid	ND	ND	2.9
	Bottom	2.7	1.2	2.8

ND – Non-detect is specified at minimum detection level of 0.95 mg/L for model comparisons

6.3.2 Metal Equilibrium Partition Coefficients

In calibrating the DCEM, the total, dissolved, and particulate metal data (10 samples) collected during the wet weather event at four locations were compared to model predicted concentration time series, as well as to vertical profiles. The wet weather field data for metals (chromium, copper, lead, and zinc) are summarized in Table 6.4. The wet weather metal concentrations were generally higher than those collected for either dry weather sampling events summarized previously in Table 4.8 and Table 5.2. A brief description of the field data are provided here.

Chromium

The chromium field data show a higher particulate fraction (an average particulate fraction of almost 70%) than to the dissolved fraction. The average equilibrium partition coefficient is similar to the average partition coefficient for the two dry weather estuary sampling events.

Copper

Copper concentrations had particulate fraction ranging from 26% to 72% with an average of 50%. The equilibrium partition coefficients for the copper samples also had a large variation between 0.03 and 0.77 L/mg with an average of 0.25 L/mg.

Lead

Lead data showed a higher particulate fraction with an average of about 90% and an average equilibrium partition coefficient of 2.4 L/mg. This equilibrium partition coefficient is nearly the same as the calibrated dry weather equilibrium partition coefficient of 2.5 L/mg.

Zinc

Similar to the dry weather estuary samples, zinc concentrations were higher than those of the other three metals. The data indicated an average particulate fraction of 20% and average equilibrium partition coefficient of 0.05 L/mg, which is lower the May 2005 average.

Table 6.4 Wet Weather Calibration Estuary Metals Field Data

Sample Location	Depth	Dissolved (µg/L)	Particulate (µg/L)	Total (µg/L)	Particulate Fraction	Equilibrium Partition Coefficient (L/mg)
Chromium						
Sepulveda	Surface	0.62	2.88	3.50	0.82	0.13
	Bottom	0.40	1.60	2.00	0.80	0.31
E. I St	Surface	0.39	1.18	1.57	0.75	0.33
	Bottom	0.32	0.57	0.89	0.64	0.64
Berth 200G	Surface	0.56	1.85	2.41	0.77	0.19
	Mid	0.54	1.55	2.09	0.74	0.22
	Bottom	0.32	0.66	0.98	0.67	0.63
Berth 173	Surface	0.57	0.92	1.49	0.62	0.45
	Mid	0.53	0.41	0.94	0.44	0.81
	Bottom	0.35	0.31	0.66	0.47	0.74
Copper						
Sepulveda	Surface	5.20	5.99	11.19	0.54	0.03
	Bottom	2.08	2.43	4.51	0.54	0.09
E. I St	Surface	1.78	3.59	5.37	0.67	0.22
	Bottom	1.11	0.98	2.09	0.47	0.32
Berth 200G	Surface	4.03	4.19	8.22	0.51	0.06
	Mid	3.12	3.14	6.26	0.50	0.08
	Bottom	0.56	1.43	1.99	0.72	0.77
Berth 173	Surface	2.88	2.35	5.23	0.45	0.23
	Mid	1.64	0.63	2.27	0.28	0.40
	Bottom	1.48	0.51	1.99	0.26	0.29
Lead						
Sepulveda	Surface	0.22	7.08	7.30	0.97	0.92
	Bottom	0.12	2.50	2.62	0.95	1.60
E. I St	Surface	0.28	4.36	4.64	0.94	1.71
	Bottom	0.11	0.84	0.95	0.88	2.73
Berth 200G	Surface	0.18	4.32	4.50	0.96	1.41
	Mid	0.16	2.94	3.10	0.95	1.41
	Bottom	0.07	0.83	0.90	0.92	3.59
Berth 173	Surface	0.18	2.25	2.43	0.93	3.47
	Mid	0.13	0.49	0.62	0.79	3.97
	Bottom	0.07	0.27	0.34	0.79	3.21
Zinc						
Sepulveda	Surface	84.2	36.2	120.4	0.30	0.01
	Bottom	39.8	10.2	50.0	0.20	0.02
E. I St	Surface	33.2	14.5	47.7	0.30	0.05
	Bottom	16.4	2.07	18.47	0.11	0.05
Berth 200G	Surface	74.4	20.7	95.1	0.22	0.02
	Mid	44.8	14.0	58.8	0.24	0.02
	Bottom	9.0	2.78	11.78	0.24	0.09
Berth 173	Surface	47.0	11.3	58.3	0.19	0.07
	Mid	15.4	1.43	16.83	0.08	0.10
	Bottom	8.65	0.68	9.33	0.07	0.07

6.4 WET WEATHER CALIBRATED RESULTS

A list of the selected wet weather calibration parameters are shown in Table 6.5. The only model parameters that differed from the dry weather calibrated parameters are the equilibrium partition coefficients for chromium and zinc, which were lower for the wet weather calibration than the dry weather calibration.

Table 6.5 DCEM Wet Weather Calibrated Parameters

MODEL PARAMETER	UNITS	VALUE
Maximum Vertical Kinematic Viscosity	m^2/sec	2E-3
Maximum Vertical Eddy Diffusivity	m^2/sec	1E-4
Equilibrium Partition Coefficient	L/mg	Cr 0.44* Cu 0.18 Pb 2.5 Zn 0.03*

** Differs from dry weather parameter*

The DCEM-predicted results based on these selected wet weather parameters were compared with field data for water surface elevations, velocities, velocity profiles, continuous salinity, salinity profiles, TSS, and metals (chromium, copper, lead, and zinc).

6.4.1 Water Elevations and Velocities

The DCEM-predicted water surface elevations between February 27 and March 16, 2006 are compared with the field data in Figure 6.5. As shown in the figure, the DCEM water surface elevations compare very well with the field data.

The wet weather DCEM-predicted velocities for S. Pacific Drive, Berth 206, and Berth 173 are compared with field measurements in Figure 6.6. Velocity data collected at Berth 200G during this time period were determined to have been affected by nearby barge activities and were not used for model comparisons. As shown in the figure, the model captured the arrival of the peak flow and the magnitude of the peak velocity at the S. Pacific Drive very well. The measured velocities at S. Pacific Drive also show the peak velocities during the March 3, 2005 rain event, which was not simulated.

The model predicted and field measured velocity profiles at S. Pacific Drive during the rain event are compared in Figure 6.7. Eleven vertical velocity profiles are compared over the course of the rain event. The top panel of the figure shows the time the profiles were taken relative to the velocity measured at S. Pacific Drive. To provide a reference to the rainfall event, the estimated time when the peak flow reached Vermont Avenue and the time when the peak velocity arrived at S. Pacific Drive are also indicated. In general, the DCEM

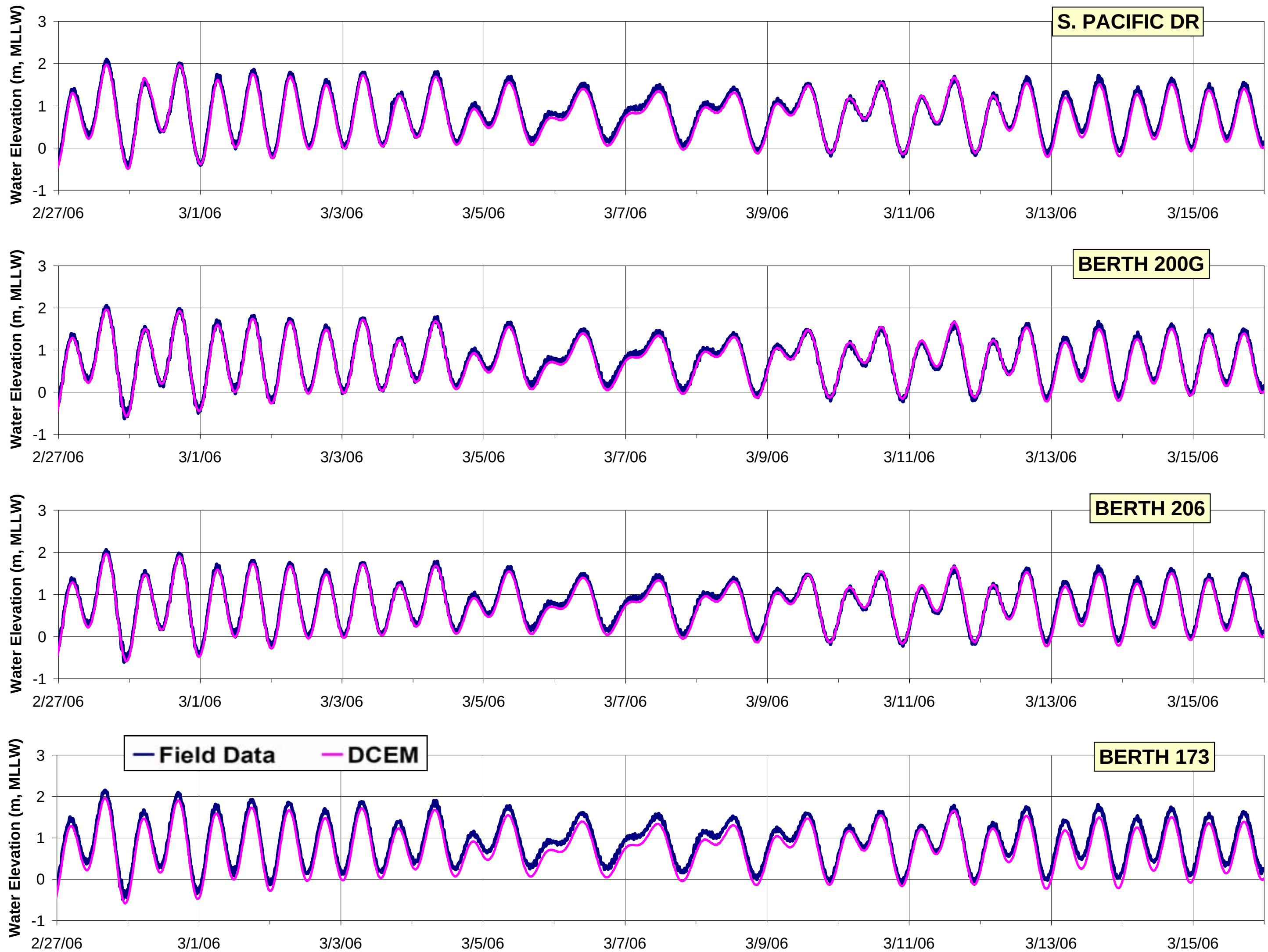

Figure 6.5 Wet Weather Calibrated Water Surface Elevations

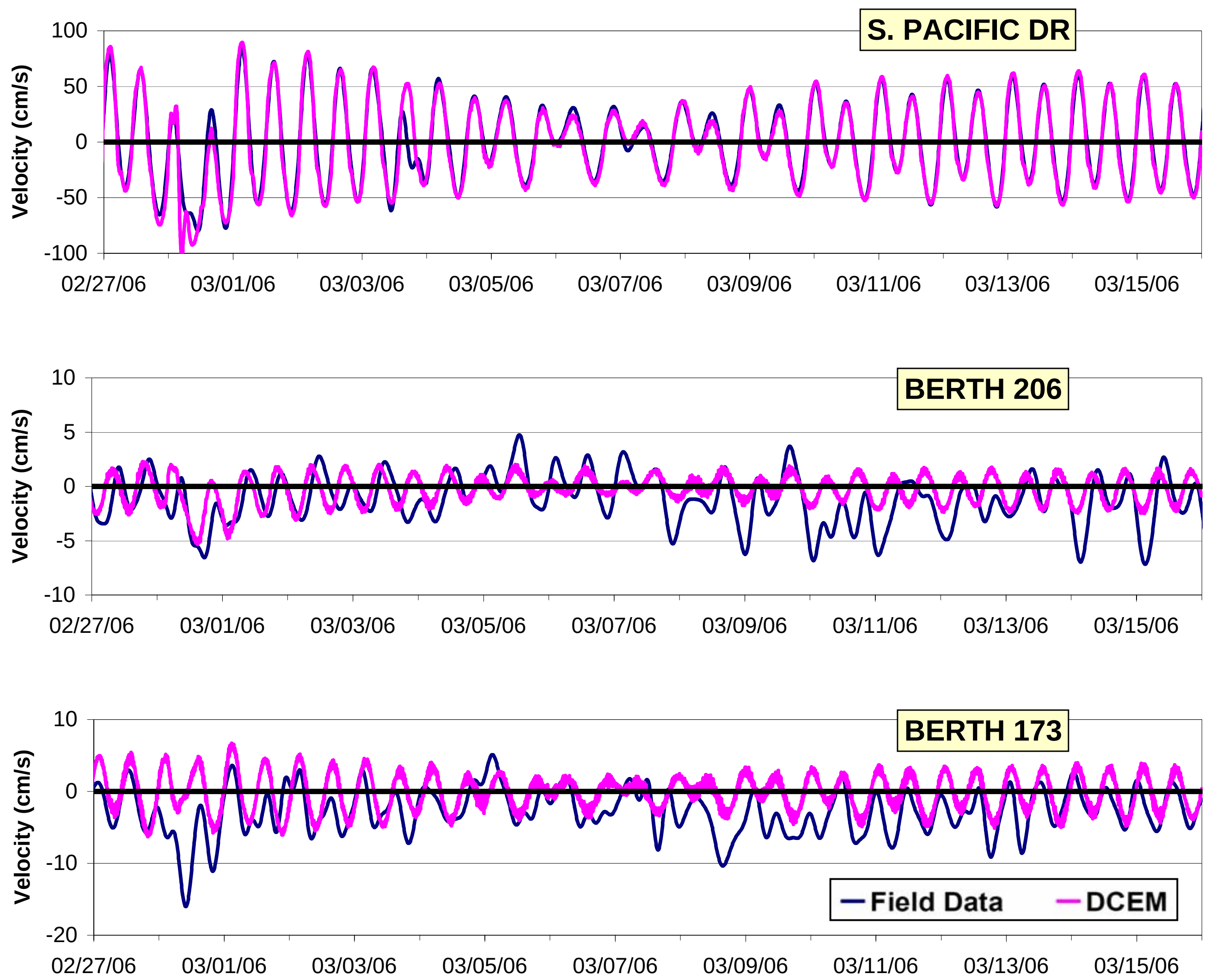

Figure 6.6 Wet Weather Calibrated Velocities

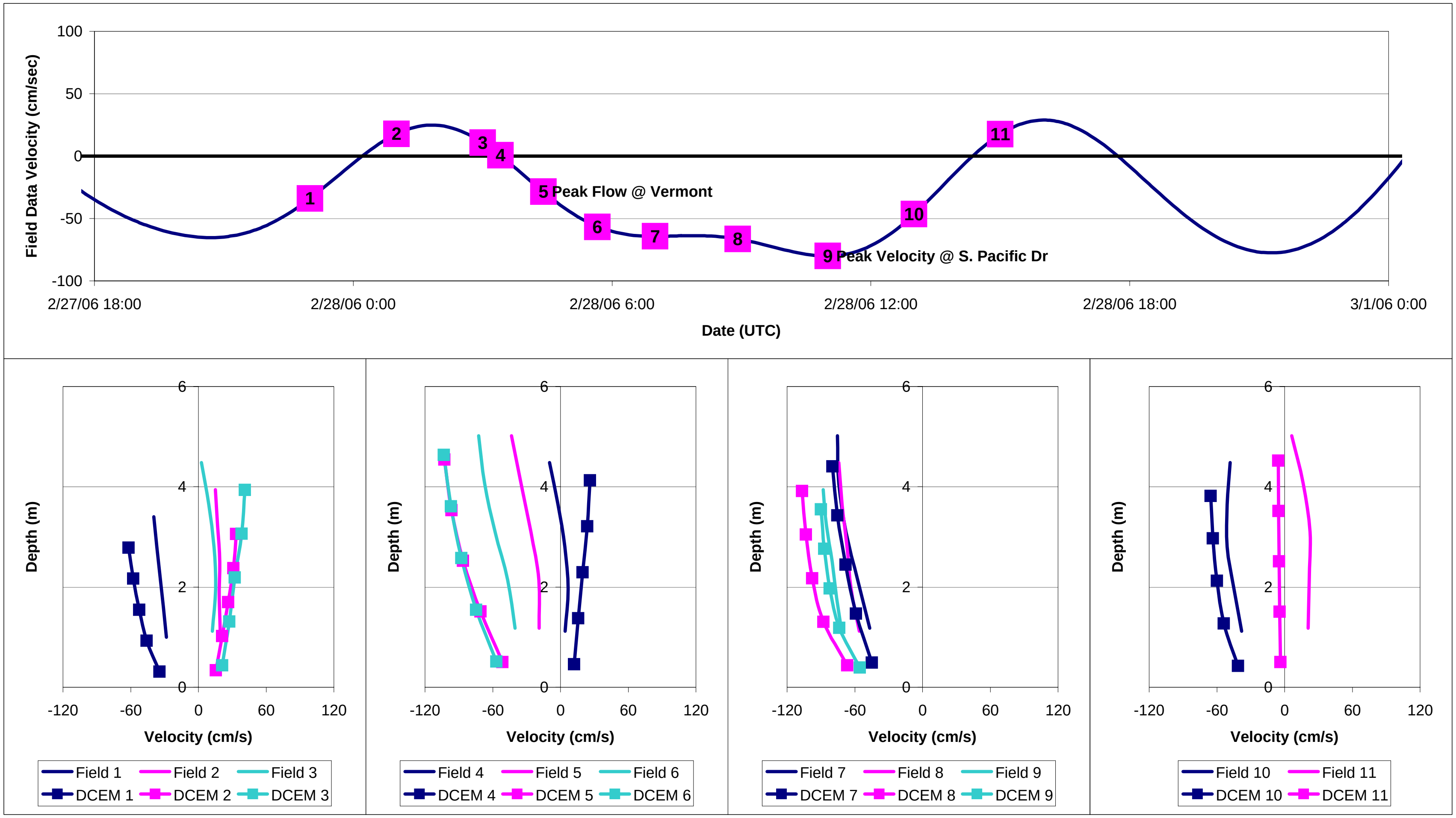

Figure 6.7 Wet Weather Calibrated Velocity Profiles

velocity profiles match well with the field data for both the magnitude and shape of the profiles.

6.4.2 Salinity

The DCEM-predicted and field-measured salinity data at Berth 200G and Berth 173 for the rain event and the recovery period (February 27 to March 16, 2006) are compared in Figure 6.8. As shown in the figure, the DCEM captured the arrival of the fresh water (both in the timing and the drop in salinity levels) at the sampling locations very well. In addition, the DCEM-simulated salinity concentrations follow the trends of the field data very well, especially at Berth 200G, including the salinity recovery over the entire 18-day simulation period.

Additional salinity profiles taken at the four CTD locations (Sepulveda, E.I. St., Berth 200G and Berth 173) and from boat transects are compared with DCEM predictions in Figure 6.9. In the figure, the salinity profiles are grouped by location and the gray-shaded charts indicate profiles taken at the CTD sampling locations. In general, the DCEM profiles match the field data, especially in the East Basin, Cerritos Channel, and Main Channel. As discussed earlier, the model under-predicts the salinity at Sepulveda.

A scatter plot comparison of the DCEM-predicted and field-measured near-surface salinity at all the salinity profile locations (shown in Figure 6.9) is shown in Figure 6.10. The comparison shows that in general, the model slightly under-predicts the near-surface salinity.

6.4.3 TSS and Metals

Figure 6.11 shows the comparison of field measured and DCEM predicted TSS results. The figure includes time series and vertical profile comparisons at the four sampling locations, and the time series which shows the cohesive sediment concentrations in the five water column layers. The results in the Dominguez Channel at Sepulveda show two peaks in concentration. The first peak corresponds to the peak inflow TSS concentration, which results in a peak in TSS loading. In addition, there is a large vertical gradient with a higher surface concentration indicating the TSS has not fully mixed vertically. The second concentration peak corresponds to the peak flow and shows uniform vertical concentration indicating a greater vertical mixing with the higher flows. These peaks also occur for the results at E. I St. with a slight lag as the flow moves from Sepulveda down to E. I St. The results for Berth 200G show the concentrations are more diffused, as opposed to the sharper peaks in the channel. The vertical gradients are attributed to the deeper water depths as the Dominguez Channel empties into the Consolidated Slip. The cohesive sediment concentrations at Berth 173 show that there has been sufficient horizontal and vertical mixing to diffuse the sediment concentrations, as such the peak concentration is

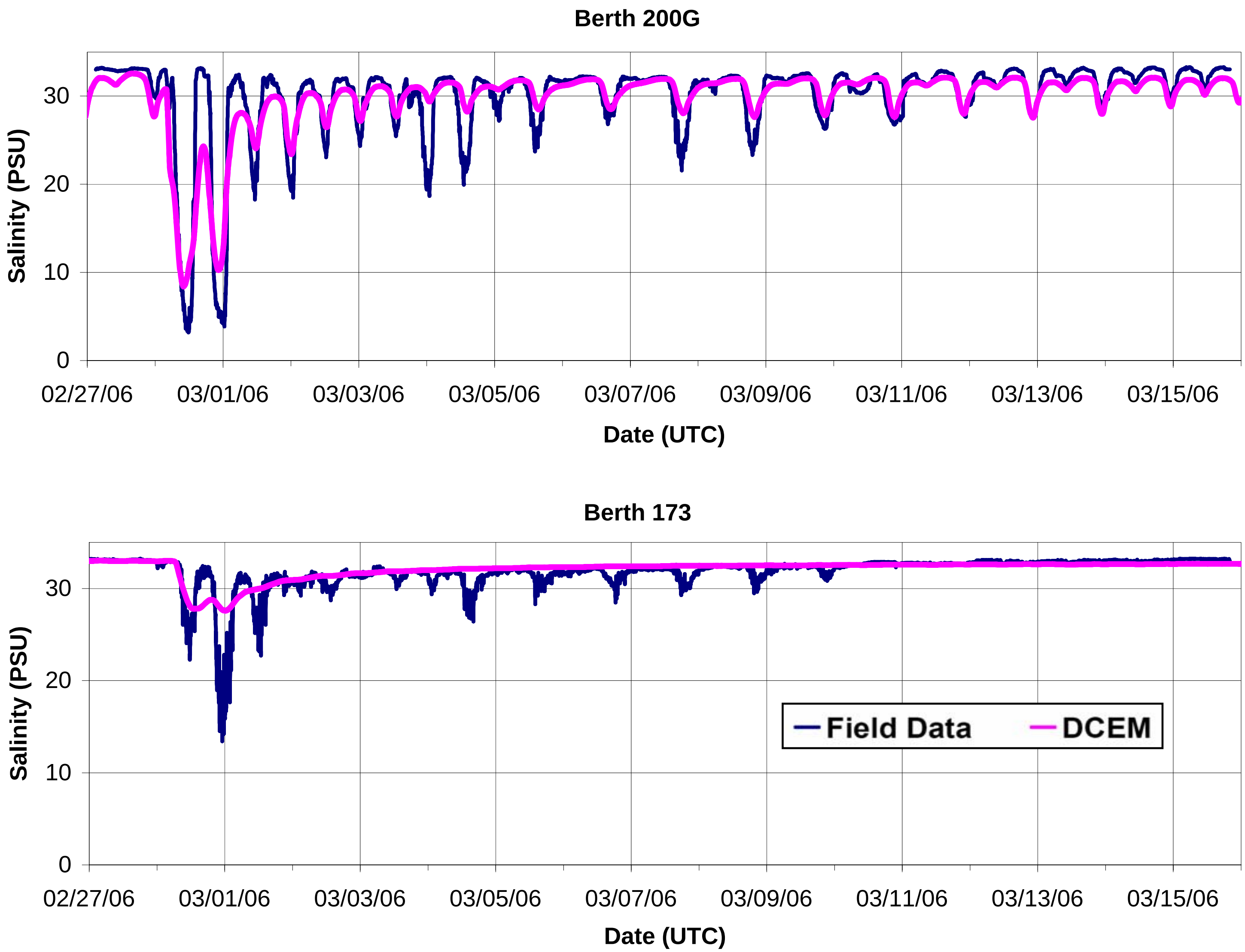

Figure 6.8 Wet Weather Calibrated Salinity

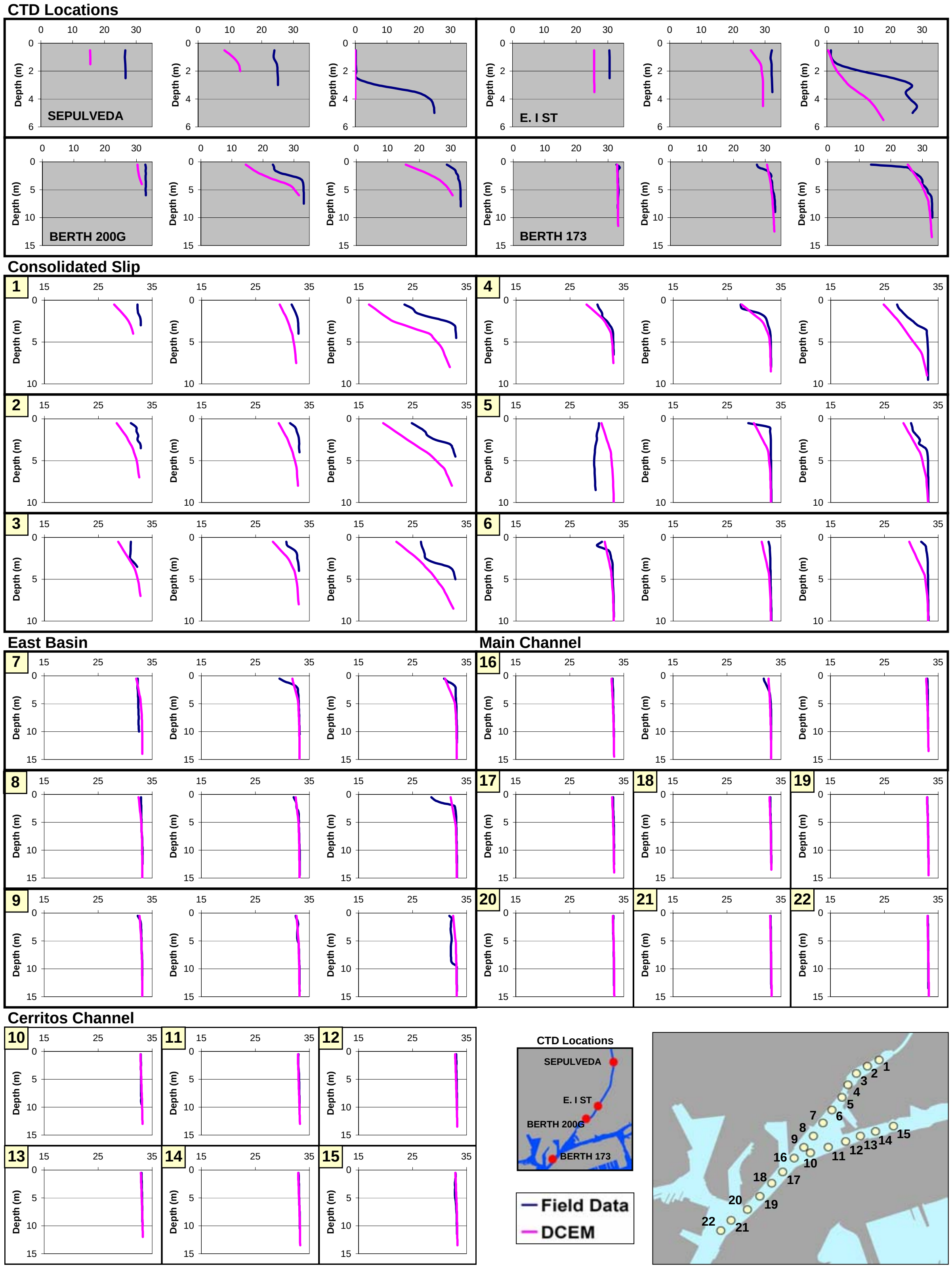

Figure 6.9 Wet Weather Calibrated Salinity Profiles

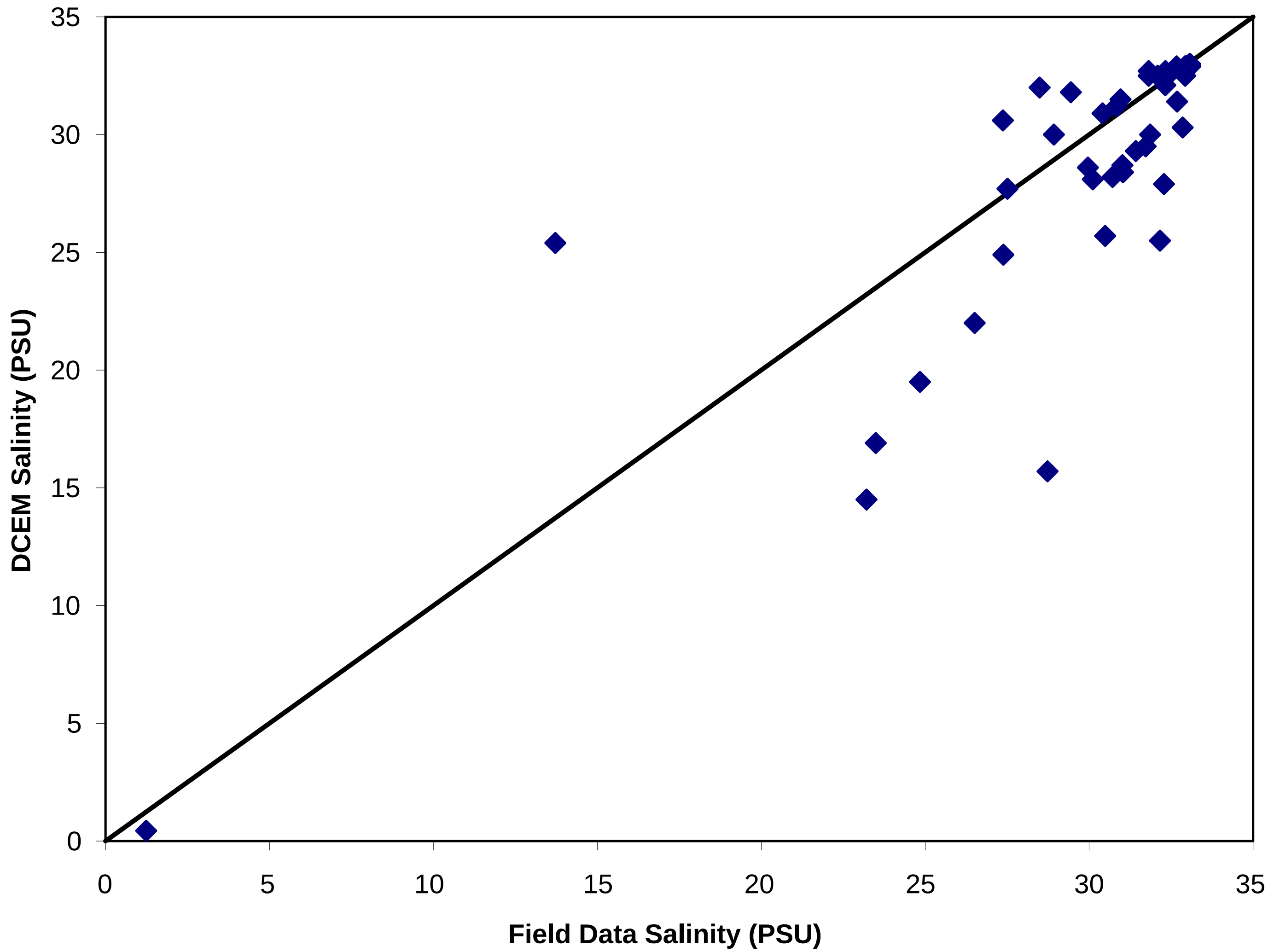

Figure 6.10 Comparison of Wet Weather Calibrated Surface Salinity with Field Data

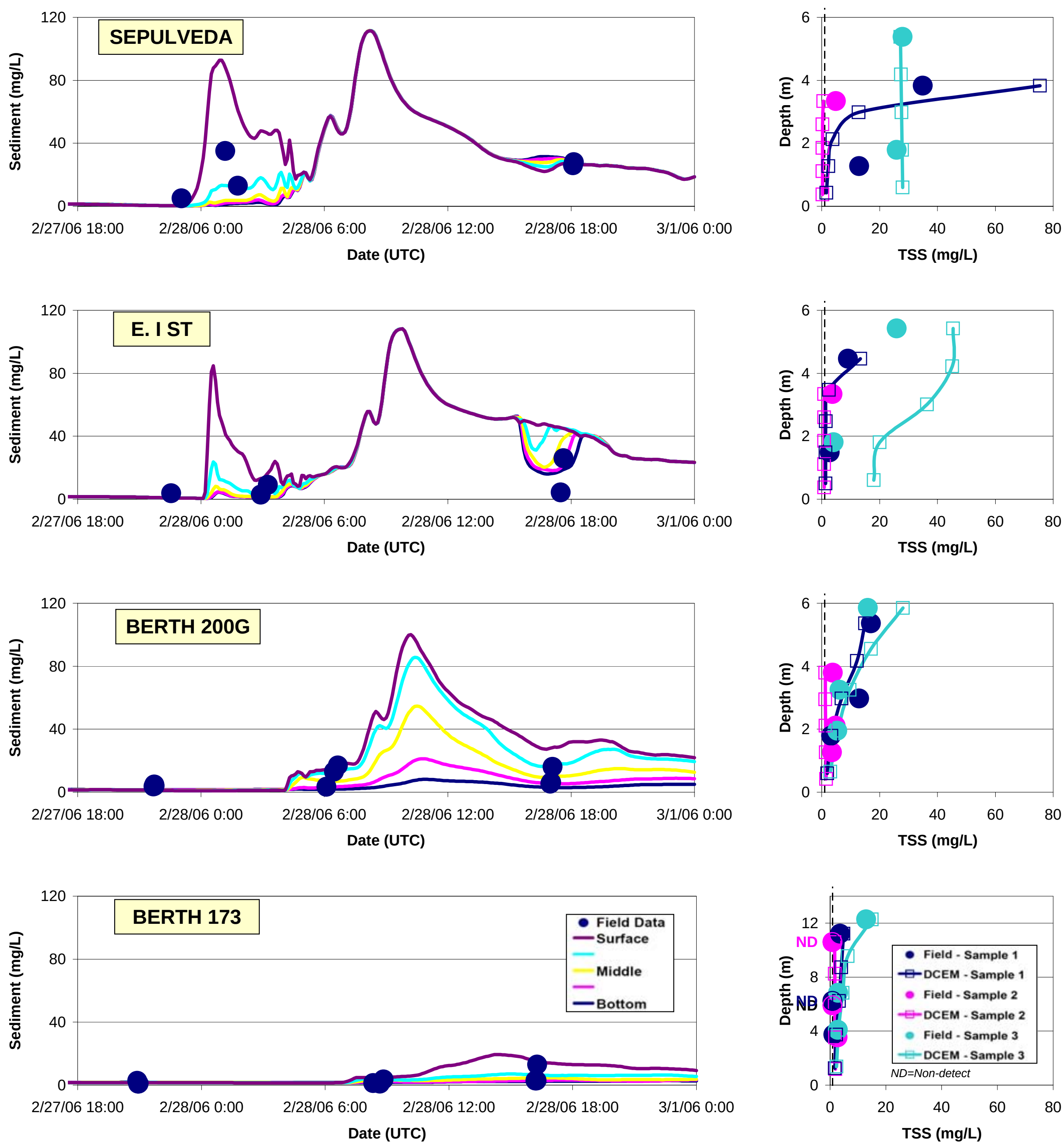

Figure 6.11 Wet Weather Calibrated TSS

barely apparent. In general, the DCEM-predicted TSS concentrations match well with the limited field measurements.

The DCEM predictions and field data concentrations for chromium, copper, lead and zinc are compared in Figure 6.12 - Figure 6.15, respectively. In the figures, the top three rows of panels show the time series of the total, dissolved, and particulate metal concentrations, and the bottom panels show the concentration profiles. The metal concentration time series follow the same trends as the sediment time series. In general, the DCEM results compare well with the field data.

The DCEM and field data metal particulate fractions for the four metals are compared in Figure 6.16, and it can be seen that the DCEM results compare well with the field data. However, the wet weather estuary sampling did not fully capture the fresh water effects on the metal equilibrium partition coefficients, as shown by the comparison of the equilibrium partition coefficient between the May 2005 dry weather estuary sampling and the February 2006 wet weather estuary sampling in Table 6.6. The field data particulate fractions for chromium and zinc were lower compared to the May 2005 samples, while the copper particulate fraction was about the same and the lead particulate fractions were slightly higher. This corresponds to the adjustment of only the chromium and zinc equilibrium partition coefficients for wet weather, but not the copper and lead.

Table 6.6 Dry and Wet Weather Equilibrium Partition Coefficient Comparisons

Location	Chromium		Copper		Lead		Zinc	
	Dry	Wet	Dry	Wet	Dry	Wet	Dry	Wet
Sepulveda Bottom	0.25	0.13	0.03	0.03	0.30	0.92	0.02	0.01
Sepulveda Surface	1.20	0.31	0.15	0.09	1.60	1.60	0.11	0.02
E. I St Bottom	1.00	0.33	0.16	0.22	1.83	1.71	0.12	0.05
E. I St Surface	1.10	0.64	0.14	0.32	1.82	2.73	0.10	0.05
200G Bottom	0.21	0.19	0.19	0.06	0.37	1.41	0.04	0.02
200G Mid	1.20	0.22	0.33	0.08	3.97	1.41	0.17	0.02
200G Surface	0.87	0.63	0.26	0.77	2.14	3.59	0.24	0.09
173 Bottom	0.88	0.45	0.21	0.23	2.03	3.47	0.10	0.07
173 Mid	0.09	0.81	0.02	0.40	0.35	3.97	0.01	0.10
173 Surface	0.42	0.74	0.18	0.29	5.15	3.21	0.19	0.07
Average	0.72	0.44	0.17	0.25	1.96	2.40	0.11	0.05
Standard Deviation	0.41	0.23	0.09	0.21	1.49	1.05	0.07	0.03

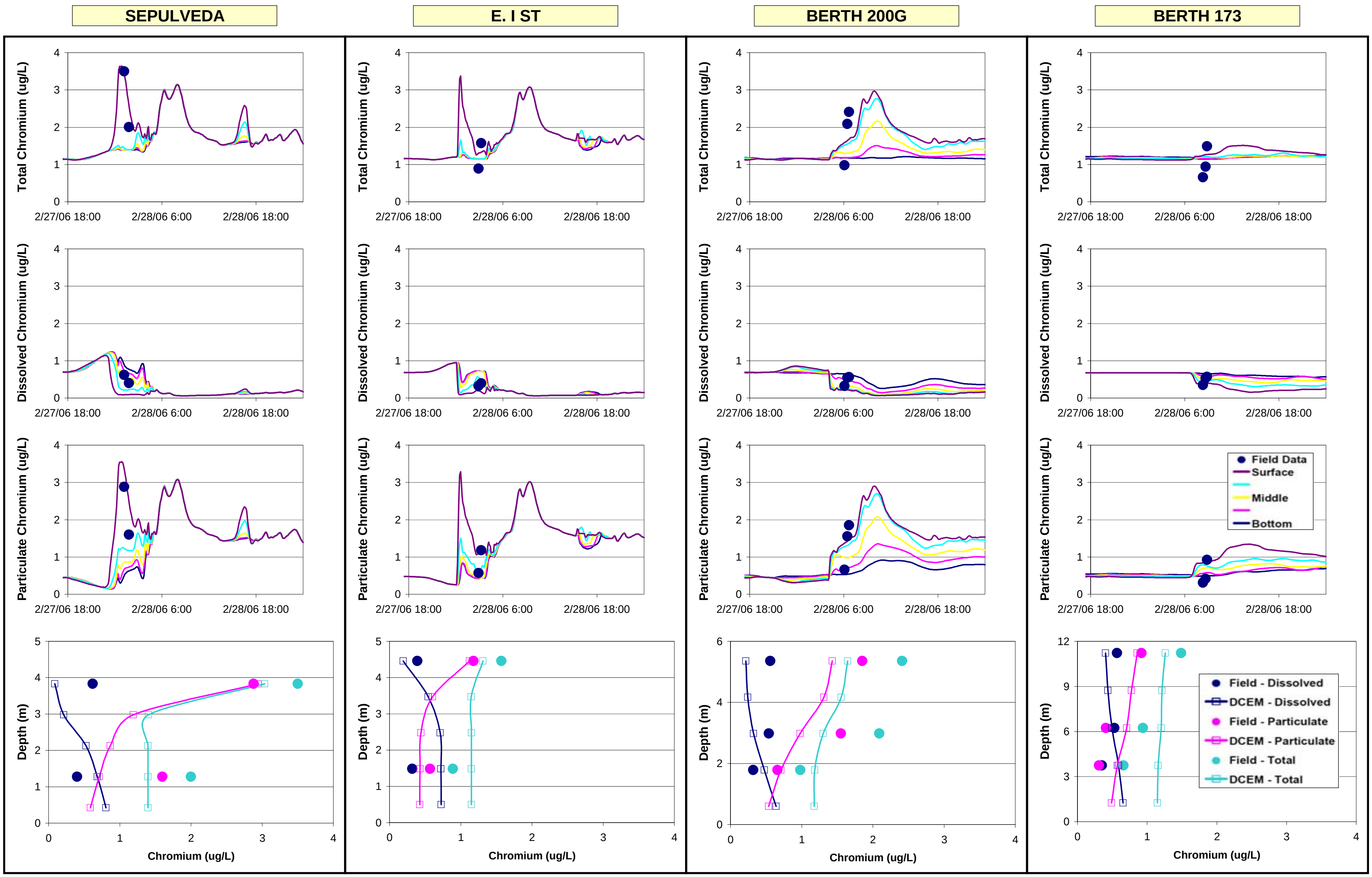

Figure 6.12 Wet Weather Calibrated Chromium

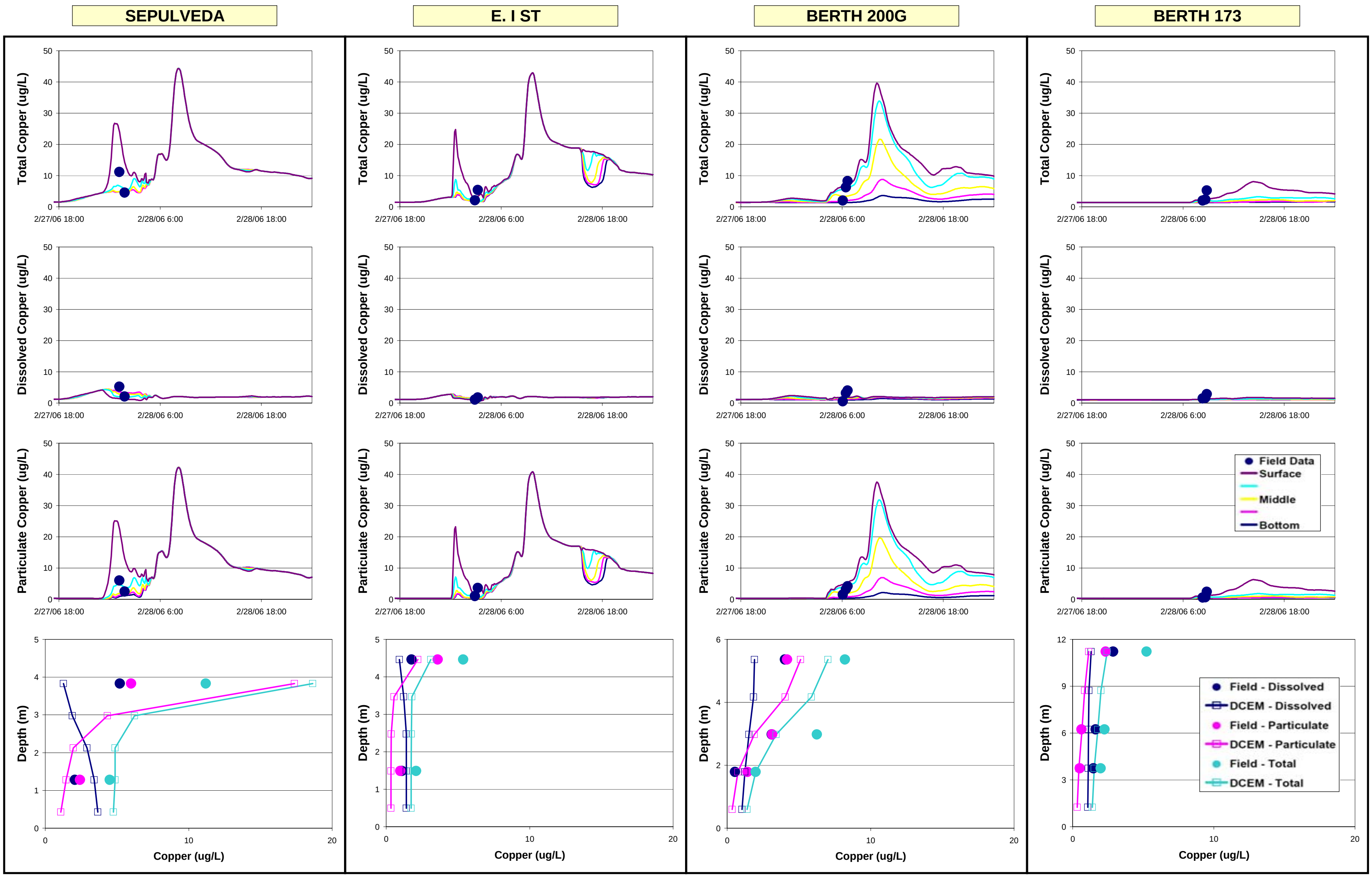

Figure 6.13 Wet Weather Calibrated Copper

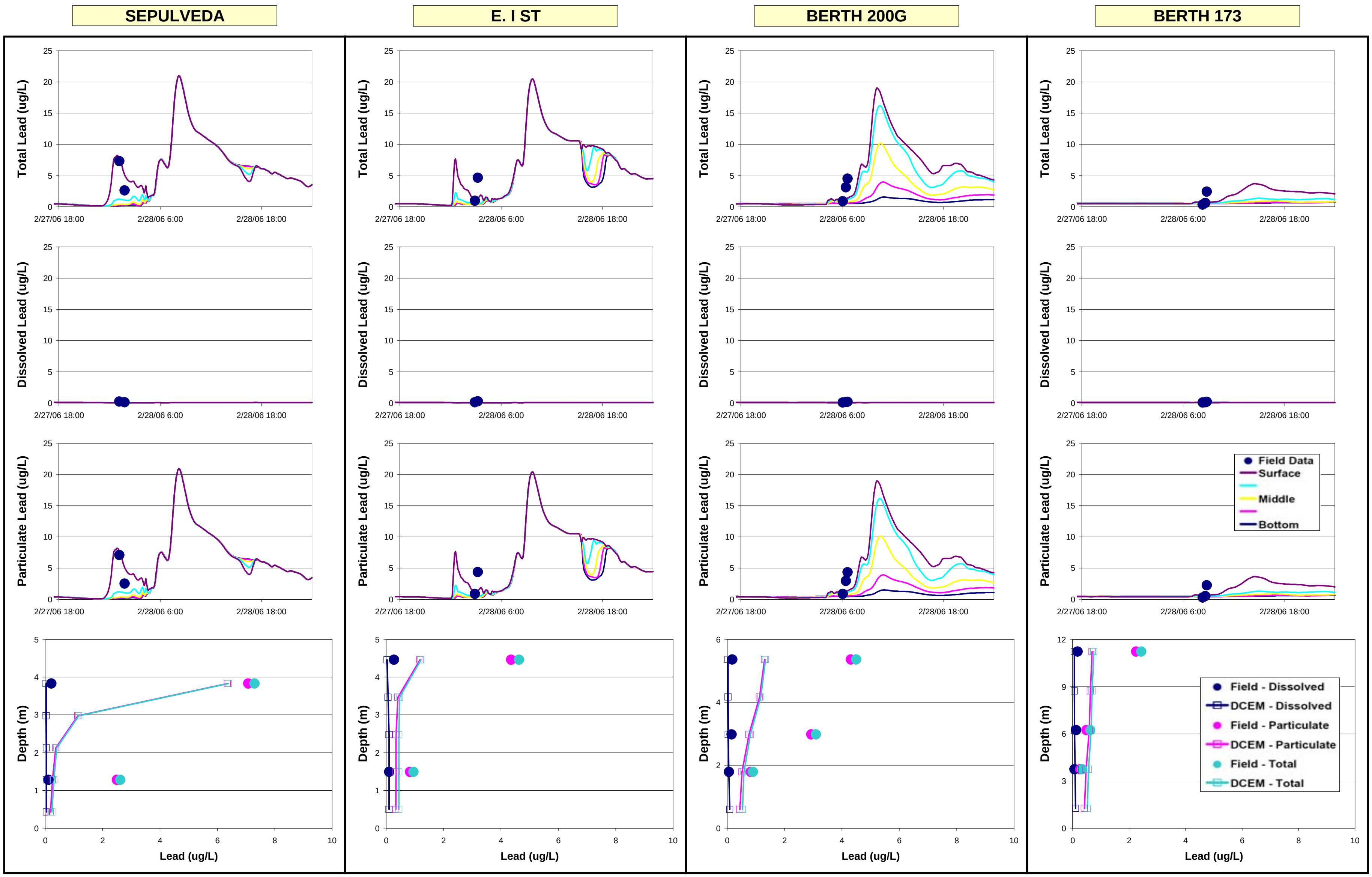

Figure 6.14 Wet Weather Calibrated Lead

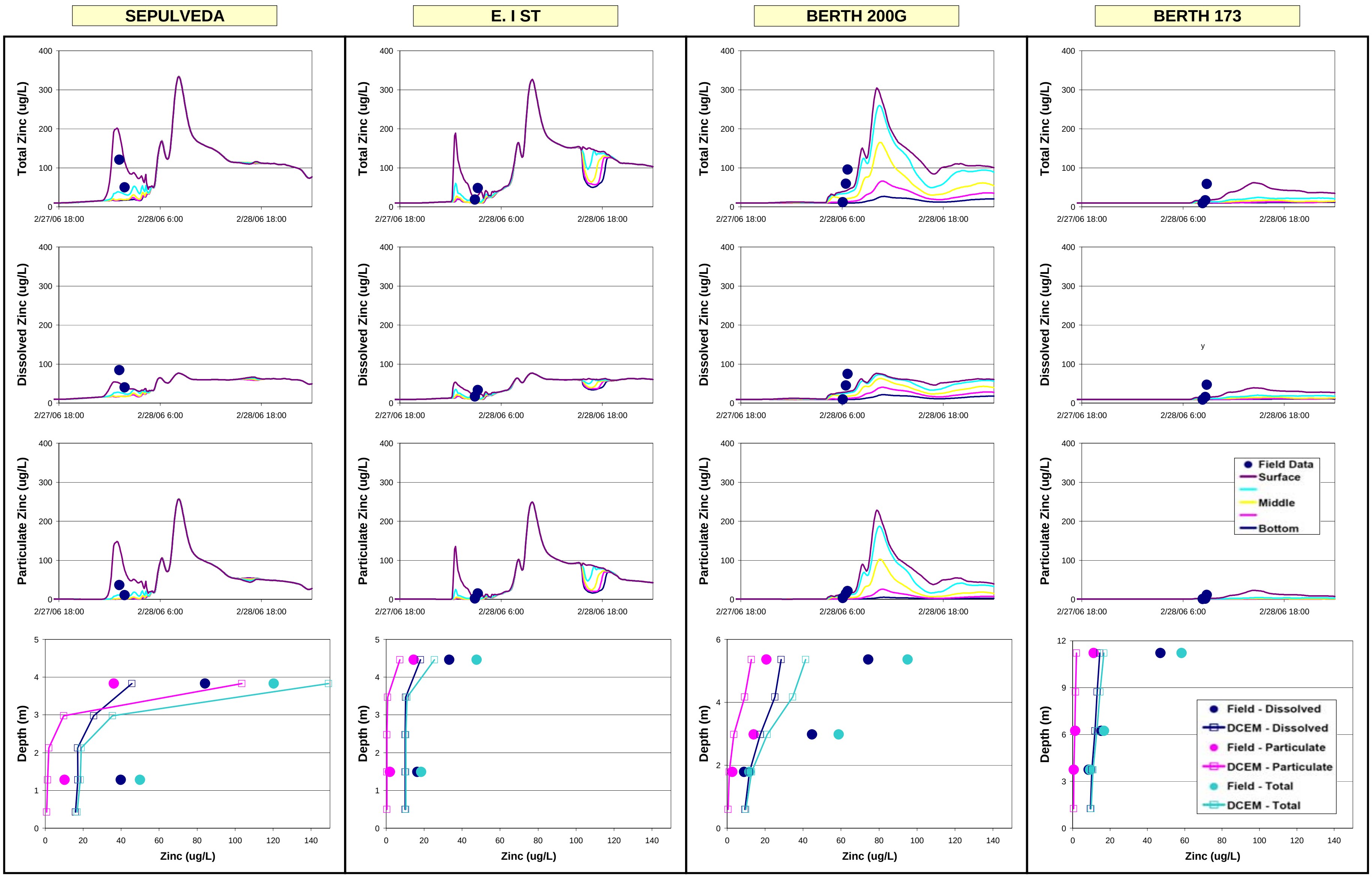

Figure 6.15 Wet Weather Calibrated Zinc

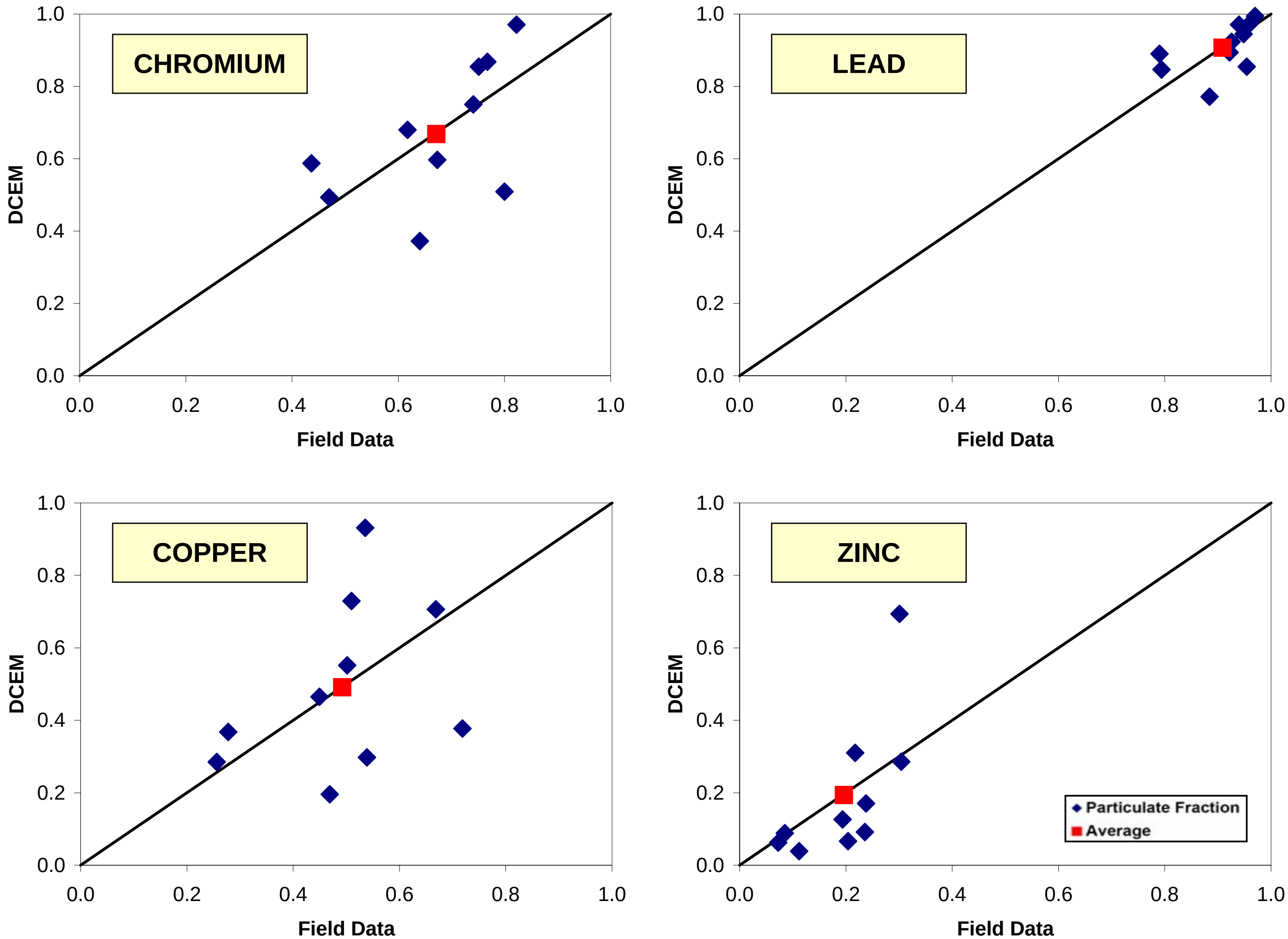

Figure 6.16 Comparison of Wet Weather Calibrated Particulate Fractions with Field Data

7. SUMMARY

The Dominguez Channel Estuary Model Study (DCEMS) was conducted to develop a calibrated 3-D hydrodynamic and water quality model (Dominguez Channel Estuary Model or DCEM) that can be used to predict water elevations, velocities, and pollutant transport in the estuarine portions of the Dominguez Channel. The Port anticipates the LARWQCB will utilize the DCEM for future development and implementation of TMDLs in the San Pedro Bay area.

This report summarized the development of the DCEM, which involved a model selection process, model setup, a field data collection program, and model calibration and verification. The Environmental Fluid Dynamic Code (EFDC) was selected for the development of DCEM. The DCEM model domain focuses on the estuary portion of the Dominguez Channel which extends from the tidally influenced portion of the Dominguez Channel at Vermont Avenue down to the Consolidated Slip. However, the model domain extends beyond the estuary portion to include the Los Angeles/Long Beach Harbors since the hydrodynamics in the estuary are dynamically linked to the harbor areas. The use of a larger model domain also facilitates future integration of the DCEM with other TMDL models being constructed for the Los Angeles/Long Beach Harbors and San Pedro Bay.

The DCEMS Field Program was designed to collect suitable data for the calibration and verification of the DCEM. The Field Program monitored hydrodynamic and water quality conditions in or near the Dominguez Estuary between February 2005 and March 2006 that included intensive dry and wet weather samplings. Data collected under the Field Program included water surface elevations, velocities, salinity, dye study, meteorological conditions, TSS, and metals. The Field Program data, along with additional data collected by others, were analyzed and processed to allow model comparisons for the calibration and verification of the DCEM.

The DCEM was calibrated for both the dry and wet weather conditions. The DCEM calibrations involved the selection of the model parameters that will provide the “best” comparison between model predicted hydrodynamics (water elevation and velocity) and water quality (salinity, dye, sediment, and metals) and field measurements. The simulation of hydrodynamics and water quality are inherently linked; for example, hydrodynamics influences salinity, but salinity also influences the hydrodynamics. Hence, the “best” calibrated model for hydrodynamics may not necessary produce the “best” calibrated results for all of the water quality constituents. The calibrated DCEM model is one that produces the overall best results for both the hydrodynamics and water quality for the study area. The dry weather calibrated parameters were then validated using another set of dry weather field data. The wet weather calibrated parameters were not validated since only one set of wet weather field data was collected.

A summary of the DCEM calibrated parameters is shown in Table 7.1. The roughness height, horizontal eddy viscosity, and sediment settling velocity were not calibrated for wet weather conditions since these parameters are not affected by fresh water inflows. It was found that the other model parameters were the same between the dry and wet weather conditions with the exception of the chromium and zinc equilibrium partition coefficients. It is expected that the metal equilibrium partition coefficients would be lower during wet weather due to lower salinity. However, most of the estuary metal samples were taken prior to the rain event flows reaching the estuary, thus the field data may not have fully reflected the changes in the metal equilibrium partition coefficients. The DCEM model files and additional information pertaining to the application of the DCEM are provided in the DCEM User's Manual (Everest 2006).

Table 7.1 Selected DCEM Calibrated Parameters

MODEL PARAMETER	UNITS	DRY WEATHER	WET WEATHER
Roughness Height – Dominguez Channel*	m	0.03	
Roughness Height – Harbor and Ocean*	m	0.02	
Horizontal Eddy Viscosity*	m^2/sec	1E-6	
Maximum Vertical Kinematic Viscosity	m^2/sec	2E-3	
Maximum Vertical Eddy Diffusivity	m^2/sec	1E-4	
Anti-Diffusion Correction for Hydrodynamics	--	Off	
Anti-Diffusion Correction for Salinity	--	Off	
Anti-Diffusion Correction for Dye	--	Off	
Anti-Diffusion Correction for Cohesive Sediment	--	On	
Anti-Diffusion Correction for Noncohesive Sediment	--	On	
Anti-Diffusion Correction for Metals	--	On	
Sediment Settling Velocity*	m/sec	3E-6	
Chromium Equilibrium Partition Coefficient	L/mg	0.9	0.44
Copper Equilibrium Partition Coefficient	L/mg	0.18	0.18
Lead Equilibrium Partition Coefficient	L/mg	2.5	2.5
Zinc Equilibrium Partition Coefficient	L/mg	0.13	0.03

* *Not weather dependent parameter*

8. REFERENCES

ACTA. 2001. Alameda Corridor Currents and Tracer Study Revised Final Report. Prepared for Alameda Corridor Transportation Authority. Prepared by Moffatt & Nichol Engineers and Reed International. May 31, 2001.

AMEC. 2002. Consolidated Slip Restoration Project – Draft Concept Plan. Prepared for Los Angeles Regional Water Quality Control Board and Port of Los Angeles Environmental Management Division. Prepared by AMEC Earth & Environmental, Inc. 2002.

AMEC. 2003. Supplemental Report Consolidated Slip Restoration Project Concept Plan. Prepared for Los Angeles Regional Water Quality Control Board and Port of Los Angeles Environmental Management Division. Prepared by AMEC Earth & Environmental, Inc. October 2003.

AMEC. 2005. Draft Dominguez Channel Sediment Investigation Report. Prepared for Los Angeles Regional Water Quality Control Board and Port of Los Angeles Environmental Management Division. Prepared by AMEC Earth & Environmental, Inc. February 2005.

Blumberg, Alan F. and Mellor, George L. 1987. A Description of a Three-Dimensional Coastal Ocean Circulation Model. *In Three Dimensional Coastal Ocean Models. Norman S. Heaps, editor.* American Geophysical Union, Washington, DC.

Chapra, Steven C. 1997. Surface Water-Quality Modeling. McGraw-Hill, Boston.

Everest. 2005. Dominguez Channel Estuary Model Study Implementation and Validation Plan Final. Prepared for the Port of Los Angeles. Prepared by Everest International Consultants, Inc. February 2005.

Everest. 2006. Dominguez Channel Estuary Model User's Manual. Prepared for the Port of Los Angeles. Prepared by Everest International Consultants, Inc. August 2006.

Galperin, B., L. Kantha, S. Hassid, and A. Rosati. 1988. A Quasi-equilibrium Turbulent Energy Model for Geophysical Flows. American Meteorological Society, Journal of the Atmospheric Sciences, Volume 45, No. 1, pp 55-62. January 1988.

Mellor, George L. and Yamada, Tetsuji. 1982. Development of a Turbulence Closure Model for Geophysical Fluid Problems. *Reviews in Geophysics and Space Physics*. Volume 20, No. 4, pp. 851-875. November 1982.

Port of Long Beach. 2002. Port of Long Beach and Los Angeles Year 2000 Biological Baseline Study of San Pedro Bay. Prepared for Port of Long Beach. Prepared by MEC Analytical Systems, Inc. in association with Science Applications International Corporation, Merkel & Associates, Inc., Keane Biological Consulting, and Everest International Consultants, Inc. June 2002.

SAIC. 2006a. Dominguez Channel Estuary Model Study Field Survey Photo Logs February 2005 through March 2006. Prepared by Science Applications International Corporation. Prepared for Everest International Consultants, Inc. April 2006.

SAIC. 2006b. Dominguez Channel Estuary Model Study Final Cumulative Survey Reports February 2005 through February 2006. Prepared by Science Applications International Corporation. Prepared for Everest International Consultants, Inc. May 2006.

Tetra Tech. 2002. EFDC Technical Memorandum – Theoretical and Computational Aspects of Sediment and Contaminant Transport in the EFDC Model. A report to U.S. Environmental Protection Agency. Tetra Tech, Inc. Fairfax, VA. 2002.

USACE. 1991. Hydraulic Design of Flood Control Channels. U.S. Army Corps of Engineers. Engineering Manual 1110-2-1601. July 1991.

USACE. 2002. Coastal Engineering Manual Volume I Part II: Coastal Hydrodynamics. Prepared by Coastal & Hydraulics Laboratory, Engineer Research and Development Center (ERDC), U.S. Army Corps of Engineers. April 2002.